

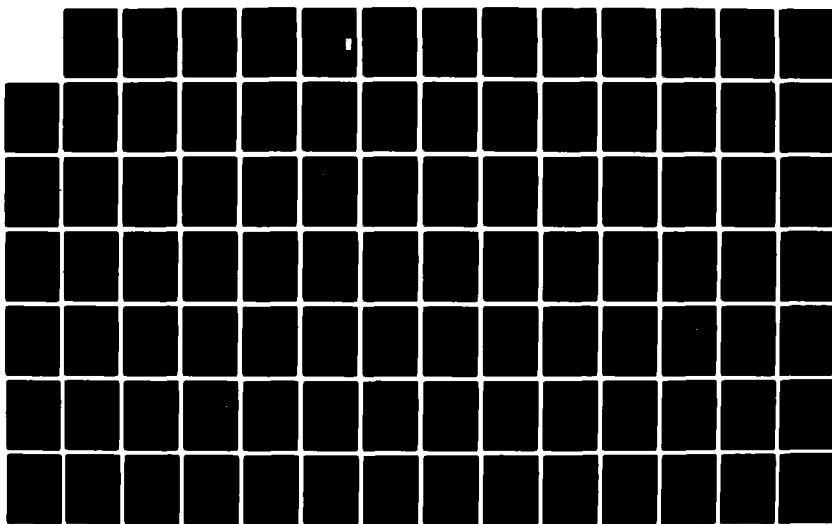
AD-A125 266

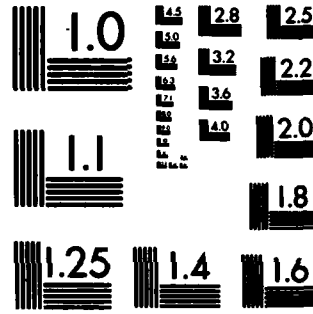
ANALYSIS OF PROGRESSIVE COLLAPSE OF COMPLEX STRUCTURES
(U) AIR FORCE INST OF TECH WRIGHT-PATTERSON AFB OH
G E RIGGS DEC 82 AFIT/CI/NR-82-63D

1/3

UNCLASSIFIED

F/G 12/1 • NL





MICROCOPY RESOLUTION TEST CHART
NATIONAL BUREAU OF STANDARDS-1963-A

AD A125266

UNCLASS

SECURITY CLASSIFICATION OF THIS PAGE (When Data Entered)

REPORT DOCUMENTATION PAGE		READ INSTRUCTIONS BEFORE COMPLETING FORM
1. REPORT NUMBER AFIT/CI/NR 82-63D	2. GOVT ACCESSION NO. <i>AD-A125266</i>	3. RECIPIENT'S CATALOG NUMBER
4. TITLE (and Subtitle) Analysis of Progressive Collapse of Complex Structures		5. TYPE OF REPORT & PERIOD COVERED THESIS/DISSERTATION
7. AUTHOR(s) Gregory Edward Riggs	6. PERFORMING ORG. REPORT NUMBER	
9. PERFORMING ORGANIZATION NAME AND ADDRESS AFIT STUDENT AT: University of Illinois	10. PROGRAM ELEMENT, PROJECT, TASK AREA & WORK UNIT NUMBERS	
11. CONTROLLING OFFICE NAME AND ADDRESS AFIT/NR WPAFB OH 45433	12. REPORT DATE <i>Dec 82</i>	
14. MONITORING AGENCY NAME & ADDRESS(if different from Controlling Office)	13. NUMBER OF PAGES 181	
16. DISTRIBUTION STATEMENT (of this Report) APPROVED FOR PUBLIC RELEASE; DISTRIBUTION UNLIMITED		15. SECURITY CLASS. (of this report) UNCLASS
17. DISTRIBUTION STATEMENT (of the abstract entered in Block 20, if different from Report)		15a. DECLASSIFICATION/DOWNGRADING SCHEDULE <i>S DTI MAR 1 1982</i>
18. SUPPLEMENTARY NOTES APPROVED FOR PUBLIC RELEASE: IAW AFR 190-17 <i>(17 Feb 73)</i>		<i>Lynn E. Wolaver</i> LYNN E. WOLAYER Dean for Research and Professional Development AFIT, Wright-Patterson AFB OH
19. KEY WORDS (Continue on reverse side if necessary and identify by block number)		
20. ABSTRACT (Continue on reverse side if necessary and identify by block number) ATTACHED		

DD FORM 1 JAN 73 1473 EDITION OF 1 NOV 68 IS OBSOLETE

UNCLASS

SECURITY CLASSIFICATION OF THIS PAGE (When Data Entered)

83 03 03 037

DMC FILE COPY

Name: Gregory Edward Riggs

Date of Degree: December, 1982

Institution: Oklahoma State University

Location: Stillwater, Oklahoma

Title of Study: ANALYSIS OF PROGRESSIVE COLLAPSE OF COMPLEX STRUCTURES

Pages in Study: 192

Candidate for Degree of Doctor of Philosophy

Major Field: Civil Engineering

Scope and Method of Study: The principal goal of the study was to evaluate an analytical procedure for predicting progressive collapse in damaged complex structures. A structure was modeled for analysis by the finite element method using relatively large, simple elements. There was little or no refinement of mesh size in areas of initial damage or damage propagation. A method was developed for determining and applying allowable stresses to help compensate for the absence of model detail. Stress results of a finite element analysis were examined by a computer post-processor program written for this study to make selective changes to the finite element model. The modified model was analyzed using the finite element method and the procedure was repeated in an iterative fashion to predict progressive collapse. Analytical results were compared to experimental test data to determine the validity of the analytical procedure.

Findings and Conclusions: The analytical procedure provided a relatively economical method for predicting progressive collapse in a complex structure. Evaluation of a complex structure subjected to three initial damage conditions showed acceptable correlation between experimental and analytical results. The method of determining appropriate allowable stresses was general enough to apply to a wide range of materials and structures. The procedure proved to be an economical estimating tool for predicting residual structural strength.

ADVISER'S APPROVAL _____



Acceptance Date	
RECEIVED	
DATE REC'D.	
UNIVERSITY LIBRARY	
JOURNAL OF APPLIED MECHANICS	
A-APPLIED MECHANICS	
DISPENSED	
A	

AFIT RESEARCH ASSESSMENT

The purpose of this questionnaire is to ascertain the value and/or contribution of research accomplished by students or faculty of the Air Force Institute of Technology (AFIT). It would be greatly appreciated if you would complete the following questionnaire and return it to:

AFIT/NR
Wright-Patterson AFB OH 45433

RESEARCH TITLE: Analysis of Progressive Collapse of Complex Structure

AUTHOR: Gregory Edward Riggs

RESEARCH ASSESSMENT QUESTIONS:

1. Did this research contribute to a current Air Force project?

() a. YES () b. NO

2. Do you believe this research topic is significant enough that it would have been researched (or contracted) by your organization or another agency if AFIT had not?

() a. YES () b. NO

3. The benefits of AFIT research can often be expressed by the equivalent value that your agency achieved/received by virtue of AFIT performing the research. Can you estimate what this research would have cost if it had been accomplished under contract or if it had been done in-house in terms of manpower and/or dollars?

() a. MAN-YEARS _____ () b. \$ _____

4. Often it is not possible to attach equivalent dollar values to research, although the results of the research may, in fact, be important. Whether or not you were able to establish an equivalent value for this research (3. above), what is your estimate of its significance?

() a. HIGHLY SIGNIFICANT () b. SIGNIFICANT () c. SLIGHTLY SIGNIFICANT () d. OF NO SIGNIFICANCE

5. AFIT welcomes any further comments you may have on the above questions, or any additional details concerning the current application, future potential, or other value of this research. Please use the bottom part of this questionnaire for your statement(s).

NAME _____ GRADE _____ POSITION _____

ORGANIZATION _____ LOCATION _____

STATEMENT(s):

FOLD DOWN ON OUTSIDE - SEAL WITH TAPE

AFTT/NR
WRIGHT-PATTERSON AFB OH 45433
OFFICIAL BUSINESS
PENALTY FOR PRIVATE USE: \$200



NO POSTAGE
NECESSARY
IF MAILED
IN THE
UNITED STATES

BUSINESS REPLY MAIL
FIRST CLASS PERMIT NO. 72220 WASHINGTON D.C.

POSTAGE WILL BE PAID BY ADDRESSEE

AFTT/ DAA
Wright-Patterson AFB OH 45433



FOLD IN

52-63D

ANALYSIS OF PROGRESSIVE COLLAPSE
OF COMPLEX STRUCTURES

By

GREGORY EDWARD RIGGS

Bachelor of Science in Civil Engineering
United States Air Force Academy
Colorado Springs, Colorado
1972

Master of Science
University of Illinois
Urbana, Illinois
1973

Submitted to the Faculty of the Graduate College
of the Oklahoma State University
in partial fulfillment of the requirements
for the Degree of
DOCTOR OF PHILOSOPHY
December, 1982

**ANALYSIS OF PROGRESSIVE COLLAPSE
OF COMPLEX STRUCTURES**

Thesis Approved:

Thesis Adviser

Dean of the Graduate College

ACKNOWLEDGMENTS

Of the many people deserving acknowledgment, it is appropriate that the first to receive thanks is Dr. Allen E. Kelly. As major adviser and chairman of my committee, he maintained a delicate balance between providing general guidance and giving full rein for me to travel my own course and learn along the way. I thank Dr. Thomas D. Jordan, a committee member, for providing background information concerning the formulation of the F-84F wing finite element model. I thank them and the other members of my committee, Dr. William P. Dawkins, Dr. John W. Harvey, and Professor Louis O. Bass, Jr., for their willingness to interrupt their own work at any time to discuss with me various aspects of the study.

I thank the Joint Technical Coordinating Group for Munitions Effectiveness for funding this study. I sincerely hope this work will provide long-term benefits for the Group in performing its mission.

Mr. Lyle Allen, senior systems analyst in Administrative Systems Development, donated his technical assistance in working within the university computer system. Joey Freeland and John Awezec, undergraduate assistants, directed their energies to both the experimental test program and to the analytical efforts that followed.

Ms. Charlene Fries receives thanks from students every semester for typing manuscripts, but such thanks severely underrate her contributions. She assumes full responsibility for administering the preparation and submission of the documents. I certainly thank her.

My wife, Jan, deserves a special thanks for her part in this program. She provided all of the encouragement and support, including assuming many of my responsibilities within our home, typical of any loving spouse behind a doctoral candidate. Beyond that, she demonstrated the analytical talents needed to assist me in portions of my course work and to recommend improvements to my research. I also thank my two young daughters, Megan and Michele, who donated a portion of their rightful time with their father during the last three months of the study.

Finally, I thank my parents, Ed and Marge Riggs, who have always been supportive. I thank especially my mother for taking the time long ago to explain to her puzzled son the difference between a noun and a verb, an adjective and an adverb. I believe her early patient effort helped immensely in my being able to progress through the formal education process.

TABLE OF CONTENTS

Chapter	Page
I. INTRODUCTION	1
II. LITERATURE REVIEW	3
2.1 General	3
2.2 Qualitative Analysis	3
2.3 Quantitative Analysis of Building Structures	4
2.4 Quantitative Analysis of Aircraft Structures	4
2.5 Analysis Method Background	5
III. SPECIFIC OBJECTIVES	7
IV. EXPERIMENTAL TEST PROGRAM	9
4.1 General	9
4.2 Specific Test Descriptions	9
4.3 Wing Support System	12
4.4 Load System	15
4.5 Deflection Measurements	15
4.6 Strain Measurements	17
V. FINITE ELEMENT MODELS	18
5.1 Background	18
5.2 Model Variations	20
5.3 Modeling Initial Damage	20
VI. ANALYSIS AUTOMATION	24
6.1 General	24
6.2 Overstressed Elements	24
6.3 Failed Elements	26
6.4 Propagation of Damage	27
6.5 Adjustment of Load	27
VII. DETERMINATION OF LIMITING STRESSES	29
7.1 Need for Limiting Stresses	29
7.2 Limiting Stresses for Rod Elements	30
7.3 Limiting Stresses for Web Elements	33
7.4 Limiting Stresses for Skin Elements	34
7.5 Damage Propagation	38

Chapter	Page
VIII. COMPARISON OF RESULTS	43
8.1 General	43
8.2 Comparison of Failure Loads	44
8.3 Load-Iteration History	45
8.4 Internal Load Paths	49
8.5 Comparison of Damage Modeling	50
8.6 Rotation of Wing Spar Roots	60
8.7 Deflections	62
IX. SUMMARY AND CONCLUSIONS	65
BIBLIOGRAPHY	68
APPENDIX A - STRAIN GAGE LOCATIONS FOR EXPERIMENTAL TESTS	71
APPENDIX B - FINITE ELEMENT MODEL NUMBERING DETAILS	76
APPENDIX C - ROD ELEMENT REPLACEMENT SYSTEMS	87
APPENDIX D - FINITE ELEMENT MODEL A LISTING	92
APPENDIX E - FINITE ELEMENT MODEL C LISTING	104
APPENDIX F - FINITE ELEMENT TORSIONAL ROD LISTING	115
APPENDIX G - INITIAL DAMAGE MODELING	117
APPENDIX H - PROGRESSIVE STRUCTURAL COLLAPSE ANALYSIS LISTING	122
APPENDIX I - PLOTS OF ANALYTICAL AND EXPERIMENTAL DATA	148
APPENDIX J - SUMMARY OF ANALYTICAL RESULTS	181

LIST OF TABLES

Table	Page
I. Designation of Finite Element Models	21
II. Limiting Stress Factors for Rod Elements	32
III. Limiting Factors for Skin Elements	36
IV. Summary of Failure Loads	45
V. Summary of Results for Test 1, Model D, Simple Damage . . .	182
VI. Summary of Results for Test 1, Model D, Detailed Damage . .	184
VII. Summary of Results for Test 2C, Model A	186
VIII. Summary of Results for Test 2C, Model D	188
IX. Summary of Results for Test 3B, Model A	190
X. Summary of Results for Test 3B, Model D	191

LIST OF FIGURES

Figure	Page
1. F-84F Wing Structure	10
2. Damage for Test 1	11
3. Damage for Test 2	13
4. Damage for Test 3	14
5. Wing Support Structure	16
6. F-84F Finite Element Model	19
7. Rod Elements for Spar Torsional Capacity	21
8. Modeling Variations for Test 1 Damage	23
9. Iterative Analysis Procedure	25
10. Cantilevered Beam Model	30
11. Cantilevered Front Spar Idealization	32
12. Typical Panel for Buckling Limits	35
13. Load-Displacement Curves for Panel Buckling	37
14. Crack Investigation Models	40
15. Propagation Stress Factor Curves	41
16. Load-Iteration Histories	46
17. Wing Model Results at Test 1 Failure	51
18. Wing Model Results at Test 2C Failure	54
19. wing Model Results at Test 3B Failure	57
20. Failure Load Profiles for Test 3B	63
21. Strain Gage Locations	73
22. Finite Element Model Numbering Details	77

Figure	Page
23. Basic Sizing of Rod Elements	90
24. Rod Element Sizing With Shear Panel Skin	91
25. PROSCAN Functional Flow Diagram	123
26. Comparison of Vertical Reaction Forces	149
27. Comparison of Strains for Test 1	155
28. Comparison of Strains for Test 2C	159
29. Comparison of Strains for Test 3B	163
30. Load Point Displacements for Test 1	167
31. Single-Point Displacements for Test 2C	169
32. Single-Point Displacements for Test 3B	175

CHAPTER I

INTRODUCTION

Many structures are susceptible to progressive collapse, a chain reaction type of failure following damage to a relatively small portion of the structure. The more specialized a structure is, the more vulnerable it is to progressive failure largely because it is designed to resist fewer possible loading conditions. As efforts increase to optimize designs within acceptable factors of safety, the risks of initiating progressive collapse through relatively minor localized damage also increase. An ability to predict analytically the response of a damaged structure would therefore be beneficial.

Although progressive collapse is normally associated with high-rise buildings, interest in it is not limited to conventional civil engineering applications. The Department of Defense needs the capability to predict the residual strength of battle-damaged aircraft and to know the role of progressive collapse in that setting. Specifically, the Department of Defense Joint Technical Coordinating Group for Munitions Effectiveness is interested in the post-damaged capabilities of potentially hostile aircraft.

In pursuit of its interest, the Group provided research funds and three F-84F aircraft wings for this study. The goal was to evaluate a potentially versatile method for predicting progressive collapse in aircraft structures. The method was to be verified by experimental testing.

Desirable characteristics to be imparted to the method would be relative simplicity in preparing for its use and relative ease and economy in its application.

The finite element method was the fundamental tool for determining stresses within the wing. In this report most discussion of the finite element method is of a general nature. The NASTRAN (National Aeronautical and Space Administration Structural Analysis) program was selected to apply the finite element method because of its versatility and its widespread availability in both industry and the defense community. The reader is assumed to be familiar with the finite element method in general. Where reference to specific program characteristics is essential, a basic familiarity with NASTRAN is also assumed.

Finally, the sponsor of this research is interested in the effectiveness of munitions in destroying combat aircraft. Consequently, any conservative assumption is one which tends to give the structure more strength than actually exists. This definition of conservative is used throughout the study. Caution must be exercised in directly extending the results of this study to more conventional applications. In such use the assumptions of this study would become unconservative.

CHAPTER II

LITERATURE REVIEW

2.1 General

Many papers have addressed the topic of progressive collapse of damaged structures, but only one has provided a general quantitative method of analysis (1). The following sections summarize the published papers while the last section details the one general approach.

2.2 Qualitative Analysis

Most studies of progressive collapse, as applied to structures conventionally associated with Civil Engineering, fit into three categories. The first addressed a need to predict statistically the frequency and severity of damaging events such as vehicle impact or explosion (2 through 8).

Another category was the qualitative analysis of a structure's ability to resist damage or to develop alternate load paths around damage. Typical topics of discussion included catenary action of slabs, beam action of adequately tied ceiling-wall-floor systems acting as wide flange sections, and the in-plane arching of walls over damage (4, 7, 9 through 14).

A third category was an effort to develop codes which mate the first two areas into economically and socially acceptable guidelines for design and construction (15 through 23). Additionally, a research workshop was

conducted in 1975 to evaluate present knowledge of the progressive collapse phenomenon and to identify areas requiring further study (24).

2.3 Quantitative Analysis of Building Structures

A smaller, fourth category addressed the need to evaluate quantitatively the behaviors occurring during a progressive collapse. Several studies have been completed, but most have considered only two-dimensional problems and most have required extensive analyst interactive involvement (25 through 29).

Smith and Epstein (30) developed a three-dimensional method to analyze the progressive collapse of a space truss roof. Their approach used the finite element method to determine structural member stresses. As a member approached its buckling load, predetermined for every member in the structure, the member was replaced by opposite equal forces representing post-buckling strength. The method did provide a three-dimensional analysis but was limited exclusively to buckling related failures. It was inappropriate for structures in which other failure modes share equal importance or are dominant.

2.4 Quantitative Analysis of Aircraft Structures

The military's need to predict the behavior of damaged aircraft has precipitated several papers of interest. Venkayya (31) outlined an empirical iterative procedure in 1978 for determining the residual strength of damaged structures. The displacements and decomposed stiffness matrix of an undamaged structure were combined with a sparse negative stiffness matrix representing damage. The result was an iteratively derived second-order Taylor series approximation of the response of the damaged structure.

The method appeared suitable for economic evaluation of initial structure response to several different damage conditions. However, when the method is applied to progressive collapse analyses, problems surface as component failure progresses toward collapse. Solution convergence times become unacceptably slow and convergence criteria become increasingly difficult to establish.

In 1976, Heard (1) proposed for the Air Force Armaments Testing Laboratory (AFATL) a method of structural modeling and analysis for progressive collapse in aircraft structures. That method, referred to in this study as the AFATL method, appeared to be the most promising general approach to a quantitative analysis of progressive collapse. The next section presents this method in some detail.

2.5 Analysis Method Background

The structure being evaluated must be represented as a computer model for finite element analysis. Because the method requires many iterative analyses to trace the progressive collapse phenomenon, economy urges the use of the largest, simplest elements which still describe the basic geometry of the structure and provide adequate precision to permit a stress-based analysis. A principal feature of the AFATL method is that little or no refinement of the model occurs in the area of damage. This feature aids the economy of the method but, because the large elements mask stress concentrations, the method must include compensating techniques. Heard employed two such techniques which are described later.

A load was applied to the model and the resulting stresses were examined in search of overstressed elements. An overstressed element was one whose stresses exceeded predefined limiting values. A solitary over-

stressed element was removed from the model as having failed. If more than one overstressed element occurred grouped together, only the most severely stressed element of the group was removed. This technique helped represent crack propagation in a model composed of large elements and was supported by studies of Sih and Hartranft (28).

Reducing the values of limiting stresses for elements bordering damage was the second technique to compensate for loss of stress concentrations around crack tips at the edges of damage. Thus the computed stress in an element bordering damage might produce element failure while a similarly stressed element away from damage remained intact. Using different values for limiting stresses complicated the process of selecting which element to fail in a group of overstressed elements. The most severely stressed element could not be determined through a direct comparison of the magnitudes of element stresses.

After the failed elements were removed, the modified model was again analyzed and the procedure was repeated. Iterations continued until the model could sustain some desired maximum load, or until failure occurred. This latter condition was sometimes determined subjectively by evaluating the structure's displaced shape rather than by its residual load-carrying capacity.

CHAPTER III

SPECIFIC OBJECTIVES

The method proposed by Heard appeared to be a versatile approach for the quantitative analysis of progressive collapse. To increase the acceptability of the method, however, four areas were identified as objectives for further study.

Validation of the method was perhaps the most important objective. Due to an absence of actual aircraft wings which his model represented, Heard was unable to substantiate with actual test data the value of his work. The first phase of this study was a laboratory test program which provided data for evaluation of analytical results. Tests of three F-84F aircraft wings measured structural performance under different damage and load combinations.

In the previous study, only one combination of elements was used for modeling the aircraft wing structure. A comparison of several element combinations was made in search of the best selection of model elements.

The actual application of the method required a great amount of manual data analysis for each iteration. A large number of elements had to be checked and compared to limiting stress values. The relative locations of overstressed elements had to be determined and caution applied to remove the appropriate element. Finally, removal of failed elements required modifications of the model. In addition to removing the failed elements, modification included reducing limiting stresses for elements

bordering the newly propagated damage. Automating the application of the method was desirable to reduce both time and expense for a complete analysis.

The final area to address was the appropriate values for limiting stresses. Heard used two levels of limiting stresses: material ultimate strength for elements away from damage, and material yield strength for elements bordering damage. A more sophisticated determination of limiting stresses had the potential for returning more realistic results.

These four areas,

1. Comparison of analytical and test results
2. Comparison of modeling elements
3. Automation of the method
4. Determination of limiting stress values,

became the specific objectives of this study.

CHAPTER IV

EXPERIMENTAL TEST PROGRAM

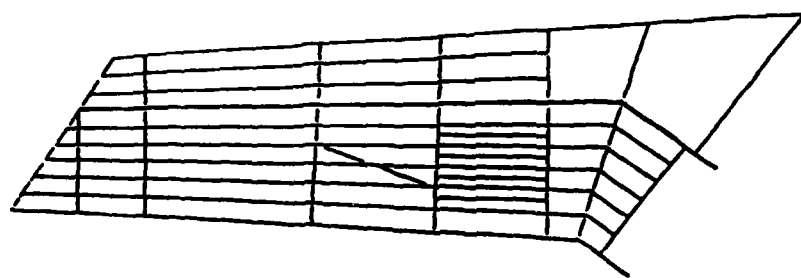
4.1 General

A major objective of this study was to use actual test data as a standard for evaluating analytical results. Three F-84F aircraft wings were tested, each with a different damage and load combination. This chapter contains descriptions of specific damage and loads and of the general test procedure. Appendix A contains diagrams showing strain gage locations for the various tests.

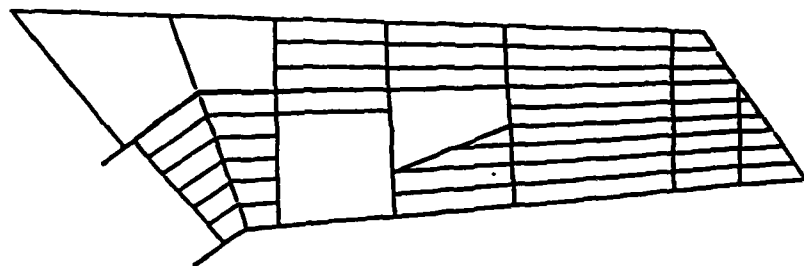
4.2 Specific Test Descriptions

The F-84F aircraft wing is a two-spar, semi-monocoque structure. For general reference, Figure 1 illustrates the upper and lower wing surfaces and the wing structural frame. All three wings were mounted upside down for testing; however, the terms "upper" and "lower" refer to the wing's upper and lower surfaces, not to their physical orientation for the tests. For all tests, the landing gear and gear doors, flaps, and ailerons were removed.

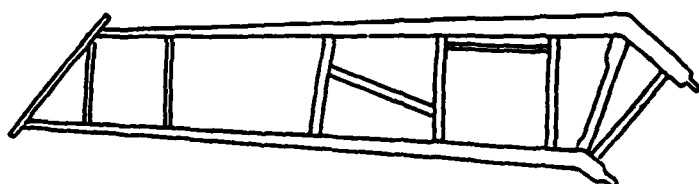
Test 1 consisted of severe damage to the upper half of the front spar as shown in Figure 2. A load applied to the front spar produced a failure with bending as the predominant behavior. The damaged area was stressed in tension.



(a) Upper Surface

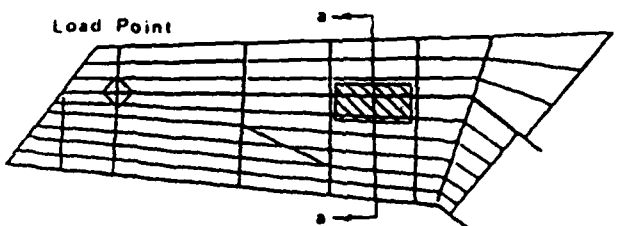


(b) Lower Surface

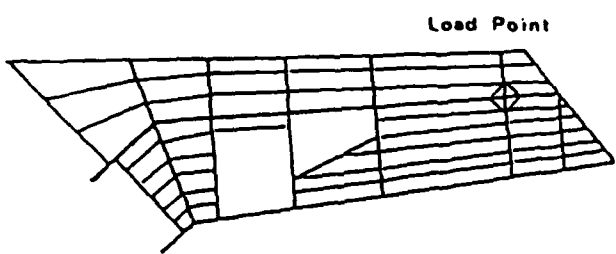


(c) Structural Frame

Figure 1. F-84F Wing Structure



Upper Surface



Lower Surface



Section a-a

■ Damage

Figure 2. Damage for Test 1

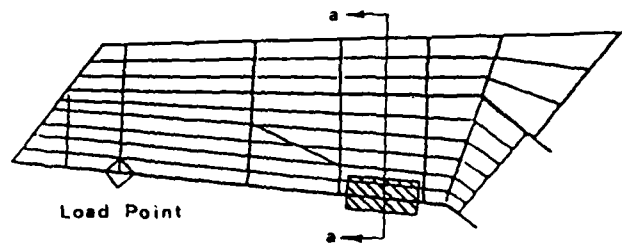
Test 2, Figure 3, was to measure behavior with a significant amount of torsion present. The rear spar was completely severed and the load was applied to the rear spar. The result was a combination of bending and torsion in the front spar. This wing could not be failed within safe limits of the laboratory loading apparatus. Consequently, three loading trials were performed on this wing and designated Tests 2A, 2B, and 2C. Each test had slightly modified damage to the skin adjacent to the severed spar. These were efforts to initiate tearing of the skin over the wheel well area; however, no propagation of that damage occurred.

Test 3 was an attempt to represent more closely the damage which could occur from a shaped-charge missile warhead. Figure 4 shows a $5\frac{1}{2}$ -inch wide strip of material removed from the lower wing surface. All skin was removed from the strip, which extended from the rear spar to the leading edge. The lower rear spar cap was removed but the web was left intact. The portion of the lower front spar cap extending from the web toward the trailing edge was also removed. The load applied to the rear spar put the damaged surface into compression.

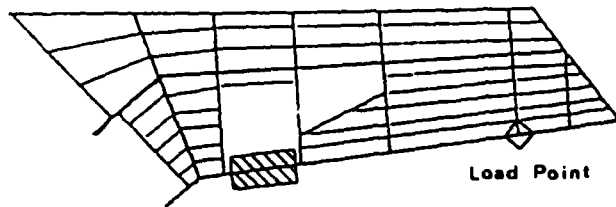
The residual strength of this wing also exceeded the safe capacity of the loading equipment. A variation of this test, designated Test 3B, included further damage to the front spar cap. Half the width of the lower spar cap extending from the web toward the leading edge was removed. A $1\frac{1}{4}$ -inch width of spar cap remained extending from the rear face of the web toward the leading edge. This additional damage led to complete structural failure.

4.3 Wing Support System

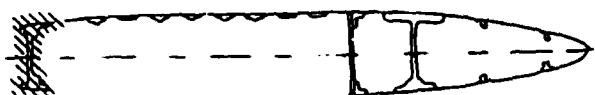
Each wing spar root mounted into a support structure as illustrated



Upper Surface



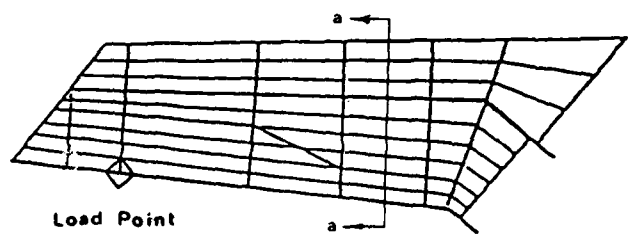
Lower Surface



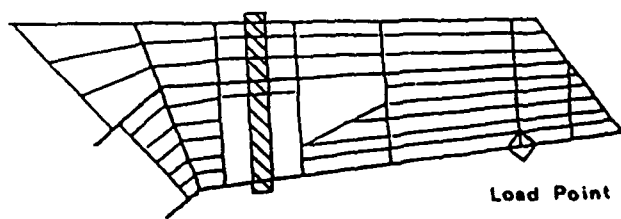
Section a-a

■ Damage

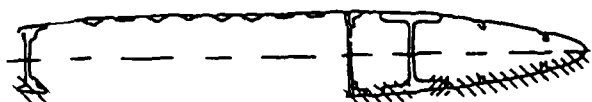
Figure 3. Damage for Test 2



Upper Surface



Lower Surface



Section a-a

- Damage
- Additional Damage for Test 3B

Figure 4. Damage for Test 3

in Figure 5. Pins secured the wings in the support structures in the same manner as the wings had been attached to aircraft fuselages. The support structures were extremely rigid compared to the wings so that no appreciable deformation occurred within the supports themselves. Three transducers supported each T-shaped support structure, permitting measurements of vertical reaction forces and reaction moments about two perpendicular horizontal axes.

The wing spar roots were aligned with the support structures and pinned into place within small tolerance; however, some motion of the wing spar roots with respect to the supports was unavoidable. For Tests 2 and 3, dial gages measured relative rotation of each wing spar root about horizontal axes parallel to and perpendicular to the root itself. These data then formed the basis for support conditions in corresponding finite element analyses. These support conditions provided a better analytical representation of wing deflections; however, support conditions assuming no relative rotation were used for stress analyses.

4.4 Load System

A movable overhead crane applied a single point load in each test. The crane was self-adjusting so the load was always applied vertically. A cable attaching the crane to the wing load point was equipped with an in-line transducer to permit continuous accurate monitoring of the actual load applied.

4.5 Deflection Measurements

Vertical deflections were measured at points along the front and rear spars corresponding to node points in the finite element model.

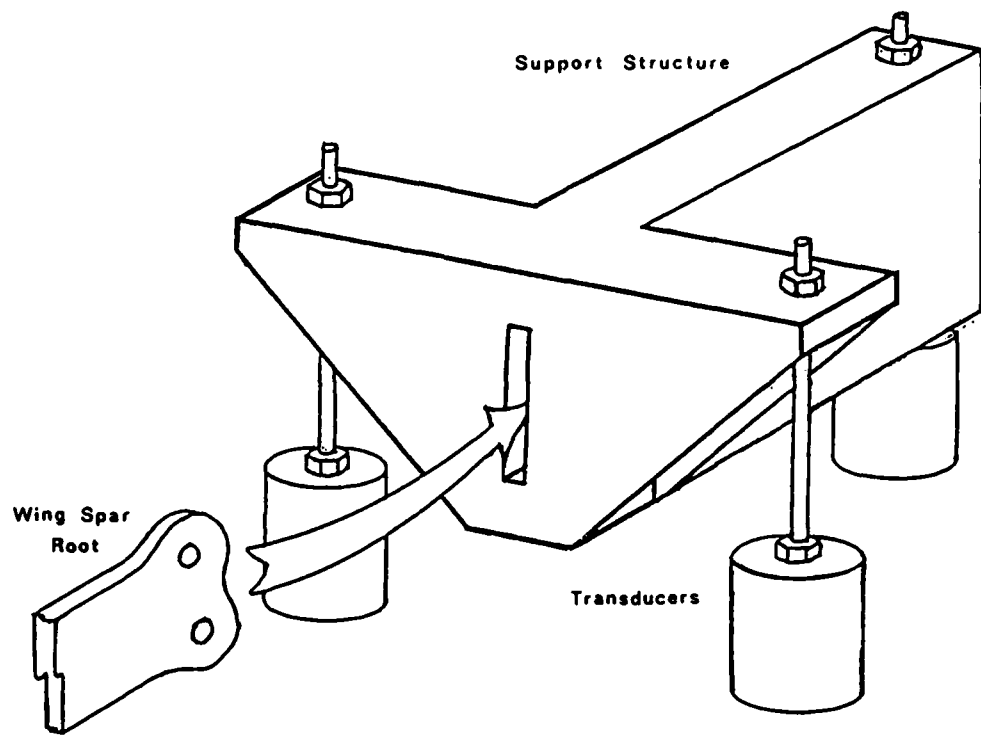


Figure 5. Wing Support Structure

Steel scales incremented to 0.01 inch were attached to the lower wing surface and measurements were read through an engineer's level. Similarly, scales were mounted on the support structures above each transducer to detect any vertical displacements there. At the load point no scale could be attached to the wing surface as at other locations along the spars. Instead, a cloth tape hung down vertically from the upper wing surface to measure deflections with respect to the laboratory floor.

4.6 Strain Measurements

Strain gages were mounted to the wing to detect changes in load paths as components failed and to detect load levels at which failures occurred. The different designs of each test and experience from previous tests led to slightly different strain gage placement for each wing. Appendix A contains specific locations.

Quarter-inch uniaxial strain gages measured outer fiber strains along spar and rib caps. Three-gage rectangular rosettes attached to selected skin panels measured panel behavior. Similar rosettes measured shear in rib and spar webs in Test 3.

Wings were first loaded enough to compensate for self-weight, and all gages were zeroed. For Test 1, all transducers and strain gages fed into a single switch and balance unit to measure output. All other tests used a Vishay Instruments Measurements Group computer-controlled data acquisition and reduction system. The System 4000 included the software program plus a Controller 4220 and two Strain Gage Scanners 4270. A Hewlett-Packard 9825B, upgraded to 9825T capabilities, served as the Executive Control Unit to complete the system hardware.

CHAPTER V

FINITE ELEMENT MODELS

5.1 Background

The fundamental modeling philosophy used by Heard (1) applied also to this study. Rod elements in combination with shear panels represented heavy structural members such as spars and ribs. Shear panel or membrane elements represented aircraft skin. Skin stiffeners were modeled by rod elements.

The specific structure for this study, the F-84F aircraft wing, was also analyzed by Jordan (32, 33). In 1976, he performed a dynamic response and small static load bending analysis of the wing. Although his objective differed from Heard's, he applied the same fundamental philosophy to develop his model of the wing. Jordan's model was the nucleus of the models evaluated in this study and is illustrated in Figure 6. Details of element numbering are presented in Appendix B.

The structure's geometry determined the size of the elements. Intersections of spars and ribs and of skin stiffeners and ribs were model node points. The node points in turn defined the elements. The procedure for assigning area properties for elements, particularly for rods, was detailed by both Heard (1) and Jordan (33). A brief summary is presented in Appendix C.

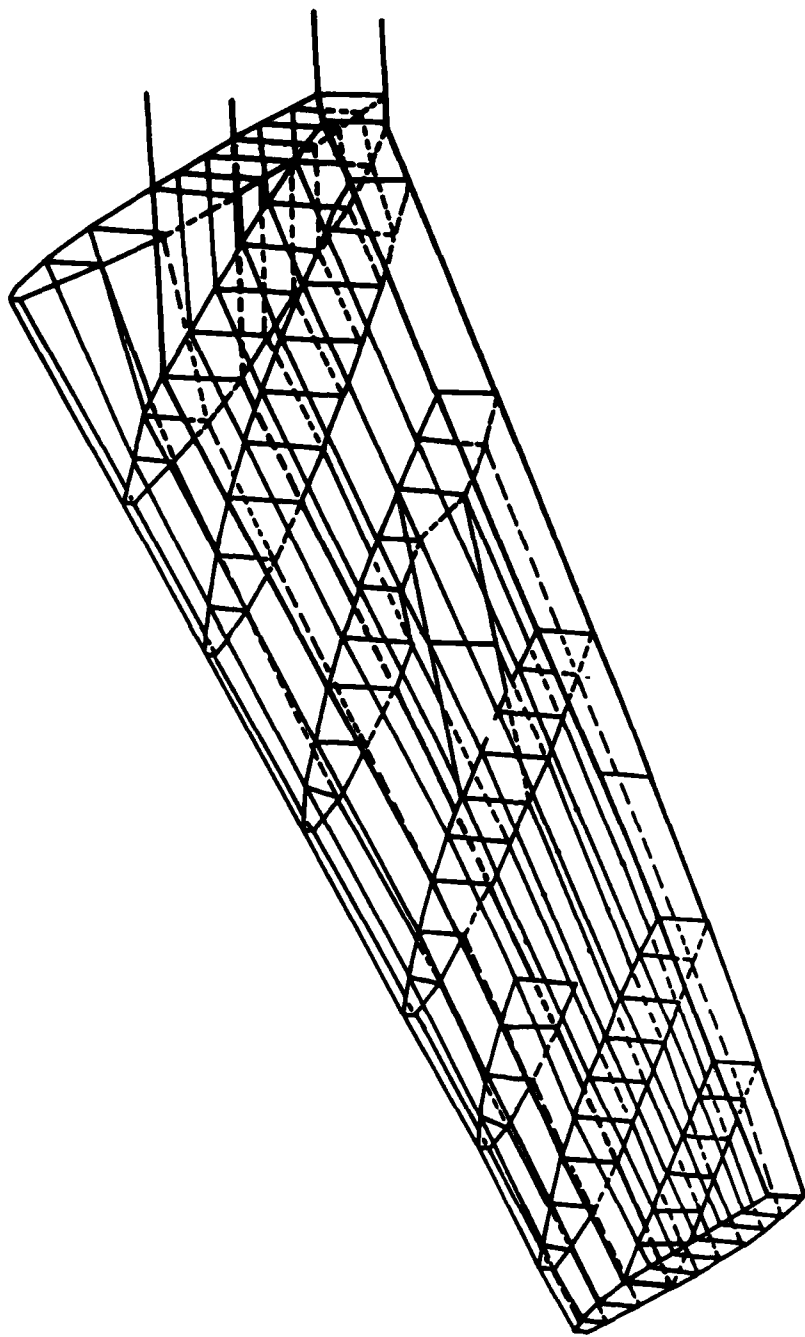


Figure 6. F-84F Finite Element Model

5.2 Model Variations

The model developed by Jordan gave him good response for conditions where bending dominated; however, it provided no torsional stiffness for the heavy structural members. To evaluate damage and load combinations producing significant torsion, model revisions included torsional stiffness for the front and rear spars.

This stiffness was provided by including rod elements along the centerlines of the spars. These elements had no axial load capacity but did provide torsional resistance. Multipoint constraint equations determined the rotation of each end of a torsion rod by using the lateral displacements of the nodes immediately above and below it. Figure 7 illustrates that the rotation, β , of the end of the centerline rod was

$$\beta = \frac{1}{h} (y_u - y_l) \quad (5.1)$$

Although modeling philosophies in the previous efforts were essentially the same, Heard used membrane elements for the skin while Jordan used shear panels. This study compared four modeling combinations. All four models used rods for skin stiffeners and for caps of spars and ribs. All used shear panels for spar and rib webs. The differences are presented in Table I. Appendix D is a listing of Model A and Appendix E is a listing of Model C. The additions for torsional resistance to convert Models A and C to Models B and D, respectively, are presented in Appendix F.

5.3 Modeling Initial Damage

To the extent possible, no special modeling techniques were applied to initial damage. Damaged shear panels or membranes were reduced in

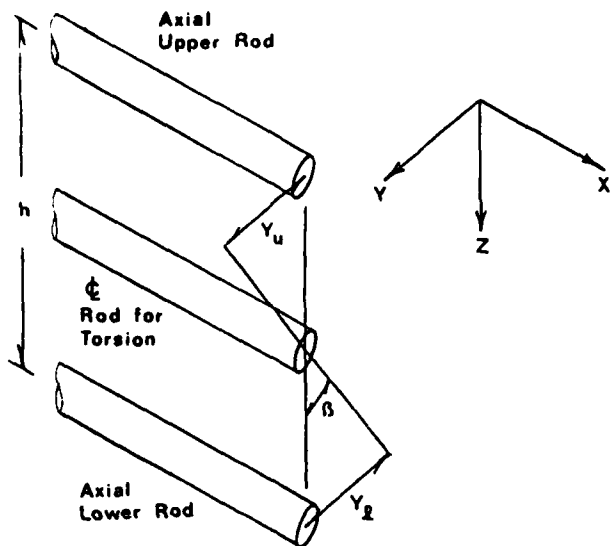
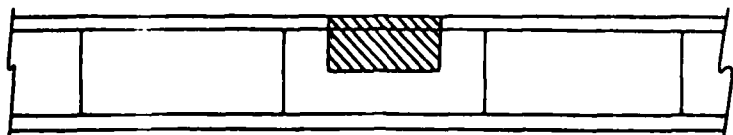


Figure 7. Rod Elements for Spar
Torsional Capacity

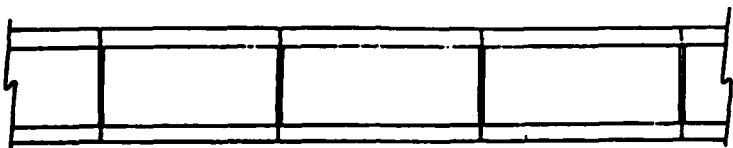
TABLE I
DESIGNATION OF FINITE ELEMENT MODELS

Model Designation	Skin Elements	Torsional Stiffness
A	Shear Panels	No
B	Shear Panels	Yes
C	Membranes	No
D	Membranes	Yes

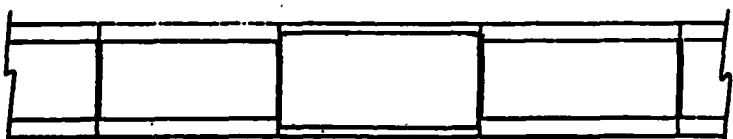
thickness or were removed when damage was severe. The rods representing damaged spars were reduced in size to maintain an equivalent moment of inertia, as presented by Jordan (32, 33). One exception to this approach was evaluated for Test 1. Damage to the front spar extended halfway into the web. Figure 8a shows a side view of the damaged front spar and Figure 8b shows modeling of the undamaged spar. The simpler modeling technique is illustrated in Figure 8c. The web element thickness was reduced to half its undamaged size. Rods representing spar caps were unmoved but reduced in size to represent the residual moment of inertia. Figure 8d shows the more detailed approach used by Jordan (32, 33) to model such severe damage. The two methods were compared. The specific changes made to Models A and C for each test are presented in Appendix G. The additional changes for Models B and D are included as part of Appendix F.



(a) Front Spar. Damaged



(b) Model. Undamaged



(c) Model. Simple Damage



(d) Model. Detailed Damage

Figure 8. Modeling Variations for Test 1 Damage

CHAPTER VI

ANALYSIS AUTOMATION

6.1 General

One shortcoming of the AFATL method cited in Chapter III was the need to examine voluminous computer output. A FORTRAN IV computer code, entitled PROSCAN for Progressive Structural Collapse Analysis, was written to alleviate the problem. PROSCAN was written to apply the method in conjunction with NASTRAN (National Aeronautics and Space Administration Structural Analysis) to perform the finite element analyses. Figure 9 illustrates the analysis procedure, and Appendix H comprises a functional flow chart and a listing of the PROSCAN program.

In exchanging information between the two computer programs, disk storage was used exclusively. All NASTRAN output was stored in punched-card format in disk files. All case control and bulk data decks were also stored on disks, and all modifications made by PROSCAN to the models were directed to those storage files.

6.2 Overstressed Elements

The first requirement in applying the AFATL method to finite element results was identifying overstressed elements. Because more than one limiting stress value was permissible, some common basis for evaluating severity of stress had to be established. The criterion selected was the margin of safety defined as

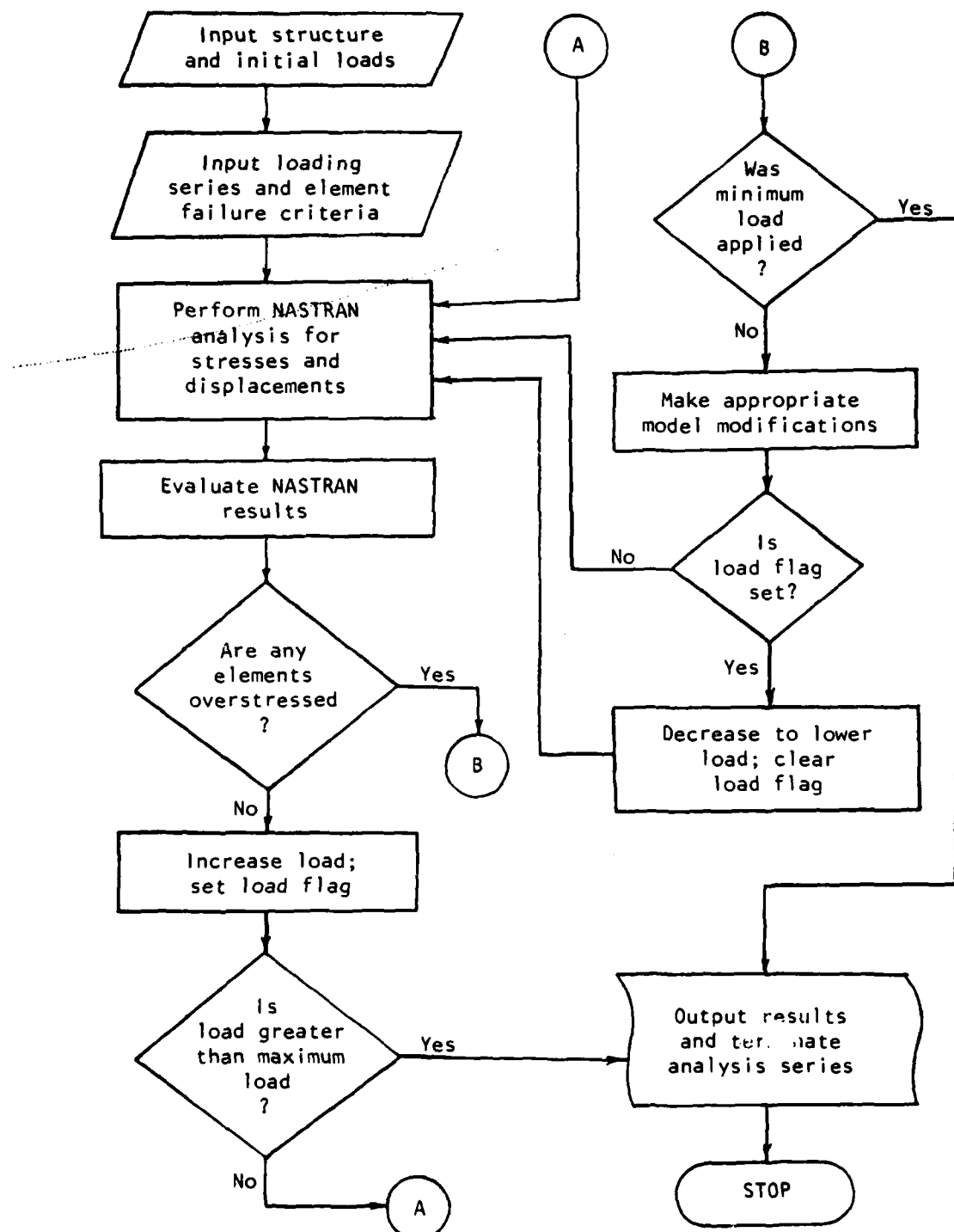


Figure 9. Iterative Analysis Procedure

$$M.S. = \frac{\text{allowable stress}}{\text{actual stress}} - 1.0 \quad (6.1)$$

Several elements within NASTRAN, rods and shear panels included, return an element margin of safety as part of the solution. For those elements which do not provide a margin of safety, PROSCAN calculated one. Element principal and maximum shear stresses were compared to analyst-provided limiting stresses for tension, compression, and shear. A margin of safety was calculated for each type of stress and the algebraically smallest value was selected as the element margin of safety. PROSCAN then identified any element with a negative margin of safety as an overstressed element.

6.3 Failed Elements

PROSCAN applied the next step of the AFATL method, grouping of overstressed elements, by node matching. The node numbers of each overstressed element were compared to those of every other overstressed element. PROSCAN designated any continuous linkage of those elements as a group, then selected the most severely stressed element from the group.

The element margin of safety again was the basis for decisions. PROSCAN selected the element of the group with the most negative margin of safety. That element became a failed element. The process of grouping and failing elements continued until all overstressed elements were considered.

PROSCAN did not actually remove a failed element from the model. Instead, PROSCAN assigned property values to the element which effectively eliminated its contribution to the structure. The failed areas and moduli of elasticity and shear were orders of magnitude below nominal values for unfailed elements.

6.4 Propagation of Damage

The failing of an element represented propagation of the damage, and as a consequence, the borders of the damage expanded. Additional elements had to be identified as bordering the new damage so they could be assigned reduced limiting stresses. Again a node matching scheme was employed. Each element which had at least one node in common with a newly failed element was examined. If it had not already failed itself or had not already bordered damage, lower limiting stresses replaced those previously used. The lowering of limiting stresses accounted for the possible presence of crack tip stress concentrations as introduced in section 2.5.

6.5 Adjustment of Load

PROSCAN had the capability of applying a new load to the model with each iteration. That capability was used in this study as explained below.

If no element failed on a particular iteration, the load was increased for the next NASTRAN analysis. This would occur until the structure sustained some maximum user-specified load without further element failure. Conversely, if an element failed on a particular iteration, PROSCAN reduced the load for the next NASTRAN analysis. The purpose was to determine the structure's ability to carry a lesser load after further weakening by the failed element. Reducing the load every time an element failed continued until the structure could not sustain a minimum load without further failure.

The analyst provided a sequence of loads to be applied, from minimum to maximum, as part of the PROSCAN input data. PROSCAN then made the

appropriate changes to the NASTRAN case control deck to reflect the structure's performance on the previous iteration. In addition to changing the load identification number, PROSCAN could assign new single point and multipoint constraint sets and identify new labels to correspond to each new load.

PROSCAN automated the entire application of the AFATL method. This began with initial viewing of NASTRAN output and finished by establishing new files containing modified case control and bulk data decks.

CHAPTER VII

DETERMINATION OF LIMITING STRESSES

7.1 Need for Limiting Stresses

Repeated reference has been made to limiting stresses. It is appropriate to address in more detail the specifics of allowable stress levels. Heard (1) used two limiting stress criteria: ultimate strength for elements away from damage, and yield strength for elements bordering damage. This study attempted to define more precisely the levels of stress which should cause failure in the model.

Ultimate strength remained the basic criterion for defining failure; but most elements, even those away from damage, were assigned limiting stresses lower than ultimate strength. Consider that a relatively large element returned a computed stress representative of a large structural region. This representative stress was unavoidably lower than the high stress within the region which would cause failure in the actual member. It was necessary then to estimate the effects of the representative stresses by using some value of limiting stress lower than ultimate strength.

Appropriate limiting stresses also estimated the nonlinear behavior experienced through the buckling of skin panels. Since the finite element analyses assumed linearly elastic behavior, the ability to compensate for skin panel buckling was incorporated to enhance results. PROSCAN had the ability to incorporate both the low stresses causing buckling and the reduced stiffnesses subsequent to buckling.

7.2 Limiting Stresses for Rod Elements

Spar and rib sections were each represented by three elements. A shear panel represented the web. One rod element represented the upper spar cap and another rod represented the lower spar cap. The rods were sized and spaced to maintain the moment of inertia about the section's neutral axis and to return outer fiber stresses.

The stress value obtained for rod elements was the average of the stresses at each end of the rod. Because rod elements in the spars were relatively long, the average stress could be substantially less than the maximum stress. A procedure to obtain limiting stresses for a similarly modeled doubly symmetric cantilevered beam served as a foundation for developing limiting stresses for the wing model. Figure 10 shows such a beam with top rod elements numbered and top nodes lettered.

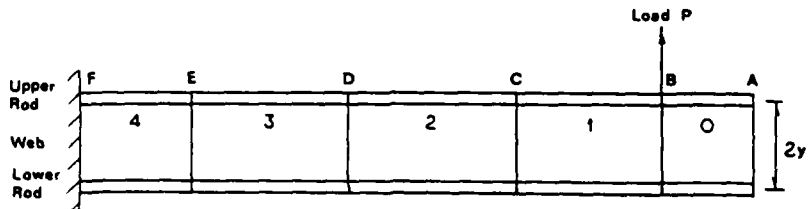


Figure 10. Cantilevered Beam Model

Using rod 3 for illustration, the maximum stress from the applied load occurred at node E, but the stress obtained was the average of

stresses at nodes D and E. Designating L_j as the length of any member j , the average stress in rod 3 was

$$\sigma_{avg} = \frac{P(L_1 + L_2 + \frac{1}{2}L_3)y}{I} \quad (7.1)$$

and the stress at node E was

$$\sigma_{max} = \frac{P(L_1 + L_2 + L_3)y}{I} \quad (7.2)$$

where I was the section moment of inertia. Designating a limiting stress factor, F_i , as the ratio of σ_{avg} to σ_{max} ,

$$F_3 = \frac{L_1 + L_2 + \frac{1}{2}L_3}{L_1 + L_2 + L_3} \quad (7.3)$$

In general terms,

$$F_i = \frac{\frac{1}{2}L_i + \sum_{j=1}^{i-1}L_j}{\sum_{j=1}^iL_j} \quad (7.4)$$

for the single point load shown. The appropriate limiting stress, σ_{L_i} , was

$$\sigma_{L_i} = F_i \sigma_{ult,i} \quad (7.5)$$

where $\sigma_{ult,i}$ was the ultimate strength for the member i .

To extend this approach for calculating stress factors to the finite element model of the wing, the wing itself was idealized as a straight cantilevered beam. The front spar dimensions were used for section lengths as shown in Figure 11. Upper surface element numbers are below each rod and corresponding node numbers are above each node.

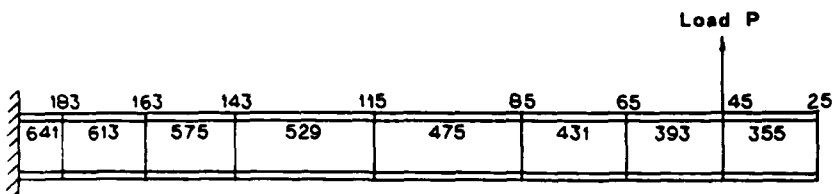


Figure 11. Cantilevered Front Spar Idealization

Factors to reduce material ultimate strength for elements inboard of the load were calculated as shown in the previous example. Elements between the load and the wing tip used the same factor as the elements immediately inboard of the load. Table II shows the limiting stress factors for the front spar rods on the upper wing surface.

TABLE II
LIMITING STRESS FACTORS FOR ROD ELEMENTS

Rod No.:	641	613	575	529	475	431	393	355
F_i :	0.950	0.937	0.921	0.855	0.788	0.735	0.500	0.500

Each rod representing a skin stiffener was approximately parallel to the spars and was assigned the same factor as its corresponding spar element. Each rib was approximately perpendicular to the spars. Each rod in a rib was assigned the factor of the spar rod immediately inboard of the spar-rib intersection.

A single concentrated load was used for analysis to correspond to the actual loading applied in the laboratory test program. However, an aerodynamic load could be represented by any approximation acceptable to the analyst. Although the mathematical expression for F_i would be more complex, the same approach to factoring for limiting stresses in rod elements could be applied.

7.3 Limiting Stresses for Web Elements

Shear panel elements represented the webs of spars and ribs. The limiting stress for shear was determined by comparing the average shearing stress in the web to the maximum shearing stress in the web. If V were designated as the shearing force in the cantilevered beam discussed in the previous section, the web element yielded a shearing stress of

$$\tau_{avg} = \frac{V}{2yt} \quad (7.6)$$

where t was the web thickness. The maximum shearing stress in the section was

$$\tau_{max} = \frac{VQ}{It} \quad (7.7)$$

The limiting stress factor, F , was the value of τ_{avg} divided by τ_{max} , so the limiting shearing stress, τ_L , was

$$\tau_L = F \tau_{ult} . \quad (7.8)$$

Calculations for typical spar cross sections showed $F = 0.85$ to be a representative value. This value was applied to all spar and rib web elements.

Proportions of spar and rib sections indicated web crippling was unlikely; therefore, no reductions in limiting stresses were developed for buckling of undamaged web members. If initial damage to the structure introduced a potential for buckling, residual member proportions dictated the appropriate reductions.

7.4 Limiting Stresses for Skin Elements

Skin panels, unlike spar and rib webs, were susceptible to buckling. Additionally, the skin could tear along rivet lines or rivets themselves could fail. Whether a panel buckled in shear or in compression, or failed along a rivet line, the result was a reduction in stiffness of the panel. Because of the similar change in behavior, panels were divided into either pre-buckling or post-buckling categories even though rivet line failure was not a buckling phenomenon.

Each skin panel on the wing had slightly different geometric properties which gave each slightly different pre- and post-buckling characteristics. Panel 106, forward of the front spar on the lower wing surface, was typical of most skin panels and was used to determine approximate values for all panels. Figure 12 shows its location in the model. The assembly used for calculations included panel 106, a stiffener attached to each long side, and a rib attached to each short side. Averaging the lengths of the two long sides and the two short sides gave a rectangular shape for calculations.

To determine pre-buckling limits, compression perpendicular to the long sides, compression perpendicular to the short sides, and a corner force producing shear were all evaluated separately. Calculations were determined according to Peery (34, Chapters 14 and 15). The average

stress causing buckling in each case was divided by the material ultimate strength to determine the limiting stress factors, F. For the two compression conditions, the more conservative value was used.

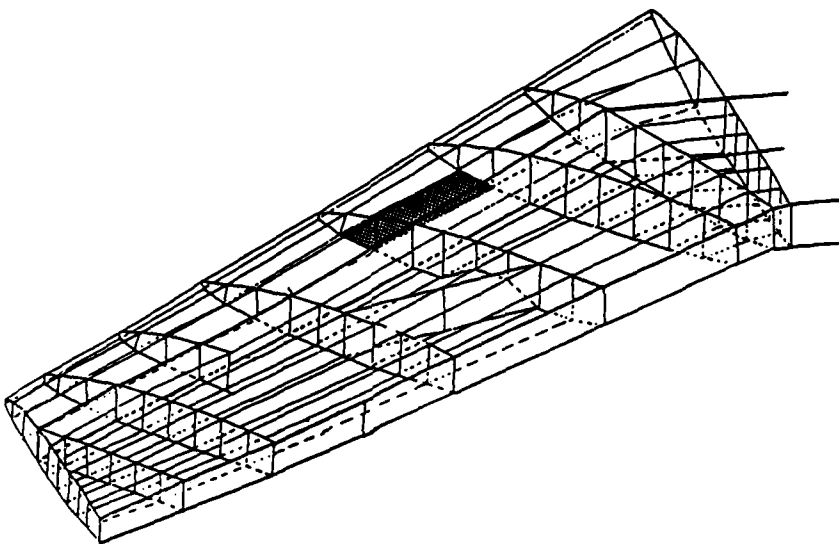


Figure 12. Typical Panel for Buckling Limits

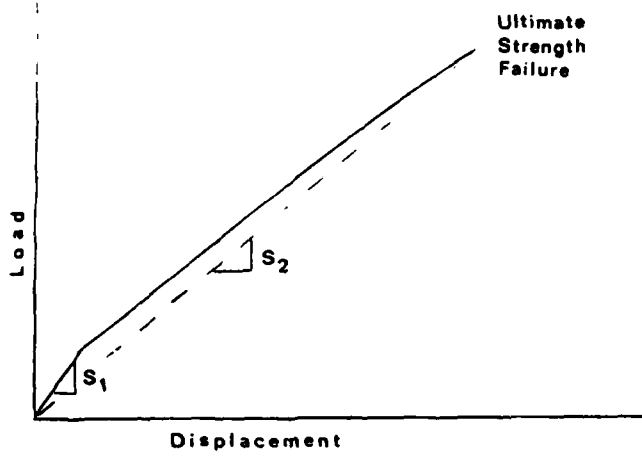
Limits for tension were obtained by calculating rivet and skin strengths along a conservative rivet line. Limiting loads, determined according to Peery (34, Chapter 12) and Bruhn (35, Chapter D1), were divided by the ultimate load, the load causing an average stress in the panel equal to the ultimate strength. The result was the limiting stress factor. Skin failure was compared to rivet failure, and the more conservative value was used.

For post-buckling behavior, the limiting stresses were returned to ultimate strength, but the elastic and shear moduli were reduced to

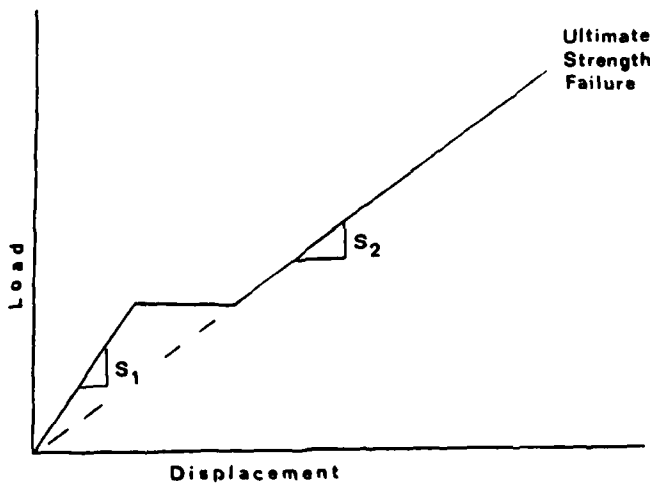
account for the reduction in stiffness following buckling. For compression buckling, bilinear behavior was assumed. The load versus displacement curve of Figure 13a assumed linear behavior prior to buckling, then linear behavior from buckling to an ultimate strength failure. The slope of the pre-buckling portion of the curve, S_1 , was divided into a secant slope, S_2 , from the origin to failure. The result was a reduction factor, M, for the elastic modulus. The same process applied to Figure 13b produced a reduction factor for the modulus of shear. Table III summarizes the results for skin buckling.

TABLE III
LIMITING FACTORS FOR SKIN ELEMENTS

Behavior	Stress Factor F	Modulus Factor M
Compression, Pre-buckling	0.17	1.00
Shear, Pre-buckling	0.32	1.00
Tension, Pre-buckling	0.55	1.00
Compression, Post-buckling	1.00	0.76
Shear, Post-buckling	1.00	0.53
Tension, Post-buckling	1.00	0.76



(a) Compression



(b) Shear

Figure 13. Load-Displacement Curves
for Panel Buckling

Although the assumption of linear behavior from buckling to ultimate failure was not correct, it was a conservative representation of the rather brittle material behavior observed in the laboratory. The result economically approximated the loss in stiffness suffered by the structure from skin buckling and rivet line failure.

7.5 Damage Propagation

No attempt was made to model ragged edges around initial damage nor to reduce element size in areas of propagating cracks. The large elements then tended to mask the stress concentrations around cracks and produced a model significantly more resistant to progressive collapse than the structure being represented.

Conventionally, the nominal stress in a cracked member would have been multiplied by a stress concentration factor, K. Its value would have been larger than 1.0 and based upon crack length and crack tip severity. The increased value for stress at the crack tip would then have been compared to an allowable stress for the member. PROSCAN used an inverse approach. Rather than increase the nominal stress returned by an element, the allowable stress was decreased by a factor F, where F essentially was the inverse of K. This further reduction of limiting stresses compensated for the absence of increased modeling detail around damage.

Any cracks occurring were assumed to originate at the initial damage or in subsequently failed elements. The further reductions in limiting stresses applied therefore only to unfailed elements bordering either initial damage or failed elements.

Separate reduction factors were determined for tension and for shear. Because cracks were assumed not to propagate in compression, no further

reduction applied to limiting compressive stresses. This portion of the investigation was patterned after similar crack propagation studies by Sih and Hartranft (28).

Two square plate models, one loaded in tension and the other in shear, provided information for reduction factors. Model detail ranged from two elements along a side to thirty-two elements along a side.

A crack initiated at the center of one edge propagated through the plate during sequential analyses. Loads remained constant through all iterations. Crack propagation was represented by creating a new node beside the tip of the crack, thus extending the crack to the next node. Figure 14 illustrates the procedure, exaggerated in scale, on a model using four elements per side. Figure 14b shows node m at the tip of the crack. The creation of node z extended the crack tip to node n in Figure 14c.

Figure 14b shows the plate cracked one-quarter of the way through its width. Stresses in the four elements connected to the node at the crack tip, those indicated by X's, were averaged and then divided into the average stress in the uncracked plate. The result was the limiting stress factor for the plate cracked through one-quarter of its width. The same procedure applied to the plate in Figure 14c produced the factor for the plate cracked halfway through its width. Figure 15 shows variation of the factor as a function of model detail and crack length. F_T represents tension loading and F_S represents shear loading.

All curves in Figure 15 appeared to approach zero slope as element size reduced. The values of F_T and F_S selected for this study were for a plate cracked one-eighth of the way through its width in a model with 32 elements along a side. For most components of the F-84F wing, this

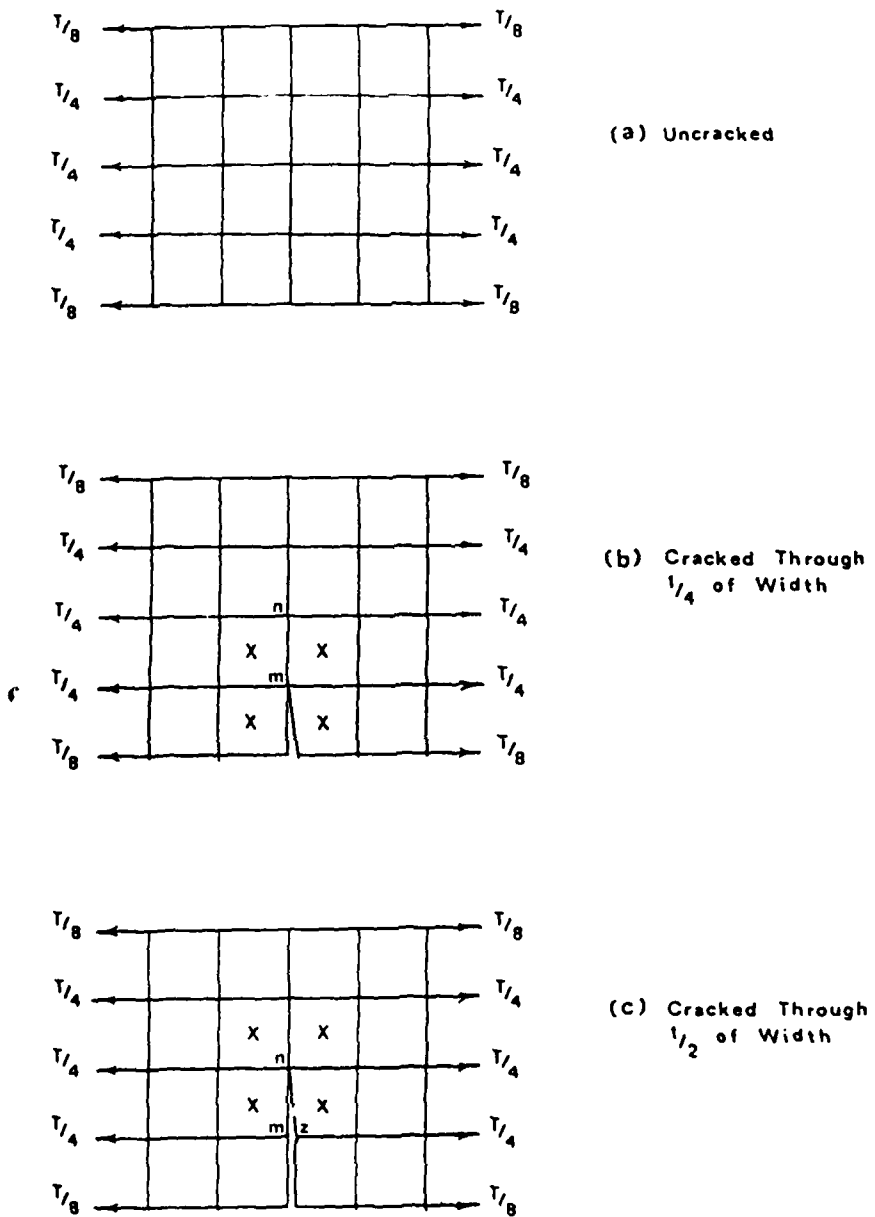
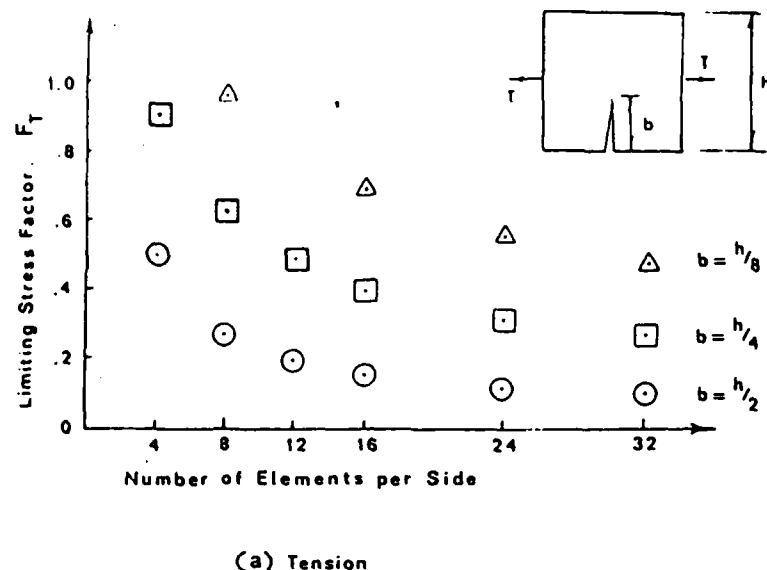
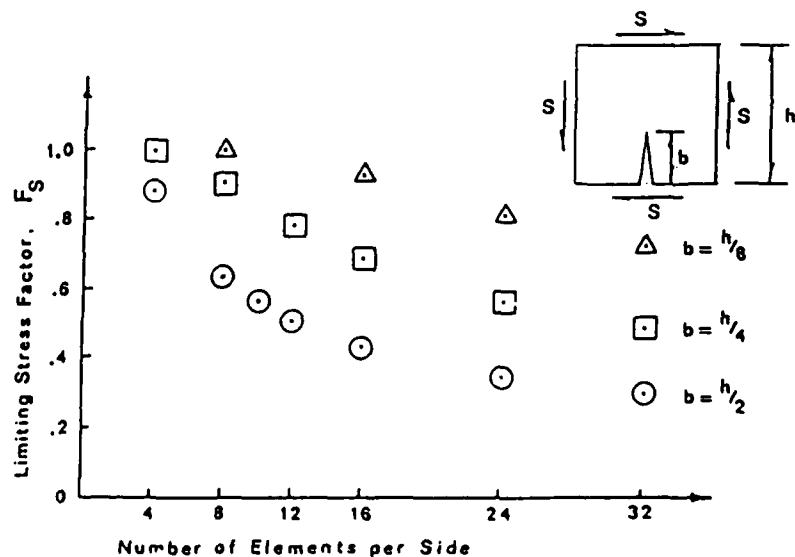


Figure 14. Crack Investigation Models



(a) Tension



(b) Shear

Figure 15. Propagation Stress Factor Curves

represented a crack less than one inch in length in the longer side of the component. The corresponding stress concentration factor was $K = 2.1$. For skin panel 106, it represented a crack 0.725 inches long with a crack tip radius of 0.30 inches calculated according to Seely and Smith (36, Chapter 12). Thus the assumed crack around damage was relatively mild and was therefore conservative.

New limiting stresses for an element bordering damage were the product of the appropriate factor, F_T or F_S or $F_C = 1.0$ for compression, and the element's previous limiting stresses. Limiting stress factors were, in this manner, cumulative. The exception was unbuckled skin panels. Their limiting stresses were not reduced to reflect cracks until after buckling stresses were exceeded.

CHAPTER VIII

COMPARISON OF RESULTS

8.1 General

Damage and load conditions for Tests 2C and 3B were analyzed using all four models for each test. Measured rotations of wing spar roots from laboratory data were enforced in the analyses. Examination of those analyses showed the addition of torsional rod elements to the spars made little difference in results. The performance of Model B was very similar to that of Model A, and the results from Model D were almost identical to those from Model C. Apparent reasons for the similarities are presented in the next section.

Further examination of the analytical results revealed unexpected stress distributions in and near the wing spar roots. The enforced rotations of wing spar roots, although developed from experimental measurements, did not produce purely rigid body motions for reasons explained in section 8.6. Consequently, the original analytical representations did not match closely enough the laboratory conditions of the experimental test program.

A second set of analyses was performed using zero support rotations for stress determination and enforced rotations for checking displacements. Tests 2C and 3B were analyzed using Models A and C for each test. Model C described the collapse phenomenon more closely than Model A as explained in section 8.4. Therefore, Model C was next compared to Model

D, the same model with the addition of torsional rod elements. The lack of significant difference between Models C and D confirmed the minimal influence of the torsional rod elements. Model B, therefore, was not analyzed further because it would produce essentially the same results as Model A. Even though torsional rod elements were not significantly affecting results, Model D was selected for the comparison of initial damage modeling since its torsional capability could provide greater latitude for an analyst to adjust model stiffness.

Model D was used to evaluate the two approaches to modeling damage for Test 1 described in section 5.3. The simpler method of modeling portrayed more accurately the pattern of failure as explained in section 8.5. The simpler method of modeling the damage was then applied to Model A for a final analysis of Test 1.

8.2 Comparison of Failure Loads

A close correlation of analytically predicted failure loads with experimentally measured failure loads would be a desirable result of evaluating the AFATL method. Table IV summarizes the failure load results. The models ranged from 5 percent to 85 percent stronger than the actual structure. Note that for Test 2 no experimental failure load was determined; therefore, conclusions about Test 2 are judgmental.

Model A gave the closest approximation for Test 3 and may have given a close approximation for Test 2. However, for reasons discussed in section 8.4, Model A was not considered the best model. Model D was more conservative than Model A in estimating wing strength. Although Model D's predicted strength for Test 2 was clearly less conservative than for Test 3, the results may have been acceptably consistent. Both approaches

for modeling Test 1 damage gave excessive predicted strengths; however, section 8.5 discusses how those figures might be improved.

TABLE IV
SUMMARY OF FAILURE LOADS

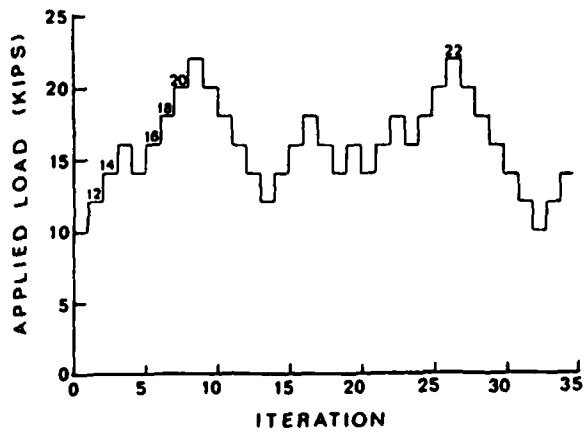
Test	Failure Loads (kips)			
	Laboratory	Model A	Model C	Model D
1	12.0	22	---	22
2	15.0*	18	20	20
3	12.4	13	19	19

* Largest load applied; no failure load determined.

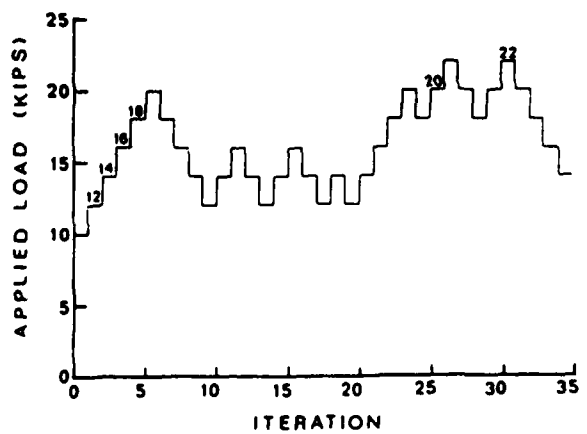
Models C and D showed no differences in failure loads and very little difference in the sequences of element failure. There are two apparent reasons for the similarity. The first is that the torsional capacities of the spars were probably underestimated when the torsional rod elements were sized. Second, bending was the dominant behavior of the F-84F wing even under extreme conditions such as those of Test 2.

8.3 Load-Iteration History

The AFATL method, as applied by PROSCAN, caused loads to vary from iteration to iteration. Figure 16 depicts the variation of load with respect to iteration for the first 35 cycles for Models A and D. The analytical data for any given load level were taken from the last cycle in which that load was applied before the model experienced a higher load. For

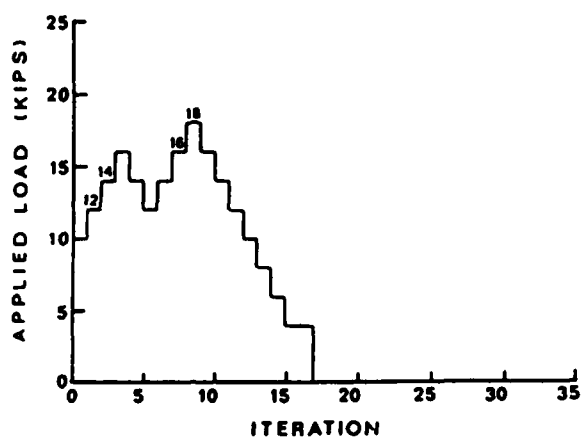


(a) Test 1, Model D (with torsional stiffness rods), Simple

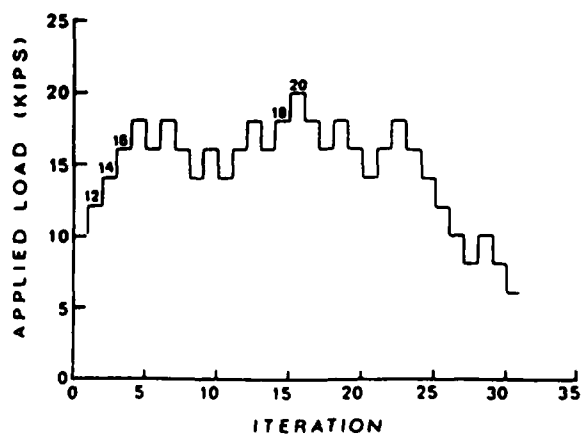


(b) Test 1, Model D (with torsional stiffness rods), Detailed

Figure 16. Load-Iteration Histories

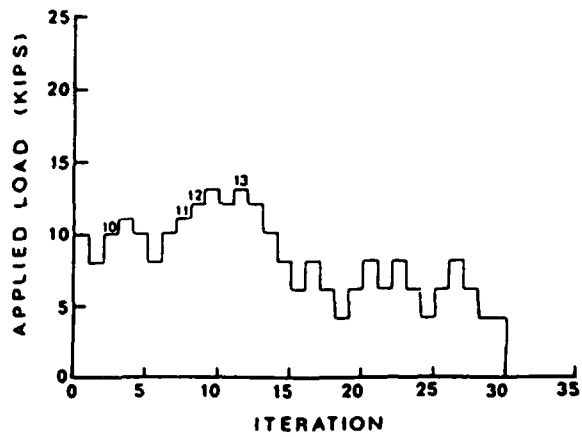


(c) Test 2C, Model A (without torsional stiffness rods)

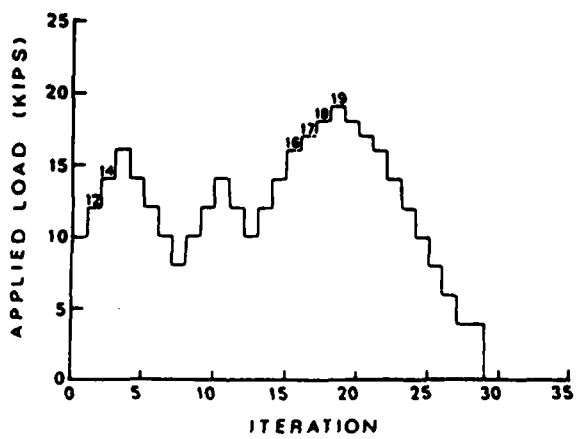


(d) Test 2C, Model D (with torsional stiffness rods)

Figure 16. (Continued)



(e) Test 3B. Model A (without torsional stiffness rods)



(f) Test 3B. Model D (with torsional stiffness rods)

Figure 16. (Continued)

example, the analytical data for the Model A analysis of Test 2C at 16 kips applied load came from iteration No. 8. As shown in Figure 16c, that was not the first application of a 16-kip load, but it was the last iteration before a higher load, 18 kips, was applied.

That procedure for selecting which iterations to use for data comparison occasionally led to gaps of several iterations between successive data-producing loads. Again as an example, Figure 16f shows 13 iterations elapsed between the 14-kip and 16-kip loads for the Model D analysis of Test 3B. During those cycles, six elements failed. This characteristic of the procedure accounted for the occasional sharp discontinuities in the plots of data.

Figure 16 also emphasizes the need for caution in setting the minimum load to be investigated. PROSCAN permitted the load to drop considerably during a series of element failures, then again rise to a high level. Figure 16a shows how the load dropped from 22 kips down to 12 kips before again climbing back up to 22 kips. Making the minimum allowable load too large could result in a premature indication of structural failure. It could occur during such a series of element failures when, in fact, the structure still possessed the capacity for loads well above the minimum level.

8.4 Internal Load Paths

The most demanding test of the models was how realistically they transferred the loads internally through the wing structure and into the supports. Figure 26 (Appendix 1) compares the vertical support reactions for experimental and analytical results. Figures 27 through 29 (also

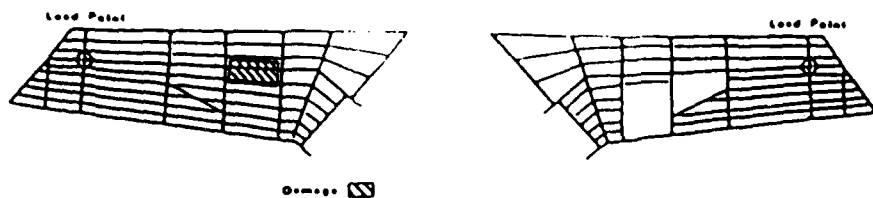
Appendix I) compare variations of strain at representative points on the wing with respect to applied load.

Examination of Figure 26 through 29 showed that neither Model A nor Model D transferred the load from the loaded spar to the unloaded spar as quickly as the actual wing did. Additionally, neither model transferred as much of the load from spar to spar as the wing did.

The most important indication for this study of how realistically the models transferred the loads internally came from Figures 17 through 19. They depict the buckled and failed elements in Models A, C, and D at their respective failure loads. For Test 3B, Figure 19, Model A did not indicate the nature of the failure as observed in the experimental test program; however, Models C and D did match closely the laboratory observations. For Test 2C, Figure 18, no failure occurred in the experimental program, but Models C and D predicted a plausible failure. Model A, however, predicted failure of the front spar at one of its strongest sections. For Test 1, Figure 17, Model D matched the laboratory failure pattern very closely using the simple modeling of initial damage. Model A, however, indicated failure of the undamaged rear spar. All models indicated more overstressing of skin elements near the wing spar roots than was observed on the actual wing. A complete summary of results for the first 35 iterations of the principal series is presented in Appendix J.

8.5 Comparison of Damage Modeling

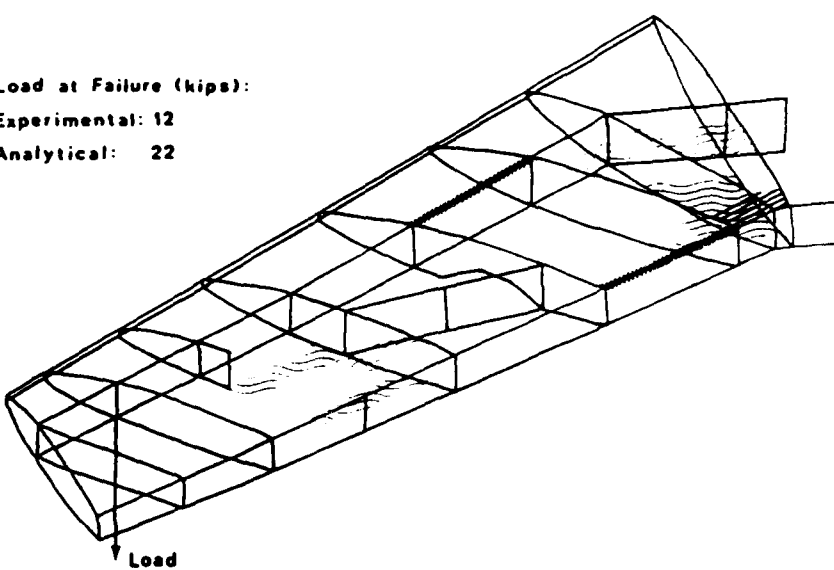
Section 5.3 introduced two approaches for modeling Test 1 damage. Both approaches predicted the same failure load, but Figure 17 illustrates that there were significant differences in which elements failed.



Load at Failure (kips):

Experimental: 12

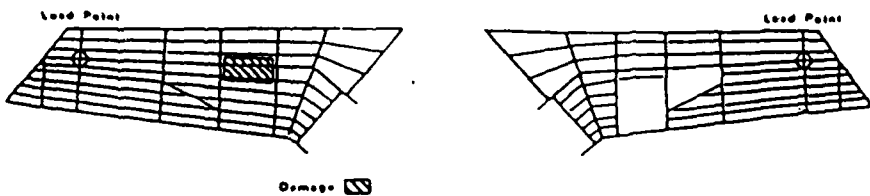
Analytical: 22



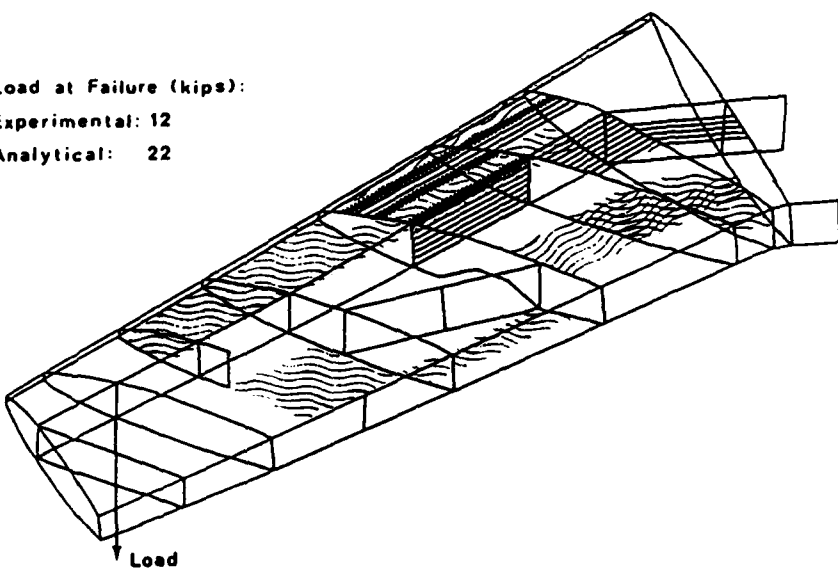
- Buckled Shear Panel Elements on Lower Surface and Leading Edge
- Buckled Shear Panel Elements on Upper Surface
- Failed Shear Panel Elements
- Failed Rod Elements

(a) Model A (without torsional stiffness rods). Simple

Figure 17. Wing Model Results at Test 1 Failure



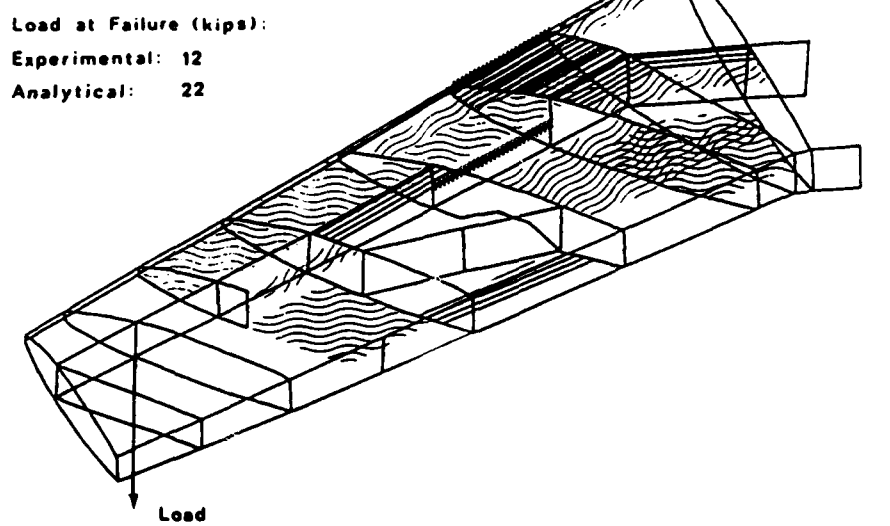
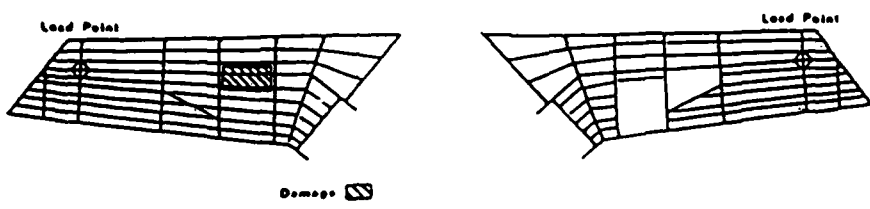
Load at Failure (kips):
Experimental: 12
Analytical: 22



-  Buckled Membrane Elements on Lower Surface and Leading Edge
-  Buckled Membrane Elements on Upper Surface
-  Failed Membrane Elements and Vertical Shear Panel Element
-  Failed Rod Elements

(b) Model D (with torsional stiffness rods). Simple

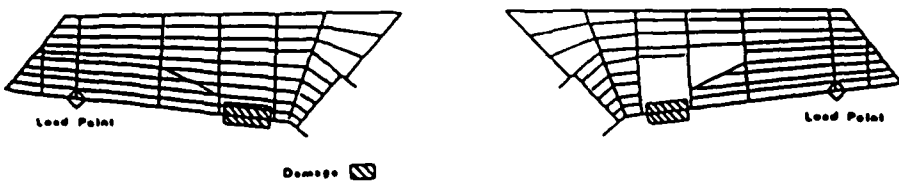
Figure 17. (Continued)



- [Wavy Line Pattern] Buckled Membrane Elements on Lower Surface and Leading Edge
- [Horizontal Line Pattern] Buckled Membrane Elements on Upper Surface
- [Solid Black Pattern] Failed Membrane Elements and Vertical Shear Panel Element
- [Solid Black Line] Failed Rod Elements

(c) Model D (with torsional stiffness rods). Detailed

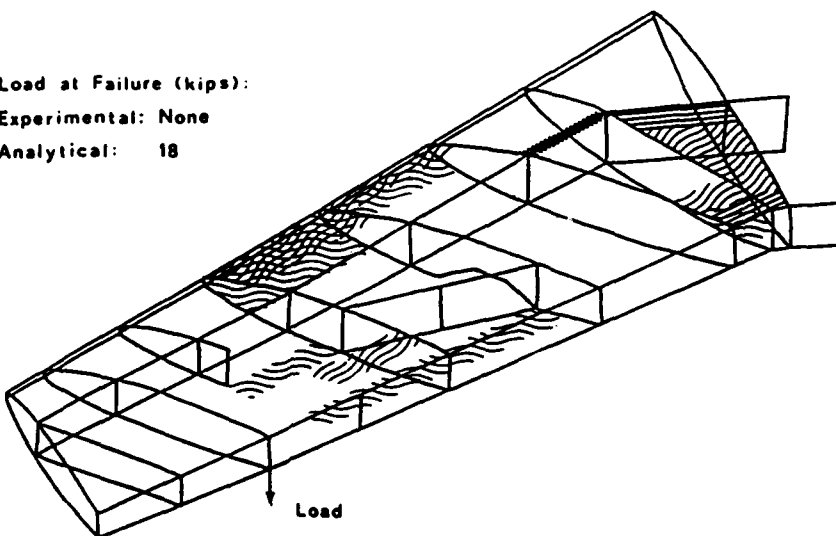
Figure 17. (Continued)



Load at Failure (kips):

Experimental: None

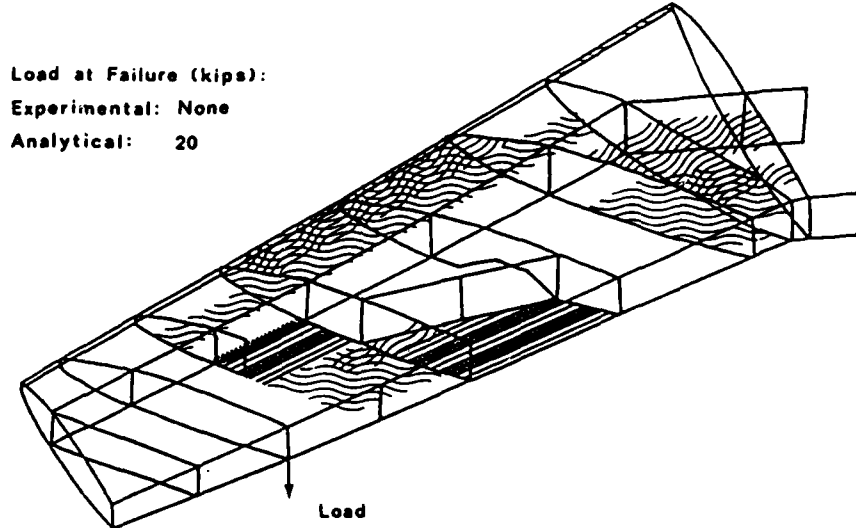
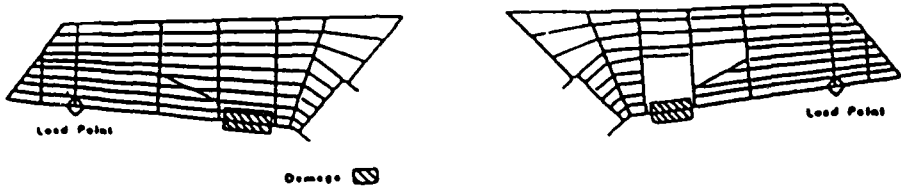
Analytical: 18



- Buckled Shear Panel Elements on Lower Surface and Leading Edge
- Buckled Shear Panel Elements on Upper Surface
- Failed Shear Panel Elements
- Failed Rod Elements

(a) Model A (without torsional stiffness rods)

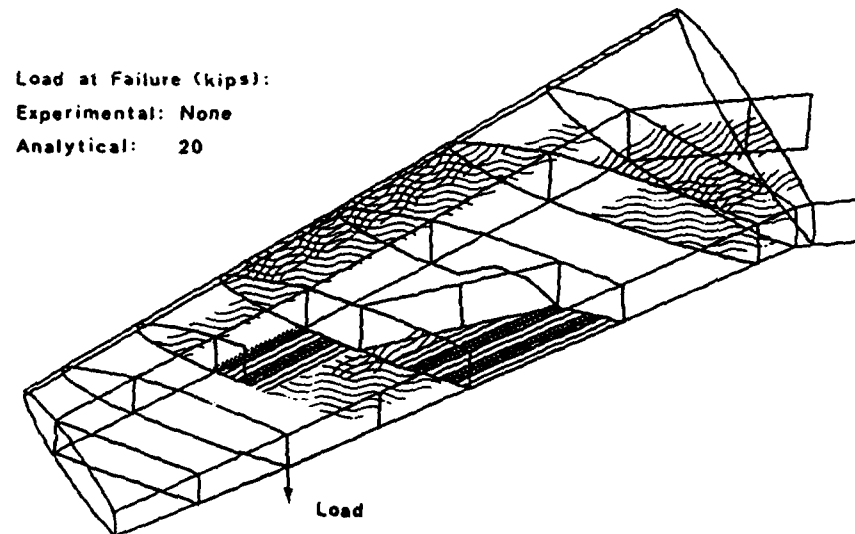
Figure 18. Wing Model Results at Test 2C Failure



- Buckled Membrane Elements on Lower Surface and Leading Edge
- Buckled Membrane Elements on Upper Surface
- Failed Membrane Elements
- Failed Rod Elements

(b) Model C (without torsional stiffness rods)

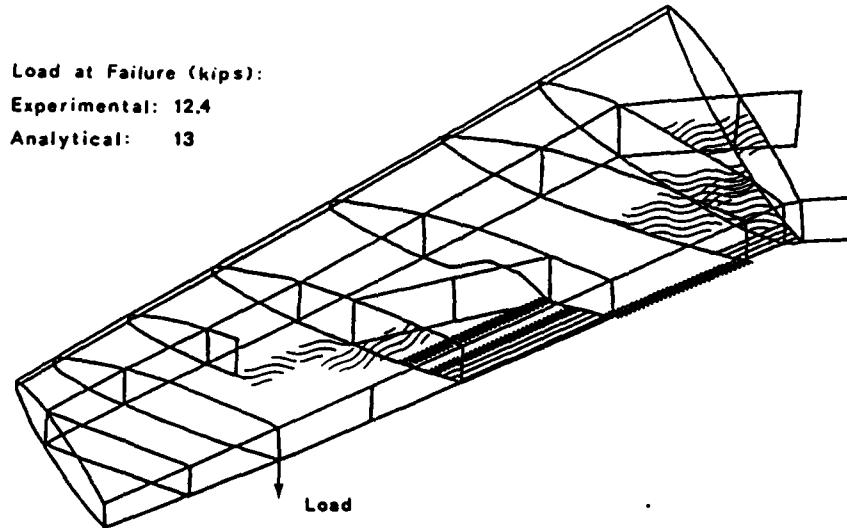
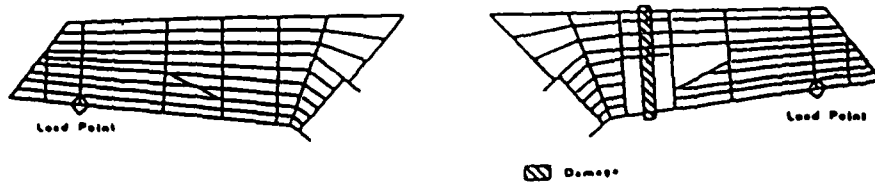
Figure 18. (Continued)



- Buckled Membrane Elements on Lower Surface and Leading Edge
- Buckled Membrane Elements on Upper Surface
- Failed Membrane Elements
- Failed Rod Elements

(c) Model D (with torsional stiffness rods)

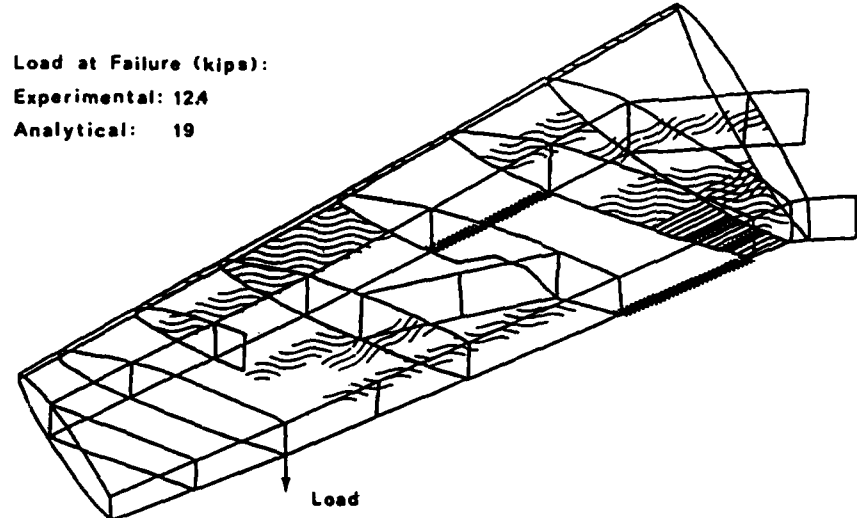
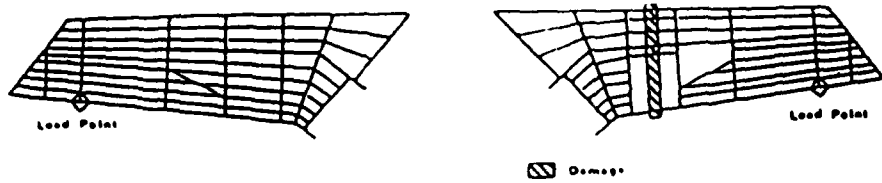
Figure 18. (Continued)



- Buckled Shear Panel Elements on Lower Surface and Leading Edge
- Buckled Shear Panel Elements on Upper Surface
- Failed Shear Panel Elements
- Failed Rod Elements

(a) Model A (without torsional stiffness rods)

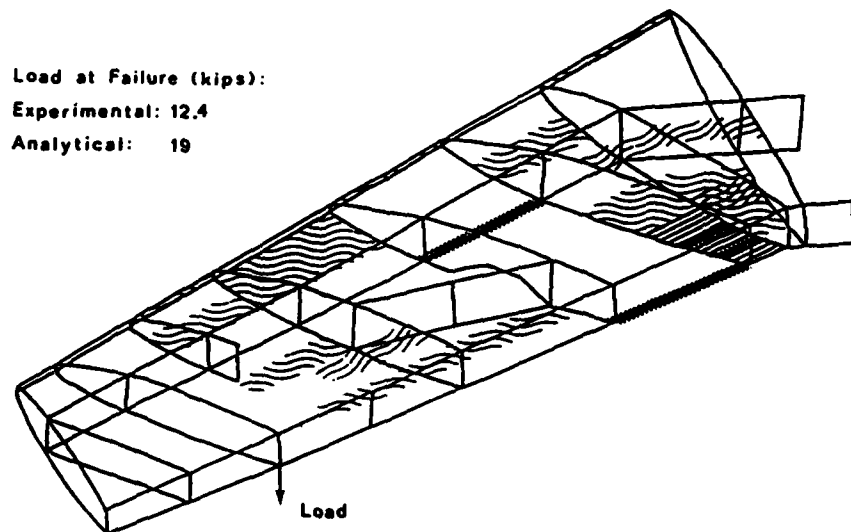
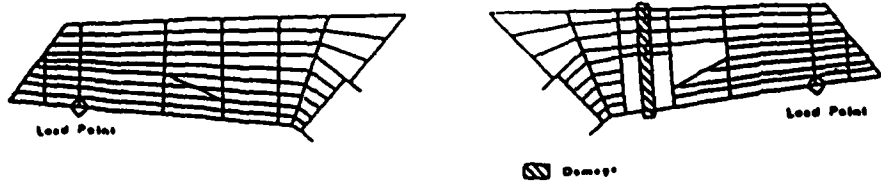
Figure 19. Wing Model Results at Test 3B Failure



- [Wavy Line Pattern] Buckled Membrane Elements on Lower Surface and Leading Edge
- [Solid Black Pattern] Buckled Membrane Elements on Upper Surface
- [Solid Black Bar] Failed Membrane Elements
- [Solid Black Line] Failed Rod Elements

(b) Model C (without torsional stiffness rods)

Figure 19. (Continued)



- Buckled Membrane Elements on Lower Surface and Leading Edge
- Buckled Membrane Elements on Upper Surface
- Failed Membrane Elements
- Failed Rod Elements

(c) Model D (with torsional stiffness rods)

Figure 19. (Continued)

Of the two approaches using Model D, the simpler approach depicted more accurately the failure as observed in the laboratory. The simple approach applied to Model A did not produce an accurate failure pattern; however, all tests indicated that Model A was less suitable for predicting the pattern of failure.

Although the Model D results suggested a preference for the simpler technique, caution is advised before reaching a firm conclusion. In all models for all tests, the webs of spars and ribs were represented by shear panels. Consequently, the front spar in Test 1 could not fail at the damage until shear limits were exceeded. The experimental program showed the damaged front spar web in Test 1 failed in bending tension, a failure mode the shear panel could not predict. For cases of initial damage where all or most of a spar cap or rib cap would be removed, the web should probably be modeled by a membrane element. Although the membrane element would be stiffer than the shear panel, it would be directly sensitive to limiting tensile and compressive stresses as well as to shear limits. Such a recommendation applied to this study may have appreciably reduced the predicted failure load for Test 1, and it may have altered the apparent value of simple modeling over the more detailed representation.

8.6 Rotation of Wing Spar Roots

Specific values of displacement were of interest in this study as an additional means of comparing analytical results to laboratory data. To obtain more accurate displacement values from the analytical method, rotations of wing spar roots were measured in the experimental test program and enforced in the analytical models. However, for most applications of

the AFATL method, rotations at structure supports would not be known. Additionally, the precise displacements of the structure probably would be unimportant. The displaced shape of the structure, which might be used to modify loading for each iteration, was available from the analyses using zero support rotations.

The enforced rotations were derived from experimental data. In translating laboratory measurements into single point constraints for NASTRAN, an assumption was made. It was assumed that the center of rotation for each spar was the point midway between the two pins securing the spar in its support structure. In fact, any point between those two pins could have been the center of rotation, and the center could have changed as loading progressed. The assumption almost certainly contributed to the introduction of erroneous stresses into the models during the first set of analyses.

Another likely contributor to those stresses was the manner in which some of the multipoint constraint equations for the models were written. A spar root was modeled by a shear panel and two rod elements, a configuration that gave the desired resistance to bending but provided no lateral restraint. The necessary lateral restraint was provided by multipoint constraints to keep each root section in line with its adjacent spar section.

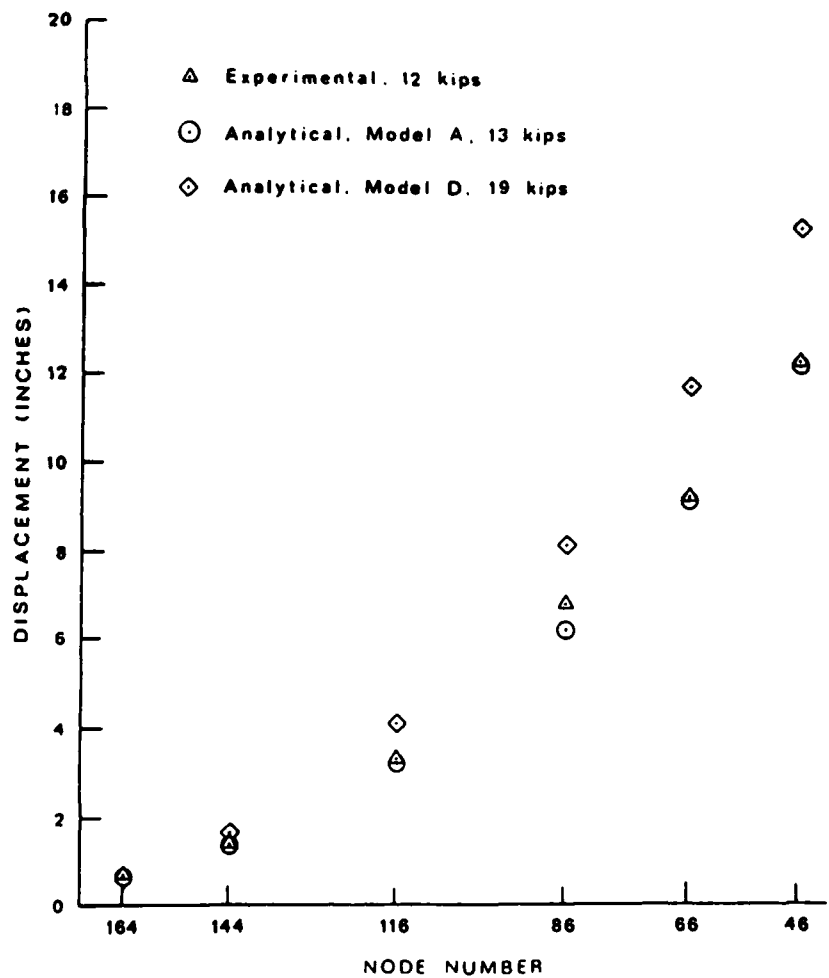
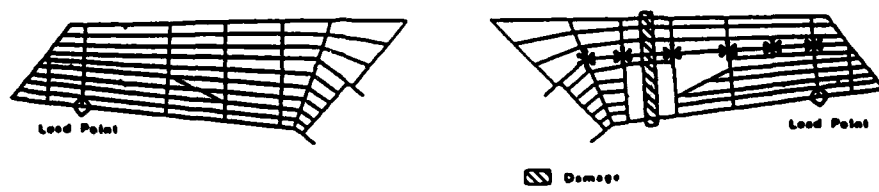
The multipoint constraint equations for the original model were formulated not in a general manner, but with an implied assumption that there was no displacement of the wing spar root nodes. Thus any attempt to enforce the measured rotations violated that assumption. The result was erroneous stresses near the base of the wing.

Of the two sources of error identified, the multipoint constraint equations could be easily corrected. The problem of precisely measuring wing spar root rotations cannot be solved without sophisticated measuring equipment. The benefits gained from precise measurements, however, would not begin to justify the added expense for normal applications of the method.

8.7 Deflections

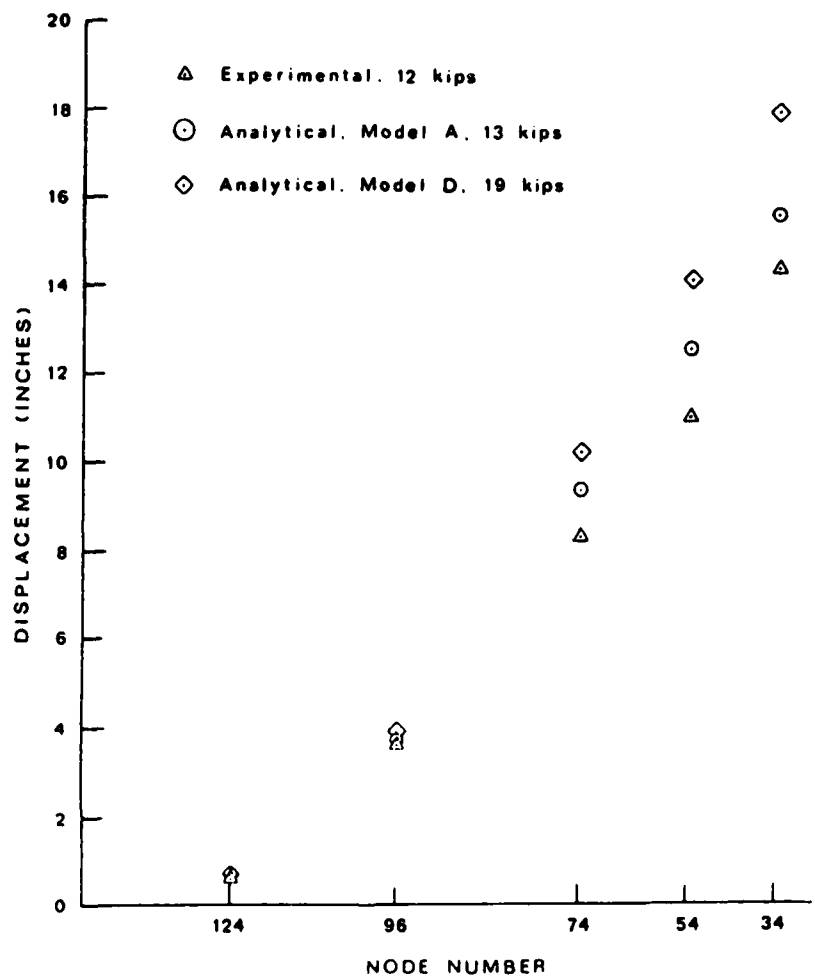
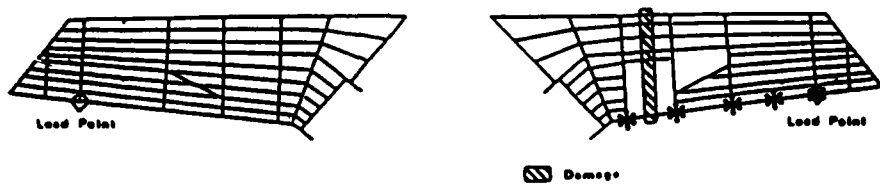
Deflections were measured in the experimental test program and were compared to analytical results. Figures 30 through 32 (Appendix I) present single-point deflection data for Models A, C, and D, and for the test program. Although Model D was selected as the best model because of its ability to predict the failure most realistically, Model A was superior for predicting displacement values. For general deflected shape, however, there was little difference between Models A and D. Figure 20 compares Test 3B profiles of the front and rear spars for Models A and D, and for the actual wing at their respective failure loads. Both models presented essentially the same deflected shape which differed only slightly from measured results.

As mentioned in the previous section, deflections are not envisioned as a critical factor in the routine application of the AFATL method. Even if deflected shape were important, Models A and D both returned approximately the same results. If specific values of displacement were to become the overriding concern in a specialized application, Model A would appear to be the better model. Otherwise, Model D provided reasonable accuracy for deflected shape.



(a) Front Spar Profile

Figure 20. Failure Load Profiles for Test 3B



(b) Rear Spar Profile

Figure 20. (Continued)

CHAPTER IX

SUMMARY AND CONCLUSIONS

The principal goal of this study was to evaluate the suitability of the AFATL method for predicting progressive collapse in complex structures. Suitability was to be investigated by determining supportable limiting stress values, selecting a good combination of finite elements for modeling, and comparing analytical to experimental results.

Limiting stresses used in this study were a direct application of classical theory. Consequently, any skilled analyst could apply the concepts to any structure. A conscious effort was made to found the work in commonly known principals of materials behavior and to avoid the structure-dependency associated with empirical formulations.

All models evaluated used axial rod and shear panel element combinations to represent spars and ribs. Model D used membrane elements to model aircraft skin and rod elements to model skin stiffeners. Additionally, it had torsional rod elements along the spar centerlines. Model A used shear panels and thickened rod elements to represent aircraft skin and skin stiffeners. Model A had no torsional rod elements.

Models A and D both overestimated the residual strength of the damaged structures. For the purposes of this study, those results were conservative. A deficiency observed in the study was the lack of consistency in the degree to which residual strength was overestimated. However, all estimates were within a factor of two of the experimental results.

Model A provided better deflection estimates than Model D. Using shear panel elements for the aircraft skin made Model A more difficult to prepare than the models using membrane elements. As explained in Appendix C, the use of shear panel elements required additional calculations for modifying rod element sizes to represent the membrane capacity of the skin. However, once Model A was developed, it was less expensive to use than models with membrane skin elements. For applications where structure displacements are of primary concern, Model A would provide better results.

Model D described more accurately the actual pattern of failure leading to structural collapse. Using membrane elements for the aircraft skin made Model D a simpler model to prepare as described in Appendix C. The membrane elements also gave a better qualitative representation of skin panel behavior. For applications where the failure pattern is of principal interest, Model D would provide better results.

PROSCAN was developed as a convenience to automate the application of the AFATL method. It proved to be more of a necessity than a convenience in processing the volumes of data generated by many iterative finite element analyses. Additionally, it provided flexibility in the selection of loading sequences and in the application of limiting stresses for elements.

The combination of automation, modeling techniques, and limiting stresses applied to the AFATL method produced a useful estimating tool for predicting progressive collapse in complex structures such as the F-84F aircraft wing. The F-84F wing is a semi-monocoque structure with a heavy two-spar skeletal frame. To further evaluate the versatility of

the method, it should also be tested using other types of structures such as different aircraft designs and components or building structures.

BIBLIOGRAPHY

- (1) Compendium of Methodologies for Assessing Aircraft Structural Damage From Multiple Fragment Impacts. 61 JTCG/ME-76-16. Joint Technical Coordinating Group for Munitions Effectiveness, Aerial Target Vulnerability, Eglin AFB, Fla., Jan. 11, 1977.
- (2) Somes, Norman F. "Progressive Collapse Risk." Proceedings, International Conference on Planning and Design of Tall Buildings. Lehigh Univ., Bethlehem, Pa., Aug., 1972, pp. 21-26.
- (3) Somes, Norman F. Abnormal Loading on Buildings and Progressive Collapse. Washington, D.C.: National Bureau of Standards, May, 1973.
- (4) Leyendecker, E. V., J. E. Breen, N. F. Somes, and M. Swatla. Abnormal Loading on Buildings and Progressive Collapse. An Annotated Bibliography. Washington, D.C.: National Bureau of Standards, Jan., 1976.
- (5) Leyendecker, E. V., V. Edgar, and Eric F. P. Burnett. The Incidence of Abnormal Loading in Residential Buildings. Washington, D.C.: National Bureau of Standards, Dec., 1976.
- (6) Woodcock, A. E. R. "Catastrophic Theory: Predicting the Unpredictable." Machine Design, Vol. 9, No. 3 (Feb. 10, 1977), pp. 86-91.
- (7) Leyendecker, E. V., and B. R. Ellingwood. Design Methods for Reducing the Risk of Progressive Collapse in Buildings. Washington, D.C.: National Bureau of Standards, Apr., 1977.
- (8) Sfintesco, Duiliu. Tall Building Criteria and Loading. New York: American Society of Civil Engineers, 1980.
- (9) Regan, P. E. "Catenary Action in Damaged Concrete Structures." Industry in Concrete Building Construction. Detroit: American Concrete Institute, 1975.
- (10) Fintel, Mark, and Donald M. Schultz. "Philosophy for Structural Integrity of Large Panel Buildings." Journal of Prestressed Concrete Institute, Vol. 21, No. 3 (May-June, 1976), pp. 46-69.
- (11) Ellingwood, B., and E. V. Leyendecker. "Approaches for Design Against Progressive Collapse." Journal of the Structural Division, ASCE, Vol. 104, No. 3 (Mar., 1978), pp. 413-423.

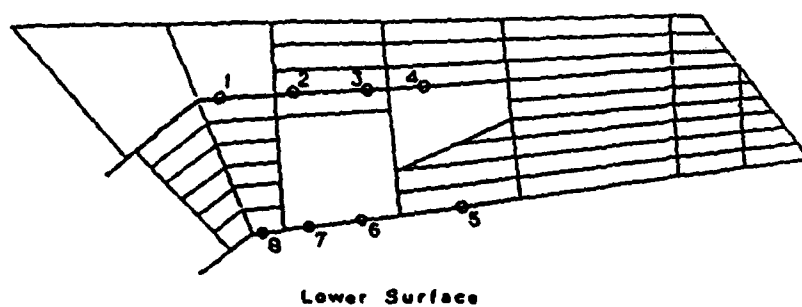
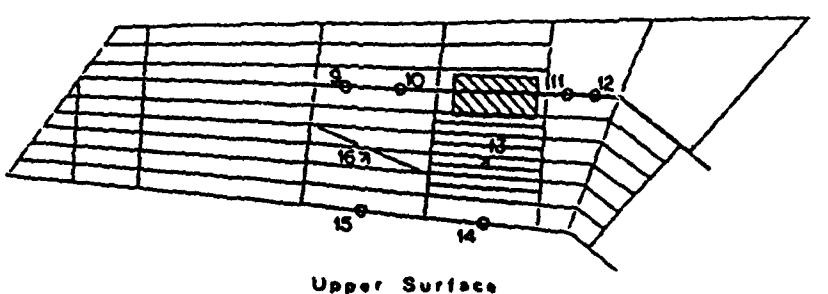
- (12) Muskivitch, John C., and Harry G. Harris. Behavior of Precast Concrete Large Panel Buildings Under Simulated Progressive Collapse Conditions. Washington, D.C.: Dept. of Housing and Urban Development, Jan., 1979.
- (13) Fintel, Mark, and Donald M. Schultz. "Structural Integrity of Large Panel Buildings," Journal of the American Concrete Institute, Vol. 76, No. 5 (May, 1979), pp. 583-620.
- (14) Girhammar, Ulf Arne. Behavior of Bolted Beam-Column Connections Under Catenary Action in Damaged Steel Structures. Stockholm, Sweden: Swedish Council for Building Research, 1980.
- (15) Ferahian, R. H. "Buildings. Design for Prevention of Progressive Collapse." Civil Engineer, Vol. 42, No. 2 (Feb., 1972), pp. 66-69.
- (16) Pinkham, C. et al. Building Practices for Disaster Mitigation. Washington, D.C.: National Bureau of Standards, Feb., 1973.
- (17) McGuire, W. Prevention of Progressive Collapse. Regional Conference on Tall Buildings, Bangkok, Thailand, Jan., 1974, pp. 851-865.
- (18) Lewicki, B., and S. O. Olesen. "Limiting the Possibility of Progressive Collapse." Building Research Practices, Vol. 2, No. 1 (Jan.-Feb., 1974), pp. 10-13.
- (19) Breen, John E. "Developing Structural Integrity in Bearing Wall Buildings." Journal of the Prestressed Concrete Institute, Vol. 25, No. 1 (Jan.-Feb., 1980), pp. 42-73.
- (20) Popoff, Alexander, Jr. "Design Against Progressive Collapse." Journal of the Prestressed Concrete Institute, Vol. 20, No. 2 (Mar.-Apr., 1975), pp. 44-57.
- (21) Yokel, F. Y., J. H. Pielert, and A. R. Schwab. The Implementation of a Provision Against Progressive Collapse. Washington, D.C.: National Bureau of Standards, Aug., 1975.
- (22) Burnett, Eric F. P. The Avoidance of Progressive Collapse: Regulatory Approaches to the Problem. Washington, D.C.: National Bureau of Standards, Oct., 1975.
- (23) Chapman, R. E., and P. F. Colwell. Economics of Protection Against Progressive Collapse. Washington, D.C.: National Bureau of Standards, Sept., 1974.
- (24) Research Workshop on Progressive Collapse of Building Structures, Held at the University of Texas at Austin, November 13-20, 1975. Washington, D.C.: National Bureau of Standards, Nov., 1975.

- (25) Watwood, Vernon B. "Mechanism Generation for Limit Analysis of Frames." Journal of the Structural Division, ASCE, Vol. 105, No. 1 (Jan., 1979), pp. 1-15.
- (26) Gross, John L., Thomas A. Mutrym, and William McGuire. "Computer Graphics and Nonlinear Frame Analysis." Seventh Conference on Electronics and Computers, St. Louis, Missouri, August 6-8, 1979. New York: American Society of Civil Engineers, 1979.
- (27) Loet Stadt, P. Interactive Simulation of the Progressive Collapse of a Building Revisited. Stockholm, Sweden: Royal Institute of Technology, 1979.
- (28) Sih, G. C., and R. J. Hartranft. "Concept of Fracture Mechanics Applied to the Progressive Failure of Structural Members." Computers and Structures, Vol. 12, No. 6 (Dec., 1980), pp. 813-818.
- (29) Girhammar, Ulf Arne. Dynamic Response of Two-Span Steel Beams Subjected to Removal of Interior Support. Stockholm, Sweden: Swedish Council for Building Research, 1980.
- (30) Smith, Erling A., and Howard I. Epstein. "Hartford Coliseum Roof Collapse: Structural Collapse Sequence and Lessons Learned," Civil Engineer, Vol. 52, No. 4 (April, 1980), pp. 59-62.
- (31) Venkayya, V. B., N. S. Khot, and F. E. Eastep. "Vulnerability Analysis of Optimized Structures." AIAA Journal, Vol. 16, No. 11 (Nov., 1978), pp. 1180-1195.
- (32) An Experimental and Analytical Study of the Static Response of an Undamaged and Damaged F-84 Wing, Vols. I and II. 61 JTCG/ME-76-11-1 and -2. Eglin AFB, Fla.: Joint Technical Coordinating Group for Munitions Effectiveness, Aug. 24, 1976.
- (33) Jordan, Thomas D. "An Analytical and Experimental Study of the Dynamic Response of a Semi-Monocoque Aircraft Wing Structure." (Unpublished Ph.D. thesis, Oklahoma State University, 1976.)
- (34) Peery, David J. Aircraft Structures. New York: McGraw-Hill, 1950.
- (35) Bruhn, E. F. Analysis and Design of Flight Vehicle Structures. Cincinnati: Tri-State Offset Company, 1973.
- (36) Seely, Fred B., and James O. Smith. Advanced Mechanics of Materials. 2nd ed. New York: John Wiley and Sons, 1952.

APPENDIX A

STRAIN GAGE LOCATIONS FOR EXPERIMENTAL PROGRAM

Three wings were tested in the experimental portion of the study. Surface strains were measured using strain gages manufactured by Micro-Measurements of Romulus, Michigan. Two types of gages were used: EA-13-125AD-120 uniaxial gages, and EA-13-250RA-120 three-gage rectangular rosettes. Figure 21 details strain gage locations for all three tests.

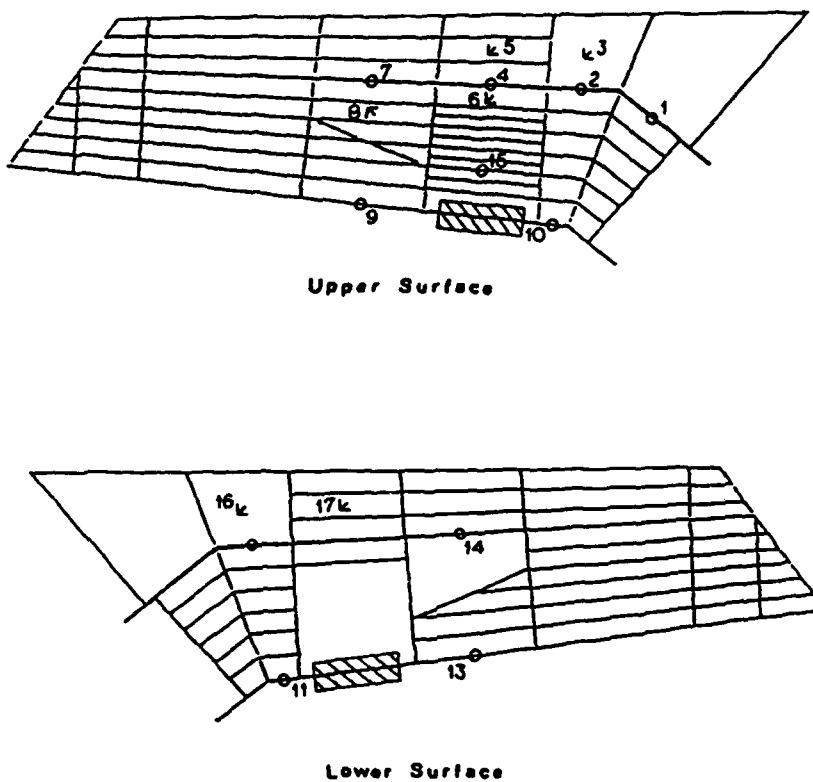


⊖ Uniaxial

↖ Rectangular Rosette

(a) Test 1

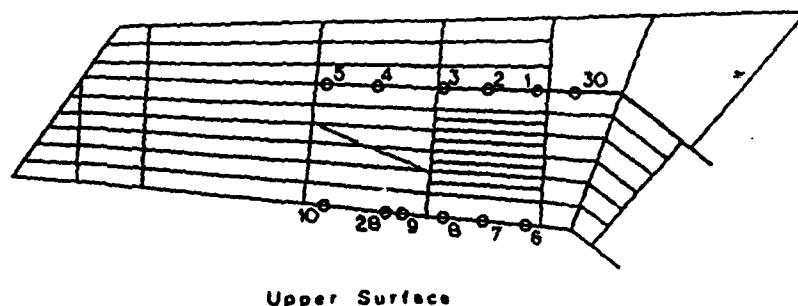
Figure 21. Strain Gage Locations



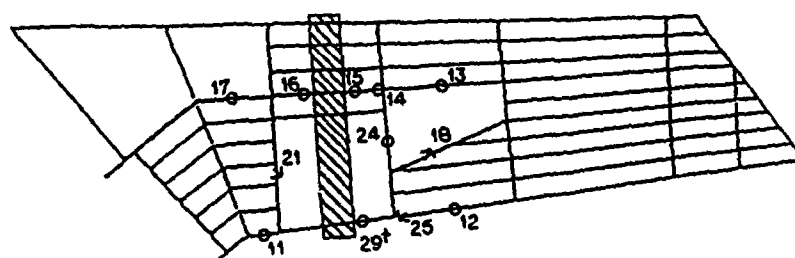
⊖ Uniaxial
↖ Rectangular Rosette

(b) Test 2

Figure 21. (Continued)



Upper Surface



Lower Surface

⊖ Uniaxial

↖ Rectangular Rosette

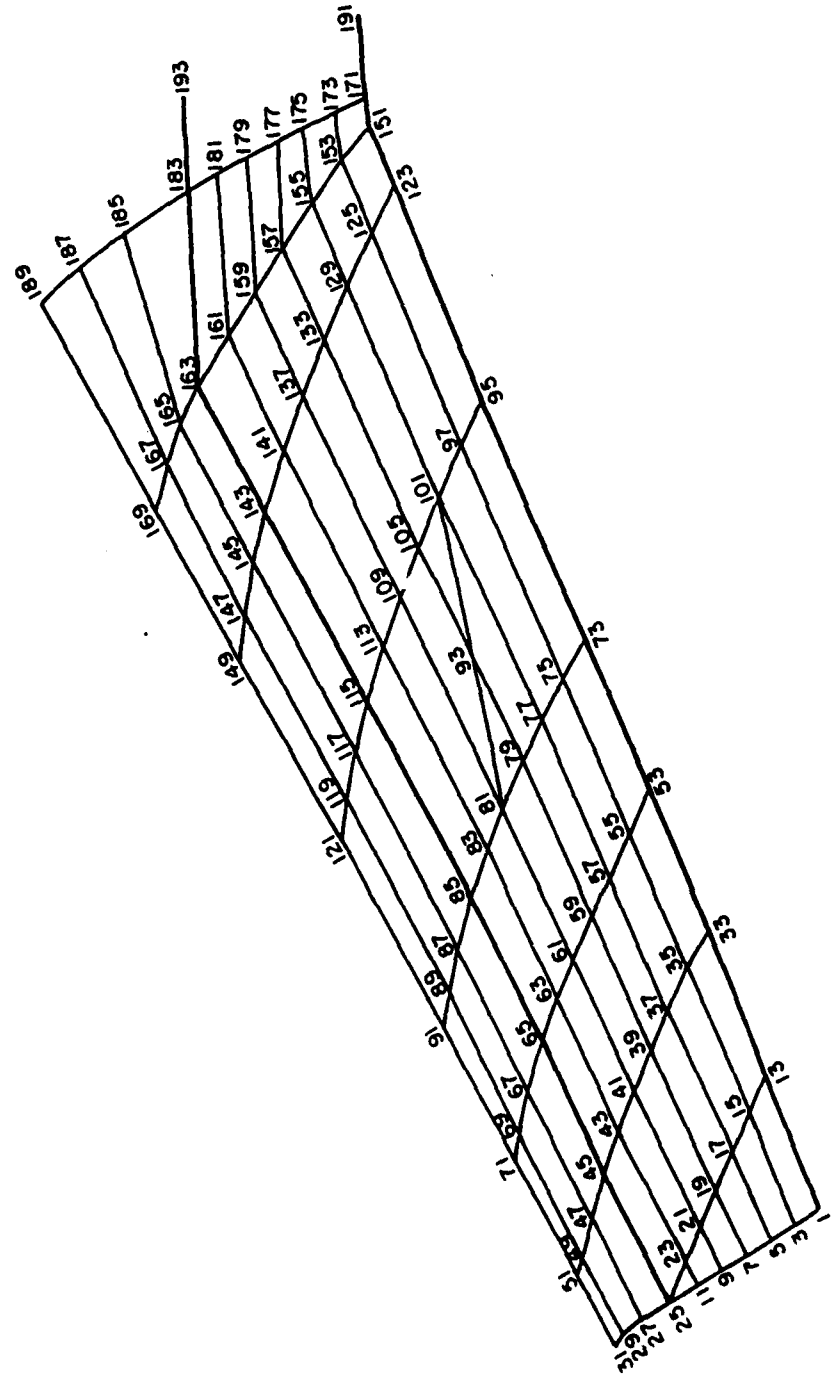
† Test 3B only

(c) Test 3

Figure 21. (Continued)

APPENDIX B

FINITE ELEMENT MODEL NUMBERING DETAILS



a. Node Numbers, Upper Surface

Figure 22. Finite Element Model Numbering Details

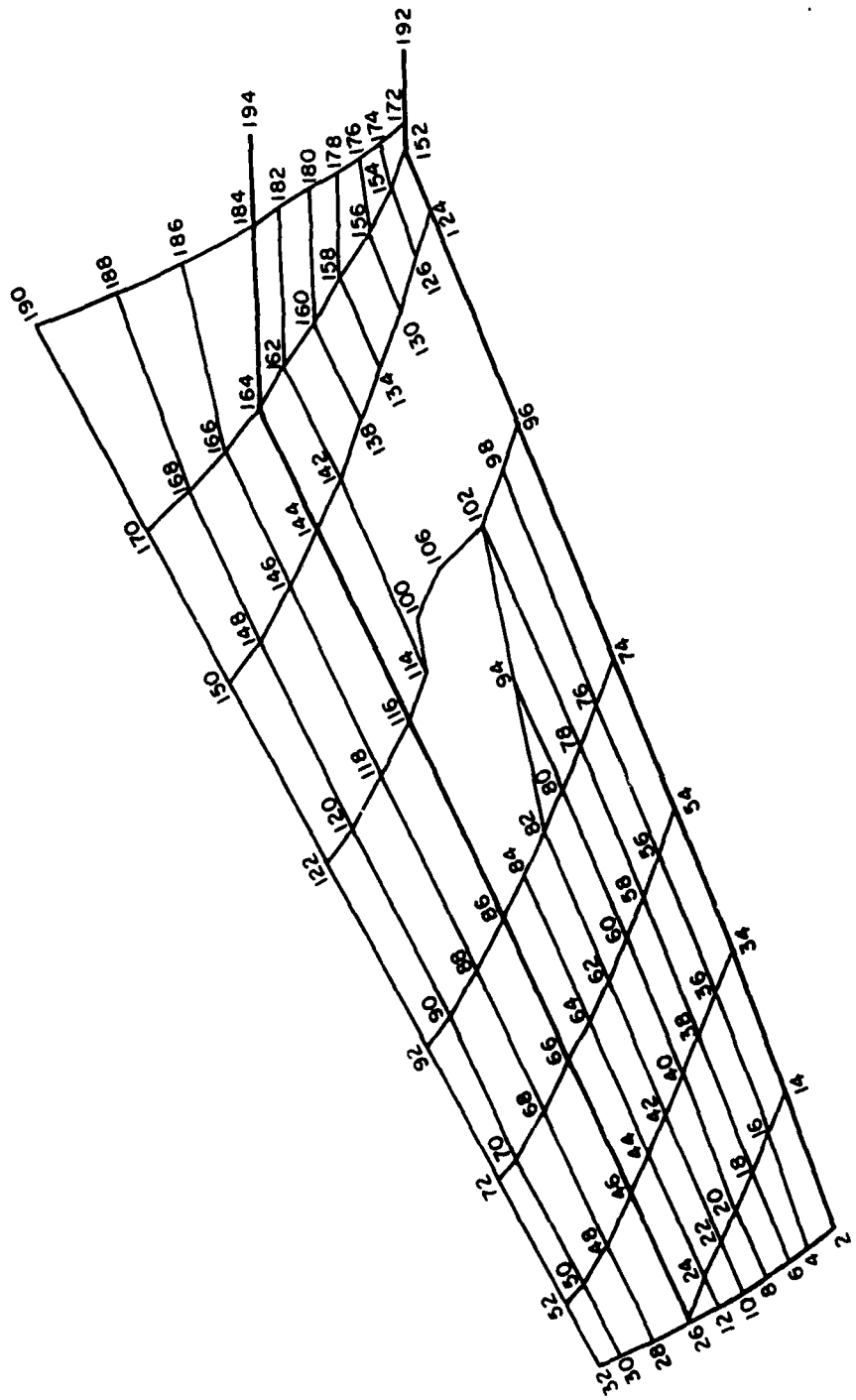
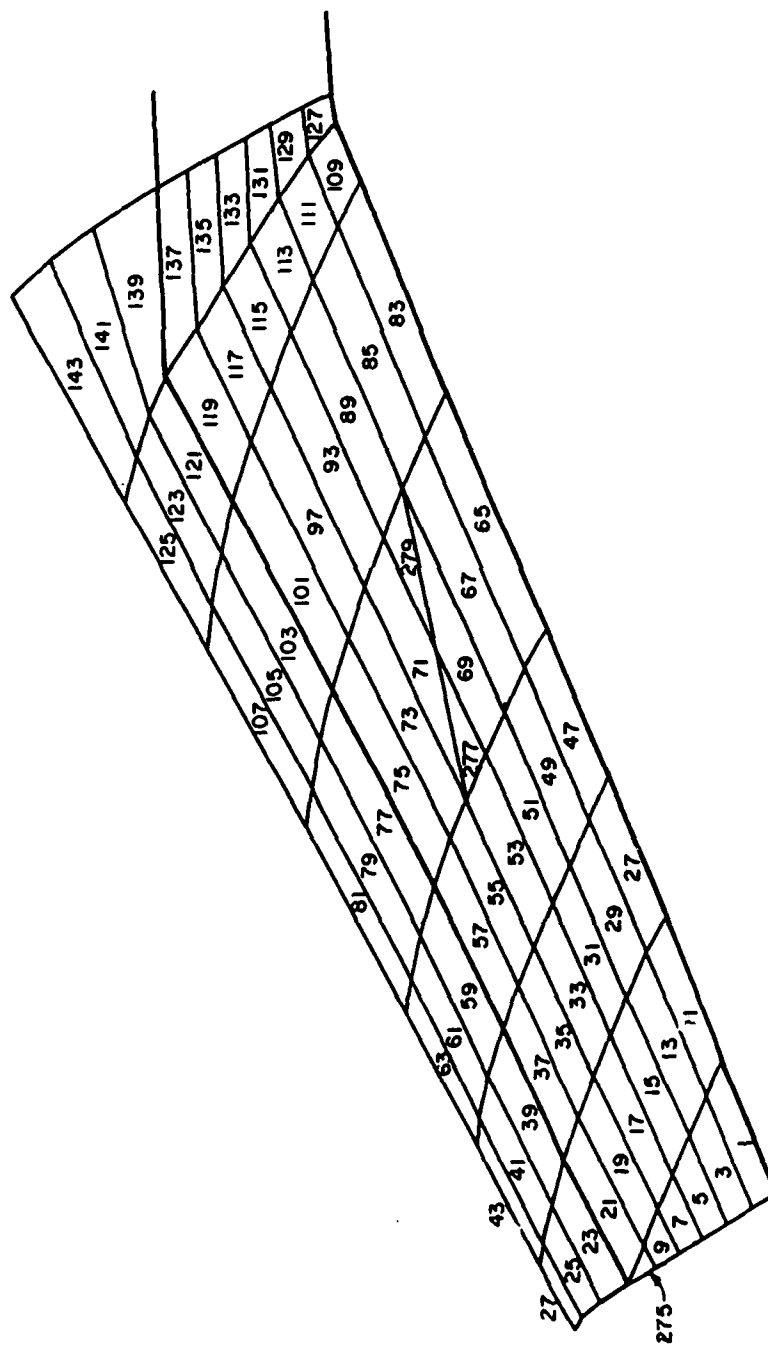
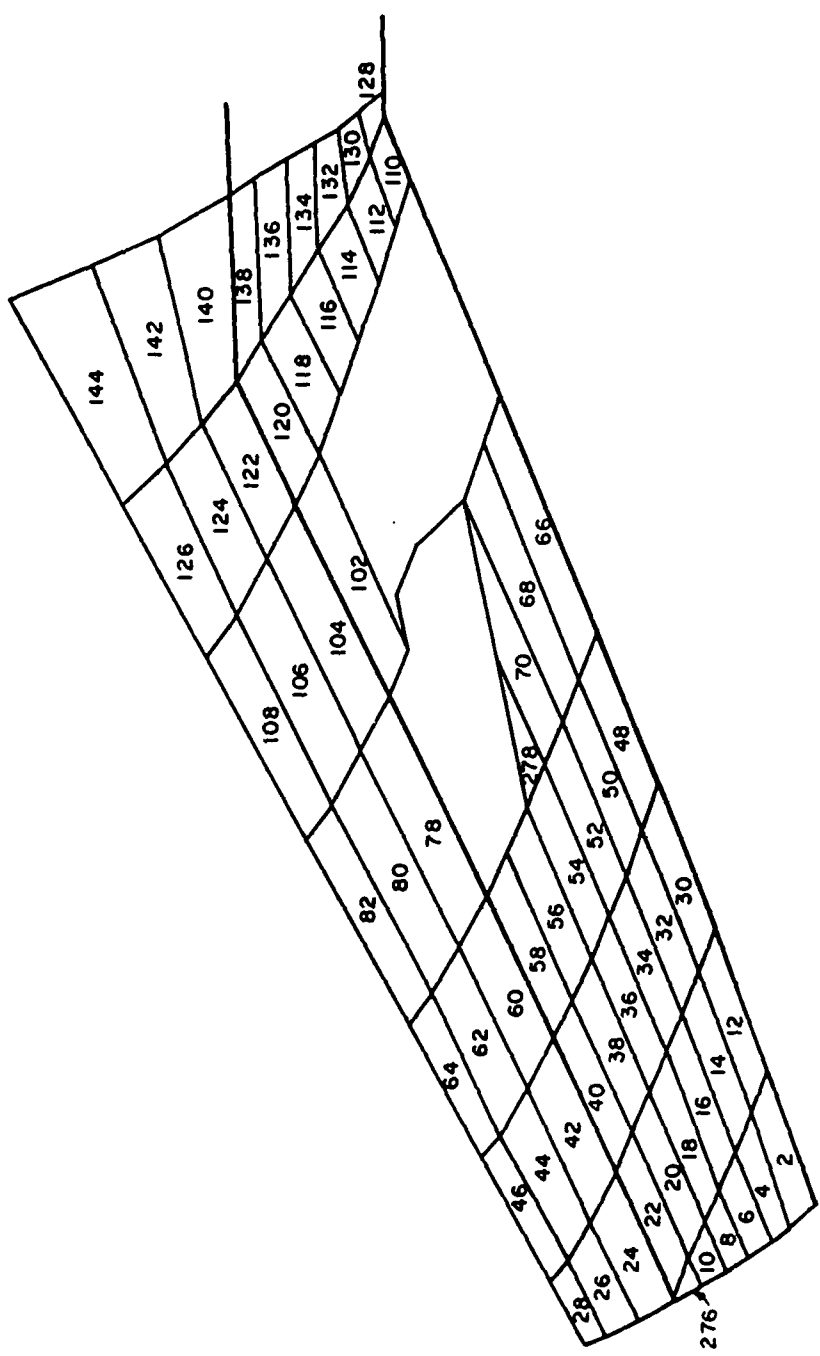


Figure 22. (Continued)

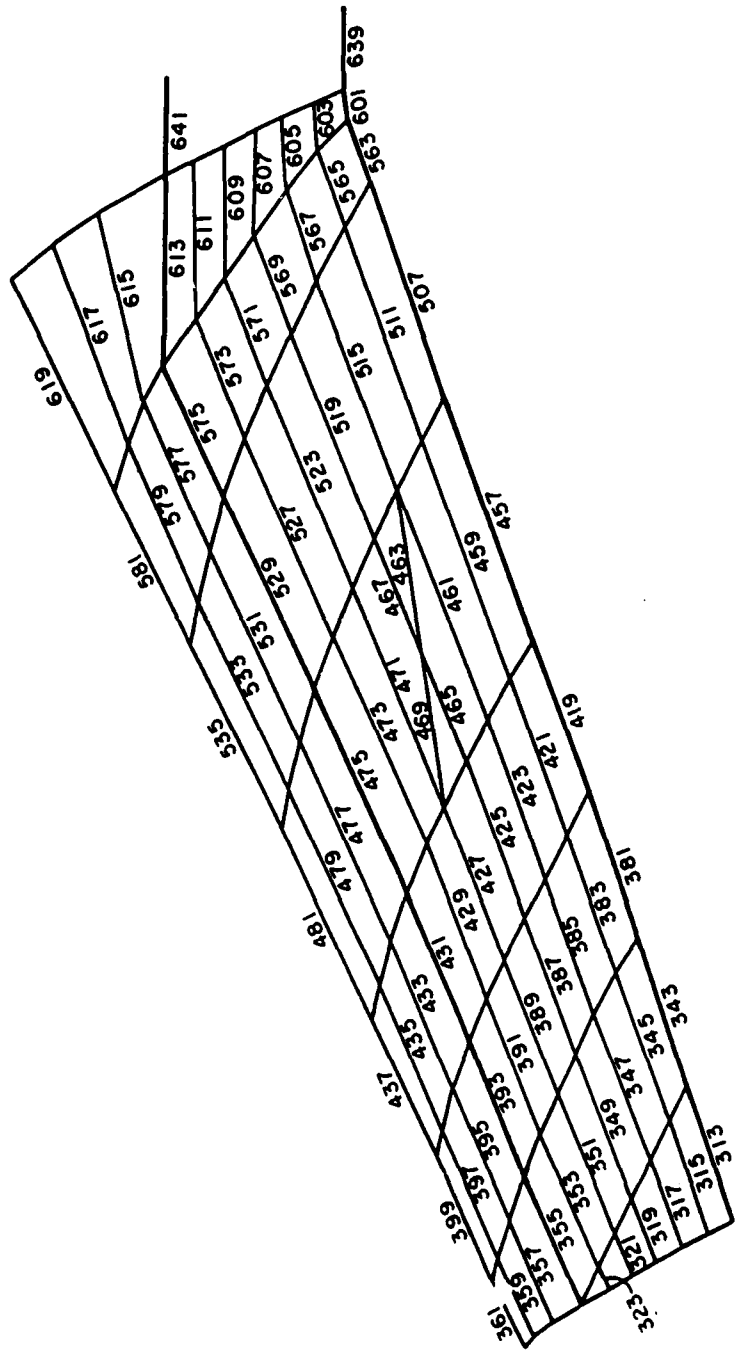


c. Skin Panels, Upper Surface
Figure 22. (Continued)



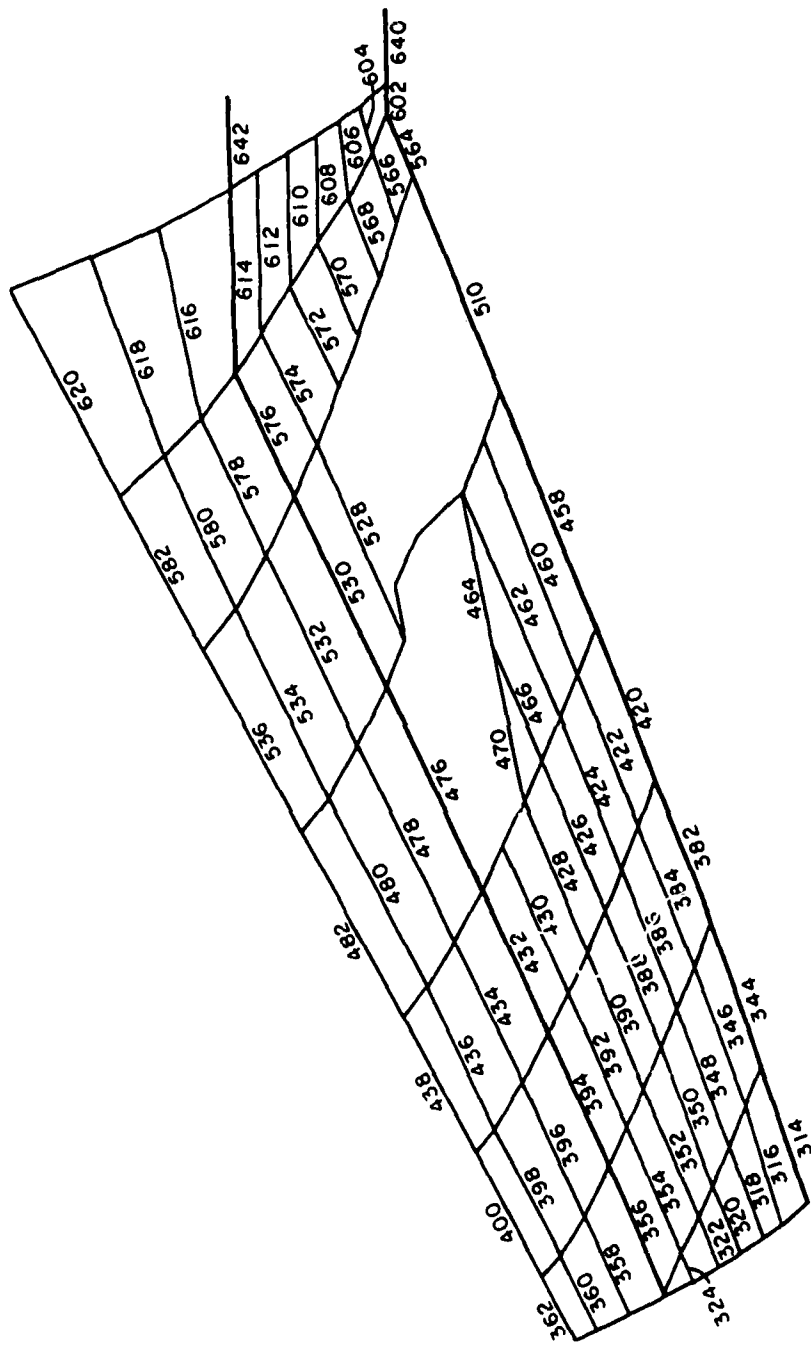
d. Skin Panels, Lower Surface

Figure 22. (Continued)



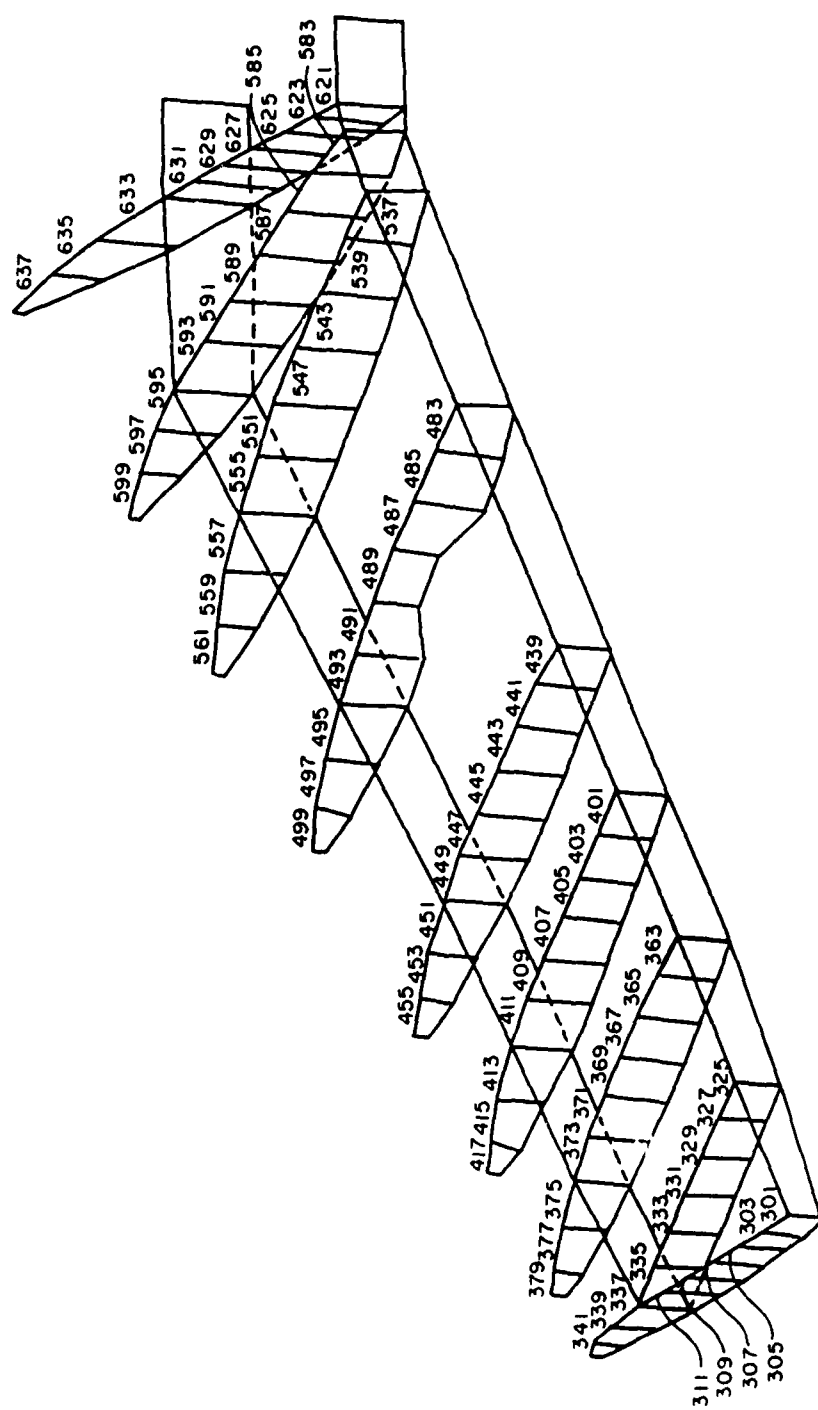
e. Spar Cap and Stiffener Rods, Upper Surface

Figure 22. (Continued)



f. Spar cap and Stiffener Rods, Lower Surface

Figure 22. (Continued)



g. Rib Cap Rods, Upper Surface

Figure 22. (Continued)

AD-A125 266

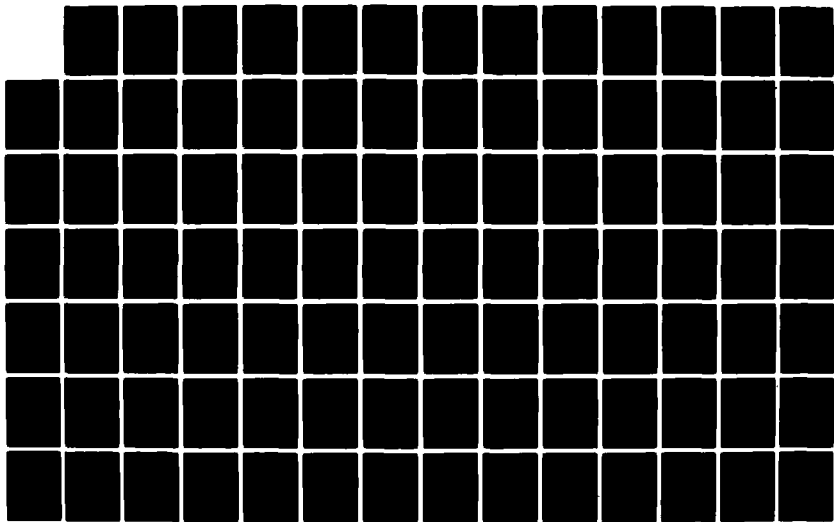
ANALYSIS OF PROGRESSIVE COLLAPSE OF COMPLEX STRUCTURES
(U) AIR FORCE INST OF TECH WRIGHT-PATTERSON AFB OH
G E RIGGS DEC 82 AFIT/CI/NR-82-63D

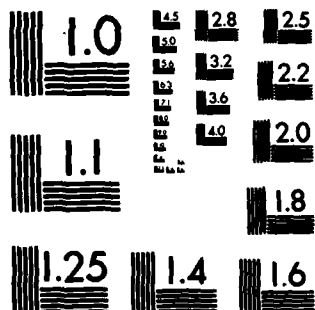
23

UNCLASSIFIED

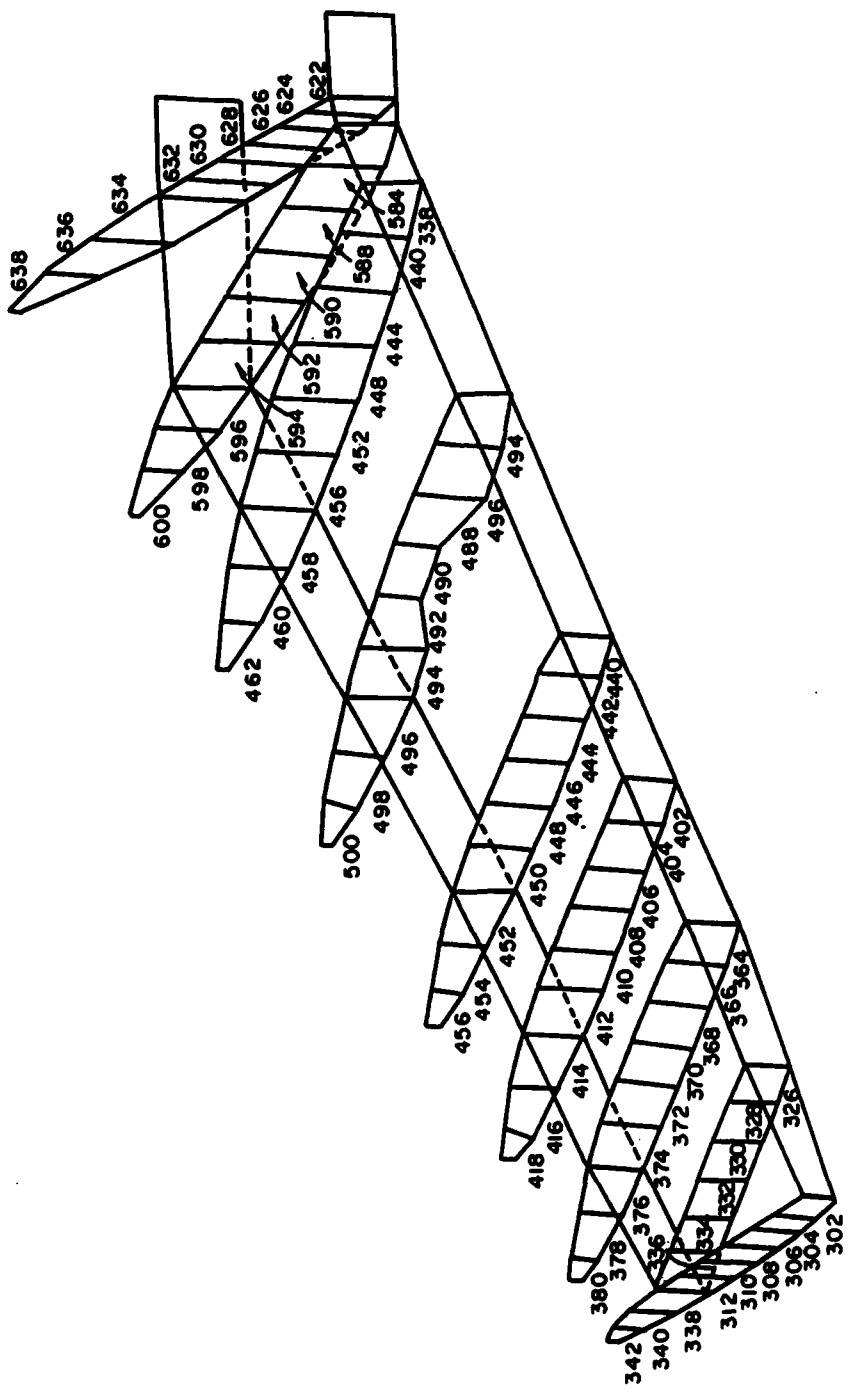
F/G 12/1

NL



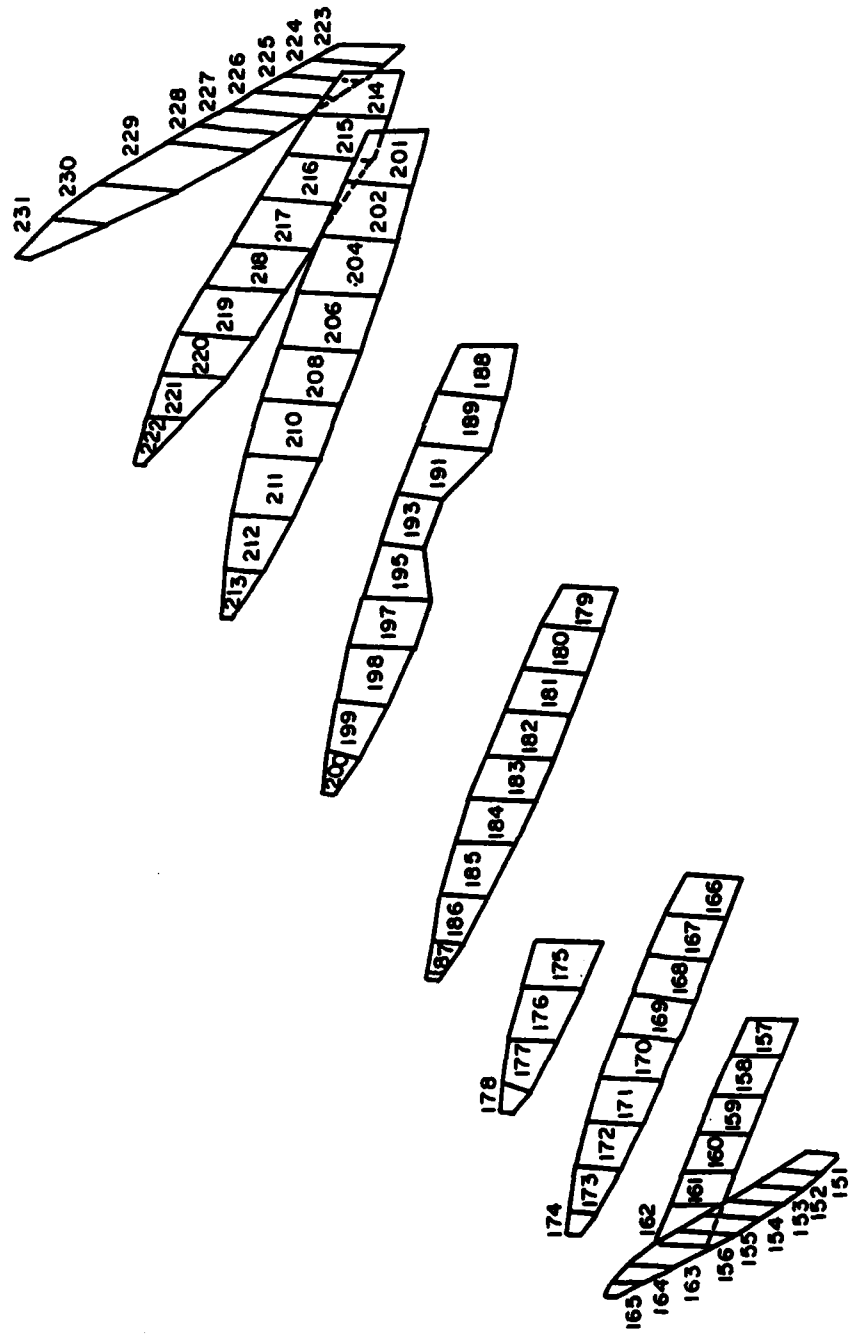


MICROCOPY RESOLUTION TEST CHART
NATIONAL BUREAU OF STANDARDS-1963-A



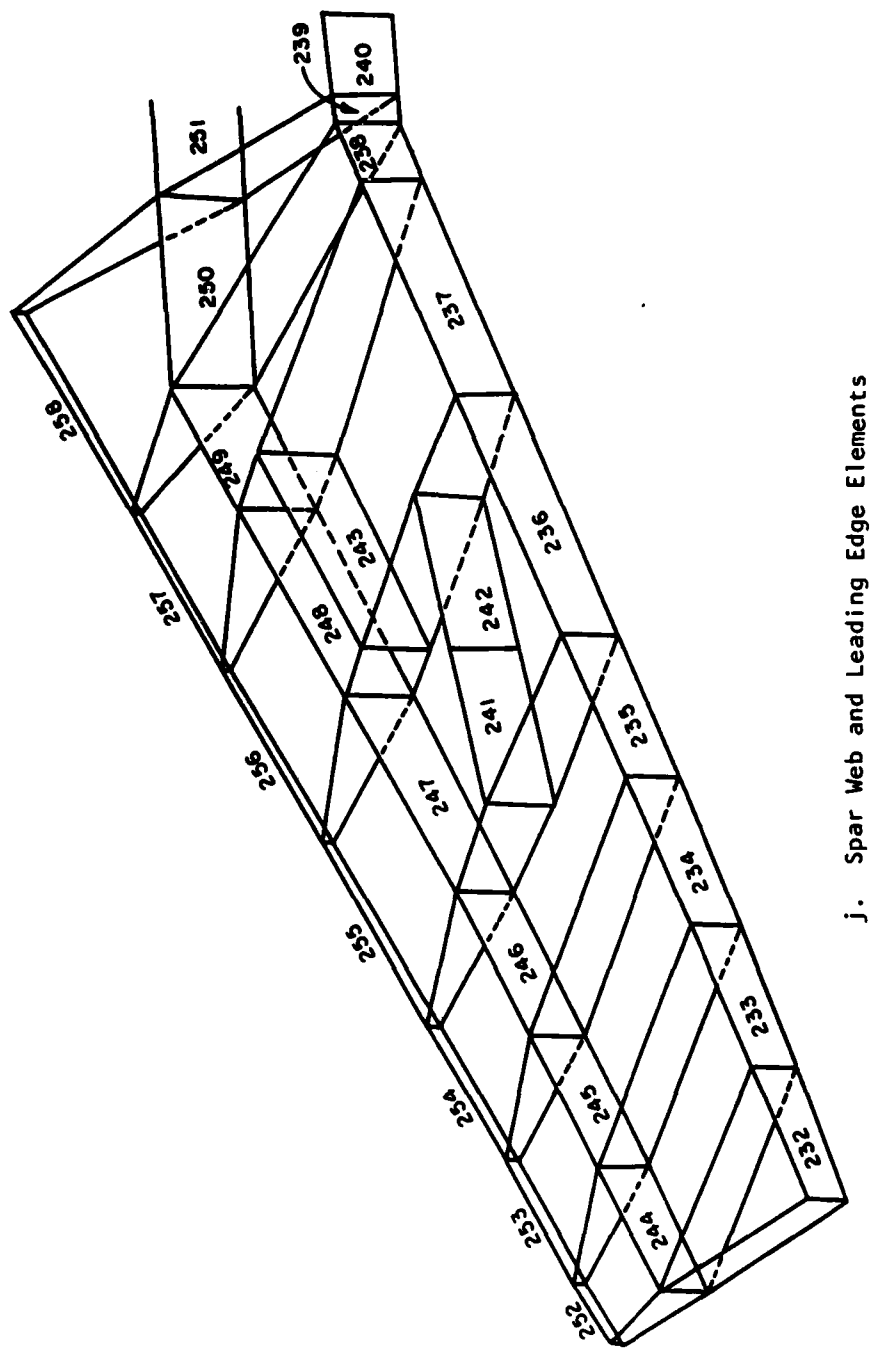
h. Rib Cap Rods, Lower Surface

Figure 22. (Continued)



i. Rib Web Elements

Figure 22. (Continued)



j. Spar Web and Leading Edge Elements

APPENDIX C

SIZING OF ROD ELEMENTS

The rationale for sizing rod elements representing spar caps or rib caps was presented by Jordan (32, 33). All symbols in the following summary of his presentation refer to Figures 23 and 24 which were extracted from Reference (32).

Property relationships were first determined for a structural member's cross section. The distance from the top surface of the section to the centroidal axis was identified as h_t . Similarly, the distance from the centroidal axis to the bottom surface of the section was labeled h_b . Maximum bending stresses at top and bottom surfaces, respectively, were

$$\sigma_T = \frac{Mh_t}{I} \quad (A.1a)$$

and

$$\sigma_B = \frac{Mh_b}{I} \quad (A.1b)$$

where M was the applied bending moment, and I was the section moment of inertia about the centroidal axis.

In the model, the rod elements were assumed to be point areas and were positioned at the top and bottom surfaces of a cross section. The rod areas were sized to maintain the location of the centroidal axis and the value of I for the actual section. Such a relationship yielded

$$A_T h_t = A_B h_b \quad (A.2)$$

with A_T and A_B being the areas of the top and bottom rods. The bending moment, M , in the model then became

$$M = \sigma_T A_T h_t + \sigma_B A_B h_b \quad (A.3)$$

Next, using actual section properties and desired model properties, the

relationships of Equations (A.1), (A.2), and (A.3) were combined to produce

$$A_T = \frac{I}{h_t(h_t + h_b)} \quad (A.4a)$$

and

$$A_B = \frac{I}{h_b(h_t + h_b)} \quad (A.4b)$$

which were the rod element areas.

Skin stiffeners also were represented by rod elements. Initially, each of those rods had the same cross sectional area and position in the structure as the stiffener it represented. However, Models A and B used shear panel elements to represent aircraft skin, so the membrane capacity of the skin panels was lost because shear panel elements do not represent membrane behavior. The membrane capacity of the skin was restored to models A and B by adding the cross sectional area of each skin panel to its bordering rod elements. This is illustrated for a typical cross section in Figure 24. Such modification of stiffener rod element areas was not necessary for Models C and D because they used membrane elements to represent the aircraft skin.

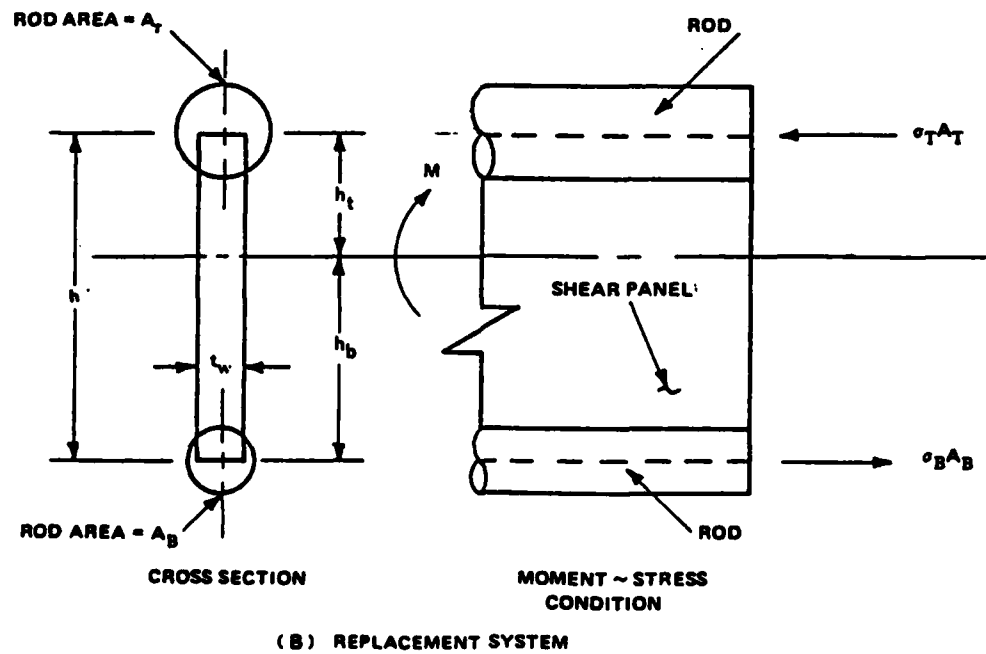
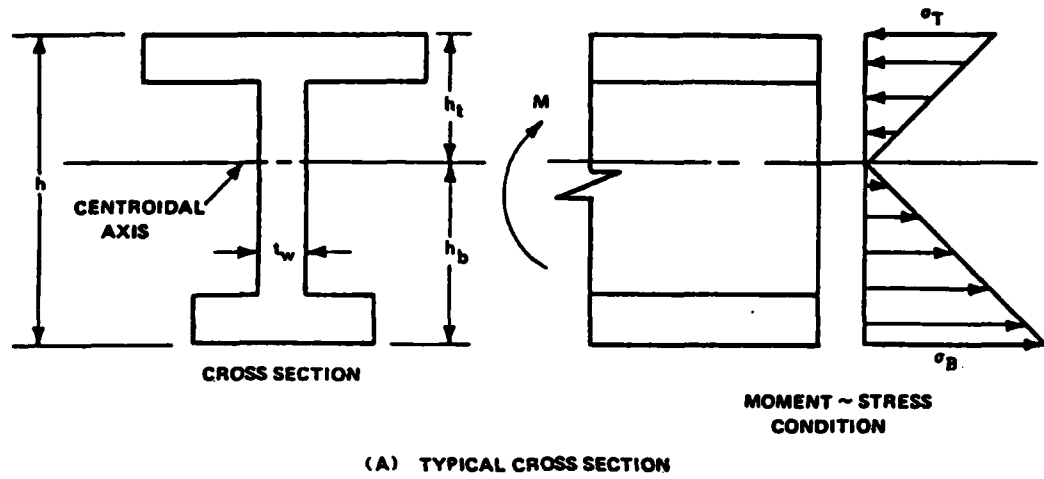


Figure 23. Basic Sizing of Rod Elements

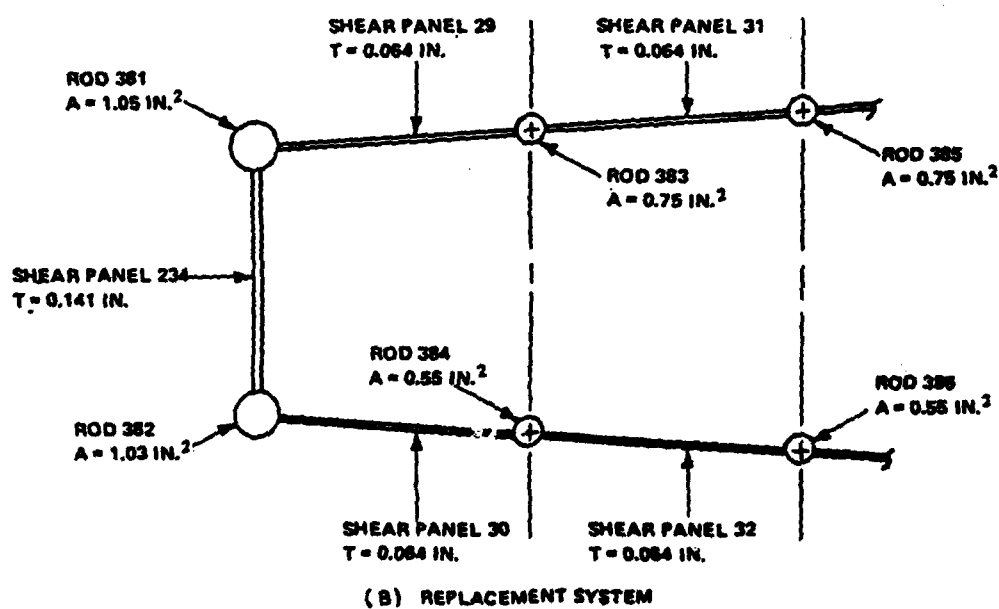
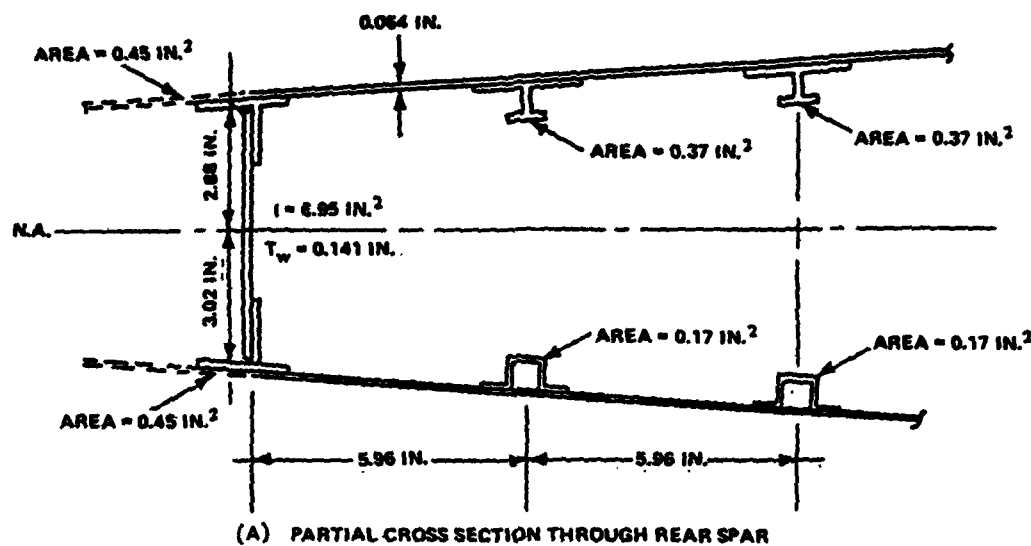


Figure 24. Rod Element Sizing With Shear Panel Skin

APPENDIX D

FINITE ELEMENT MODEL A LISTING

SHEET PANELS - Definition of	
1	15
2	20
3	25
4	30
5	35
6	40
7	45
8	50
9	55
10	60
11	65
12	70
13	75
14	80
15	85
16	90
17	95
18	100
19	105
20	110
21	115
22	120
23	125
24	130
25	135
26	140
27	145
28	150
29	155
30	160
31	165
32	170
33	175
34	180
35	185
36	190
37	195
38	200
39	205
40	210
41	215
42	220
43	225
44	230
45	235
46	240
47	245
48	250
49	255
50	260
51	265
52	270
53	275
54	280
55	285
56	290
57	295
58	300
59	305
60	310
61	315
62	320
63	325
64	330
65	335
66	340
67	345
68	350
69	355
70	360
71	365
72	370
73	375
74	380
75	385
76	390
77	395
78	400
79	405
80	410
81	415
82	420
83	425
84	430
85	435
86	440
87	445
88	450
89	455
90	460
91	465
92	470
93	475
94	480
95	485
96	490
97	495
98	500
99	505
100	510
101	515
102	520
103	525
104	530
105	535
106	540
107	545
108	550
109	555
110	560
111	565
112	570
113	575
114	580
115	585
116	590
117	595
118	600
119	605
120	610
121	615
122	620
123	625
124	630
125	635
126	640
127	645
128	650
129	655
130	660
131	665
132	670
133	675
134	680
135	685
136	690
137	695
138	700
139	705
140	710
141	715
142	720
143	725
144	730
145	735
146	740
147	745
148	750
149	755
150	760
151	765
152	770
153	775
154	780
155	785
156	790
157	795
158	800
159	805
160	810
161	815
162	820
163	825
164	830
165	835
166	840
167	845
168	850
169	855
170	860
171	865
172	870
173	875
174	880
175	885
176	890
177	895
178	900
179	905
180	910
181	915
182	920
183	925
184	930
185	935
186	940
187	945
188	950
189	955
190	960
191	965
192	970
193	975
194	980
195	985
196	990
197	995
198	1000
199	1005
200	1010
201	1015
202	1020
203	1025
204	1030
205	1035
206	1040
207	1045
208	1050
209	1055
210	1060
211	1065
212	1070
213	1075
214	1080
215	1085
216	1090
217	1095
218	1100
219	1105
220	1110
221	1115
222	1120
223	1125
224	1130
225	1135
226	1140
227	1145
228	1150
229	1155
230	1160
231	1165
232	1170
233	1175
234	1180
235	1185
236	1190
237	1195
238	1200
239	1205
240	1210
241	1215
242	1220
243	1225
244	1230
245	1235
246	1240
247	1245
248	1250
249	1255
250	1260
251	1265
252	1270
253	1275
254	1280
255	1285
256	1290
257	1295
258	1300
259	1305
260	1310
261	1315
262	1320
263	1325
264	1330
265	1335
266	1340
267	1345
268	1350
269	1355
270	1360
271	1365
272	1370
273	1375
274	1380
275	1385
276	1390
277	1395
278	1400
279	1405
280	1410
281	1415
282	1420
283	1425
284	1430
285	1435
286	1440
287	1445
288	1450
289	1455
290	1460
291	1465
292	1470
293	1475
294	1480
295	1485
296	1490
297	1495
298	1500
299	1505
300	1510
301	1515
302	1520
303	1525
304	1530
305	1535
306	1540
307	1545
308	1550
309	1555
310	1560
311	1565
312	1570
313	1575
314	1580
315	1585
316	1590
317	1595
318	1600
319	1605
320	1610
321	1615
322	1620
323	1625
324	1630
325	1635
326	1640
327	1645
328	1650
329	1655
330	1660
331	1665
332	1670
333	1675
334	1680
335	1685
336	1690
337	1695
338	1700
339	1705
340	1710
341	1715
342	1720
343	1725
344	1730
345	1735
346	1740
347	1745
348	1750
349	1755
350	1760
351	1765
352	1770
353	1775
354	1780
355	1785
356	1790
357	1795
358	1800
359	1805
360	1810
361	1815
362	1820
363	1825
364	1830
365	1835
366	1840
367	1845
368	1850
369	1855
370	1860
371	1865
372	1870
373	1875
374	1880
375	1885
376	1890
377	1895
378	1900
379	1905
380	1910
381	1915
382	1920
383	1925
384	1930
385	1935
386	1940
387	1945
388	1950
389	1955
390	1960
391	1965
392	1970
393	1975
394	1980
395	1985
396	1990
397	1995
398	2000
399	2005
400	2010
401	2015
402	2020
403	2025
404	2030
405	2035
406	2040
407	2045
408	2050
409	2055
410	2060
411	2065
412	2070
413	2075
414	2080
415	2085
416	2090
417	2095
418	2100
419	2105
420	2110
421	2115
422	2120
423	2125
424	2130
425	2135
426	2140
427	2145
428	2150
429	2155
430	2160
431	2165
432	2170
433	2175
434	2180
435	2185
436	2190
437	2195
438	2200
439	2205
440	2210
441	2215
442	2220
443	2225
444	2230
445	2235
446	2240
447	2245
448	2250
449	2255
450	2260
451	2265
452	2270
453	2275
454	2280
455	2285
456	2290
457	2295
458	2300
459	2305
460	2310
461	2315
462	2320
463	2325
464	2330
465	2335
466	2340
467	2345
468	2350
469	2355
470	2360
471	2365
472	2370
473	2375
474	2380
475	2385
476	2390
477	2395
478	2400
479	2405
480	2410
481	2415
482	2420
483	2425
484	2430
485	2435
486	2440
487	2445
488	2450
489	2455
490	2460
491	2465
492	2470
493	2475
494	2480
495	2485
496	2490
497	2495
498	2500
499	2505
500	2510
501	2515
502	2520
503	2525
504	2530
505	2535
506	2540
507	2545
508	2550
509	2555
510	2560
511	2565
512	2570
513	2575
514	2580
515	2585
516	2590
517	2595
518	2600
519	2605
520	2610
521	2615
522	2620
523	2625
524	2630
525	2635
526	2640
527	2645
528	2650
529	2655
530	2660
531	2665
532	2670
533	2675
534	2680
535	2685
536	2690
537	2695
538	2700
539	2705
540	2710
541	2715
542	2720
543	2725
544	2730
545	2735
546	2740
547	2745
548	2750
549	2755
550	2760
551	2765
552	2770
553	2775
554	2780
555	2785
556	2790
557	2795
558	2800
559	2805
560	2810
561	2815
562	2820
563	2825
564	2830
565	2835
566	2840
567	2845
568	2850
569	2855
570	2860
571	2865
572	2870
573	2875
574	2880
575	2885
576	2890
577	2895
578	2900
579	2905
580	2910
581	2915
582	2920
583	2925
584	2930
585	2935
586	2940
587	2945
588	2950
589	2955
590	2960
591	2965
592	2970

.064	.001	.001	.001	.001
.128	.001	.001	.001	.001
.256	.001	.001	.001	.001
.512	.001	.001	.001	.001
.1	.001	.001	.001	.001
.2	.001	.001	.001	.001
.4	.001	.001	.001	.001
.8	.001	.001	.001	.001
1.6	.001	.001	.001	.001
3.2	.001	.001	.001	.001
6.4	.001	.001	.001	.001
12.8	.001	.001	.001	.001
25.6	.001	.001	.001	.001
51.2	.001	.001	.001	.001
102.4	.001	.001	.001	.001
204.8	.001	.001	.001	.001
409.6	.001	.001	.001	.001
819.2	.001	.001	.001	.001
1638.4	.001	.001	.001	.001
3276.8	.001	.001	.001	.001
6553.6	.001	.001	.001	.001
13107.2	.001	.001	.001	.001
26214.4	.001	.001	.001	.001
52428.8	.001	.001	.001	.001
104857.6	.001	.001	.001	.001
209715.2	.001	.001	.001	.001
419430.4	.001	.001	.001	.001
838860.8	.001	.001	.001	.001
1677721.6	.001	.001	.001	.001
3355443.2	.001	.001	.001	.001
6710886.4	.001	.001	.001	.001
13421772.8	.001	.001	.001	.001
26843545.6	.001	.001	.001	.001
53687091.2	.001	.001	.001	.001
107374182.4	.001	.001	.001	.001
214748364.8	.001	.001	.001	.001
429496729.6	.001	.001	.001	.001
858993459.2	.001	.001	.001	.001
1717986918.4	.001	.001	.001	.001
3435973836.8	.001	.001	.001	.001
6871947673.6	.001	.001	.001	.001
13743895347.2	.001	.001	.001	.001
27487790694.4	.001	.001	.001	.001
54975581388.8	.001	.001	.001	.001
109951162777.6	.001	.001	.001	.001
219902325555.2	.001	.001	.001	.001
439804651110.4	.001	.001	.001	.001
879609302220.8	.001	.001	.001	.001
1759218604401.6	.001	.001	.001	.001
3518437208803.2	.001	.001	.001	.001
7036874417606.4	.001	.001	.001	.001
14073748835212.8	.001	.001	.001	.001
28147497670425.6	.001	.001	.001	.001
56294995340851.2	.001	.001	.001	.001
11258999068162.4	.001	.001	.001	.001
22517998136324.8	.001	.001	.001	.001
45035996272649.6	.001	.001	.001	.001
90071992545299.2	.001	.001	.001	.001
180143985090598.4	.001	.001	.001	.001
360287970181196.8	.001	.001	.001	.001
720575940362393.6	.001	.001	.001	.001
144115188072586.4	.001	.001	.001	.001
288230376145172.8	.001	.001	.001	.001
576460752290345.6	.001	.001	.001	.001
115292150580686.4	.001	.001	.001	.001
230584301161372.8	.001	.001	.001	.001
461168602322745.6	.001	.001	.001	.001
922337204645491.2	.001	.001	.001	.001
184467440929092.4	.001	.001	.001	.001
368934881858184.8	.001	.001	.001	.001
737869763716369.6	.001	.001	.001	.001
147573952743279.2	.001	.001	.001	.001
295147905486558.4	.001	.001	.001	.001
590295810973116.8	.001	.001	.001	.001
1180591621946233.6	.001	.001	.001	.001
2361183243892467.2	.001	.001	.001	.001
4722366487784934.4	.001	.001	.001	.001
9444732975569868.8	.001	.001	.001	.001
1888946595113977.6	.001	.001	.001	.001
3777893190227955.2	.001	.001	.001	.001
7555786380455910.4	.001	.001	.001	.001
15111572760911820.8	.001	.001	.001	.001
30223145521823641.6	.001	.001	.001	.001
60446291043647283.2	.001	.001	.001	.001
120892582087294566.4	.001	.001	.001	.001
241785164174589132.8	.001	.001	.001	.001
483570328349178265.6	.001	.001	.001	.001
967140656698356531.2	.001	.001	.001	.001
1934281313396713062.4	.001	.001	.001	.001
3868562626793426124.8	.001	.001	.001	.001
7737125253586852249.6	.001	.001	.001	.001
1547425051717370449.2	.001	.001	.001	.001
3094850103434740898.4	.001	.001	.001	.001
6189700206869481796.8	.001	.001	.001	.001
1237940041373896353.6	.001	.001	.001	.001
2475880082747792707.2	.001	.001	.001	.001
4951760165495585414.4	.001	.001	.001	.001
9903520322991170828.8	.001	.001	.001	.001
1980704064582240165.6	.001	.001	.001	.001
3961408129164480331.2	.001	.001	.001	.001
7922816258328960662.4	.001	.001	.001	.001
15845632516657921324.8	.001	.001	.001	.001
31691265033315842649.6	.001	.001	.001	.001
63382530066631685299.2	.001	.001	.001	.001
12676506013326336058.4	.001	.001	.001	.001
25353012026652672116.8	.001	.001	.001	.001
50706024053305344233.6	.001	.001	.001	.001
10141204810661068846.4	.001	.001	.001	.001
20282409621322137692.8	.001	.001	.001	.001
40564819242644275385.6	.001	.001	.001	.001
81129638485288550771.2	.001	.001	.001	.001
16225927690561710142.4	.001	.001	.001	.001
32451855381123420284.8	.001	.001	.001	.001
64903710762246840569.6	.001	.001	.001	.001
12980742152449368119.2	.001	.001	.001	.001
25961484304898736238.4	.001	.001	.001	.001
51922968609797472476.8	.001	.001	.001	.001
10384593721959494493.6	.001	.001	.001	.001
20769187443918988987.2	.001	.001	.001	.001
41538374887837977974.4	.001	.001	.001	.001
83076749775675955948.8	.001	.001	.001	.001
16615349555135911189.6	.001	.001	.001	.001
33230699110271822379.2	.001	.001	.001	.001
66461398220543644758.4	.001	.001	.001	.001
13292279641086728916.8	.001	.001	.001	.001
26584559282173457833.6	.001	.001	.001	.001
53169118564346915667.2	.001	.001	.001	.001
10633823712869383134.4	.001	.001	.001	.001
21267647425738766268.8	.001	.001	.001	.001
42535294851477532537.6	.001	.001	.001	.001
85070589702955065075.2	.001	.001	.001	.001
17014117940590513010.4	.001	.001	.001	.001
34028235881181026020.8	.001	.001	.001	.001
68056471762362052041.6	.001	.001	.001	.001
13611294352472410403.2	.001	.001	.001	.001
27222588704944820806.4	.001	.001	.001	.001
54445177409889641612.8	.001	.001	.001	.001
10889035401977928324.4	.001	.001	.001	.001
21778070803955856648.8	.001	.001	.001	.001
43556141607911713297.6	.001	.001	.001	.001
87112283215823426595.2	.001	.001	.001	.001
17422456643664685390.4	.001	.001	.001	.001
34844913287329370780.8	.001	.001	.001	.001
69689826574658741561.6	.001	.001	.001	.001
13937965314931748322.4	.001	.001	.001	.001
27875930629863496644.8	.001	.001	.001	.001
55751861259726993289.6	.001	.001	.001	.001
11150372251945398658.4	.001	.001	.001	.001
22300744503890797316.8	.001	.001	.001	.001
44601489007781594633.6	.001	.001	.001	.001
89202978015563189267.2	.001	.001	.001	.001
17840595603112637854.4	.001	.001	.001	.001
35681191206225275708.8	.001	.001	.001	.001
71362382412450551417.6	.001	.001	.001	.001
14272476482495110235.2	.001	.001	.001	.001
28544952964980220470.4	.001	.001	.001	.001
57089855929960440940.8	.001	.001	.001	.001
11417971185980888180.16	.001	.001	.001	.001
22835942371961776360.32	.001	.001	.001	.001
45671884743923552720.64	.001	.001	.001	.001
91343769487847105441.28	.001	.001	.001	.001
18268753895669421082.56	.001	.001	.001	.001
36537507791338842165.12	.001	.001	.001	.001
73075015582677684330.24	.001	.001	.001	.001
14615003116535336860.48	.001	.001	.001	.001
29230006233070673720.96	.001	.001	.001	.001
58460012466141347441.92	.001	.001	.001	.001
11692002492282685482.36	.001	.001	.001	.001
23384004984565370964.72	.001	.001	.001	.001
46768009969130741929.44	.001	.001	.001	.001
93536019938261483858.88	.001	.001	.001	.001
187072039876522967717.76	.001	.001	.001	.001
374144079753045935435.52	.001	.001	.001	.001
74828815950609187087.04	.001	.001	.001	.001
149657631901218374154.08	.001	.001	.001	.001
299315263802436748308.16	.001	.001	.001	.001
598630527604873496616.32	.001	.001	.001	.001
119726105208974699332.64	.001	.001	.001	.001
239452210417949398665.28	.001	.001	.001	.001
478904420835898797330.56	.001	.001	.001	.001
957808841671797594661.12	.001	.001	.001	.001
191561768334359518922.24	.001	.001	.001	.001
383123536668719037844.48	.001	.001	.001	.001
766247073337438075688.96	.001	.001	.001	.001
1532494146674876151777.92	.001	.001	.001	.001
3064988293349752303555.84	.001	.001	.001	.001
6129976586699504607111.68	.001	.001	.001	.001
1225995317339875921423.36	.001	.001	.001	.001
2451990634679751842846.72	.001	.001	.001	.001
4903981269359503685693.44	.001	.001	.001	.001
9807962538719007371386.88	.001	.001	.001	.001
1961592507743801474773.76	.001	.001	.001	.001
3923185015487602949547.52	.001	.001	.001	.001
7846370030975205899095.04	.001	.001	.001	.001
1569274061955041789590.08	.001	.001	.001	.001
3138548123910083579180.16	.001	.001	.001	.001
6277096247820167158360.32	.001	.001	.001	.001
1255419249644034317672.64	.001	.001	.001	.001
2510838499288068635345.28	.001	.001	.001	.001
5021676998576137270690.56	.001	.001	.001	.001
10043353997152654541381.12	.001	.001	.001	.001
20086707994305309082762.24	.001	.001	.001	.001
40173415988610618165524.48	.001	.001	.001	.001
80346831977221236331048.96	.001	.001	.001	.001
16069366395444467266209.92	.001	.001	.001	.001

PROPERTY CARDS FOR BLOCKED SKIN PANELS ADJACENT TO DAMAGE

.064	32322	4	.001
.128	32324	4	.001
.064	32326	4	.005
.16	32328	4	.212
.16	32330	4	.411
.204	32332	4	.263
.097	32334	4	.182
.097	32336	4	.095
.16	32338	4	.3
.065	32340	4	.161
.219	32342	4	.30
.219	32344	4	.246
.32	32346	4	.4
.32	32348	4	.5
	32350	4	
	32352	4	.081
	32354	4	
	32356	4	
	32358	4	
	32360	4	
	32362	4	
	32364	4	
	32366	4	
	32368	4	
	32370	4	
	32372	4	
	32374	4	
	32376	4	
	32378	4	
	32380	4	
	32382	4	
	32384	4	
	32386	4	
	32388	4	
	32390	4	
	32392	4	
	32394	4	
	32396	4	
	32398	4	
	32400	4	
	32402	4	
	32404	4	
	32406	4	
	32408	4	
	32410	4	
	32412	4	
	32414	4	
	32416	4	
	32418	4	
	32420	4	
	32422	4	
	32424	4	
	32426	4	
	32428	4	
	32430	4	
	32432	4	
	32434	4	
	32436	4	
	32438	4	
	32440	4	
	32442	4	
	32444	4	
	32446	4	
	32448	4	
	32450	4	
	32452	4	
	32454	4	
	32456	4	
	32458	4	
	32460	4	
	32462	4	
	32464	4	
	32466	4	
	32468	4	
	32470	4	
	32472	4	
	32474	4	
	32476	4	
	32478	4	
	32480	4	
	32482	4	
	32484	4	
	32486	4	
	32488	4	
	32490	4	
	32492	4	
	32494	4	
	32496	4	
	32498	4	
	32500	4	
	32502	4	
	32504	4	
	32506	4	
	32508	4	
	32510	4	
	32512	4	
	32514	4	
	32516	4	
	32518	4	
	32520	4	
	32522	4	
	32524	4	
	32526	4	
	32528	4	
	32530	4	
	32532	4	
	32534	4	
	32536	4	
	32538	4	
	32540	4	
	32542	4	
	32544	4	
	32546	4	
	32548	4	
	32550	4	
	32552	4	
	32554	4	
	32556	4	
	32558	4	
	32560	4	
	32562	4	
	32564	4	
	32566	4	
	32568	4	
	32570	4	
	32572	4	
	32574	4	
	32576	4	
	32578	4	
	32580	4	
	32582	4	
	32584	4	
	32586	4	
	32588	4	
	32590	4	
	32592	4	
	32594	4	
	32596	4	
	32598	4	
	32600	4	
	32602	4	
	32604	4	
	32606	4	
	32608	4	
	32610	4	
	32612	4	
	32614	4	
	32616	4	
	32618	4	
	32620	4	
	32622	4	
	32624	4	
	32626	4	
	32628	4	
	32630	4	
	32632	4	
	32634	4	
	32636	4	
	32638	4	
	32640	4	
	32642	4	
	32644	4	
	32646	4	
	32648	4	
	32650	4	
	32652	4	
	32654	4	
	32656	4	
	32658	4	
	32660	4	
	32662	4	
	32664	4	
	32666	4	
	32668	4	
	32670	4	
	32672	4	
	32674	4	
	32676	4	
	32678	4	
	32680	4	
	32682	4	
	32684	4	
	32686	4	
	32688	4	
	32690	4	
	32692	4	
	32694	4	
	32696	4	
	32698	4	
	32700	4	
	32702	4	
	32704	4	
	32706	4	
	32708	4	
	32710	4	
	32712	4	
	32714	4	
	32716	4	
	32718	4	
	32720	4	
	32722	4	
	32724	4	
	32726	4	
	32728	4	
	32730	4	
	32732	4	
	32734	4	
	32736	4	
	32738	4	
	32740	4	
	32742	4	
	32744	4	
	32746	4	
	32748	4	
	32750	4	
	32752	4	
	32754	4	
	32756	4	
	32758	4	
	32760	4	
	32762	4	
	32764	4	
	32766	4	
	32768	4	
	32770	4	
	32772	4	
	32774	4	
	32776	4	
	32778	4	
	32780	4	
	32782	4	
	32784	4	
	32786	4	
	32788	4	
	32790	4	
	32792	4	
	32794	4	
	32796	4	
	32798	4	
	32800	4	
	32802	4	
	32804	4	
	32806	4	
	32808	4	
	32810	4	
	32812	4	
	32814	4	
	32816	4	
	32818	4	
	32820	4	
	32822	4	
	32824	4	
	32826	4	
	32828	4	
	32830	4	
	32832	4	
	32834	4	
	32836	4	
	32838	4	
	32840	4	
	32842	4	
	32844	4	
	32846	4	
	32848	4	
	32850	4	
	32852	4	
	32854	4	
	32856	4	
	32858	4	
	32860	4	
	32862	4	
	32864	4	
	32866	4	
	32868	4	
	32870	4	
	32872	4	
	32874	4	
	32876	4	
	32878	4	
	32880	4	
	32882	4	
	32884	4	
	32886	4	
	32888	4	
	32890	4	
	32892	4	
	32894	4	
	32896	4	
	32898	4	
	32900	4	
	32902	4	
	32904	4	
	32906	4	
	32908	4	
	32910	4	
	32912	4	
	32914	4	
	32916	4	
	32918	4	
	32920	4	
	32922	4	
	32924	4	
	32926	4	
	32928	4	
	32930	4	
	32932	4	
	32934	4	
	32936	4	
	32938	4	
	32940	4	
	32942	4	
	32944	4	
	32946	4	
	32948	4	
	32950	4	
	32952	4	
	32954	4	
	32956	4	
	32958	4	
	32960	4	
	32962	4	
	32964	4	
	32966	4	
	32968	4	
	32970	4	
	32972	4	
	32974	4	
	32976	4	
	32978	4	
	32980	4	
	32982	4	
	32984	4	
	32986	4	
	32988	4	
	32990	4	
	32992	4	
	32994	4	
	32996	4	
	32998	4	
	33000	4	

ESTATE PLANNING FOR THE RETIRED COUPLE

卷之三

PROPERTY CLAIMS FOR UNINSURED SWIM PAMES AND HOME OWNAGE

PROPERTY DAMAGE FOR INJURIES TO 3RD PARTIES AND COSTS TO DAMAGE

PROPERTY CARES FOR YOUR SKIN WHILE AWAY FROM HOME.

• REPORTS OF UNUSUAL SKIN PALSIES AWAY FROM DAMAGE

PROPERTY CLASS FOR UNLICENSED SKIN PANELS ADJACENT TO DAWA

										Vertical Mods																																																																																																																																																																																																																																																																																																																																																																																																																																																																																																																																																																																																																																																																																																																																																																																																																																																																																																																																																																																																																																																																																																																																																																																																																																																																																																																								
1	2	3	4	5	6	7	8	9	10	11	12	13	14	15	16	17	18	19	20	21	22	23	24	25	26	27	28	29	30	31	32	33	34	35	36	37	38	39	40	41	42	43	44	45	46	47	48	49	50	51	52	53	54	55	56	57	58	59	60	61	62	63	64	65	66	67	68	69	70	71	72	73	74	75	76	77	78	79	80	81	82	83	84	85	86	87	88	89	90	91	92	93	94	95	96	97	98	99	100	101	102	103	104	105	106	107	108	109	110	111	112	113	114	115	116	117	118	119	120	121	122	123	124	125	126	127	128	129	130	131	132	133	134	135	136	137	138	139	140	141	142	143	144	145	146	147	148	149	150	151	152	153	154	155	156	157	158	159	160	161	162	163	164	165	166	167	168	169	170	171	172	173	174	175	176	177	178	179	180	181	182	183	184	185	186	187	188	189	190	191	192	193	194	195	196	197	198	199	200	201	202	203	204	205	206	207	208	209	210	211	212	213	214	215	216	217	218	219	220	221	222	223	224	225	226	227	228	229	230	231	232	233	234	235	236	237	238	239	240	241	242	243	244	245	246	247	248	249	250	251	252	253	254	255	256	257	258	259	260	261	262	263	264	265	266	267	268	269	270	271	272	273	274	275	276	277	278	279	280	281	282	283	284	285	286	287	288	289	290	291	292	293	294	295	296	297	298	299	300	301	302	303	304	305	306	307	308	309	310	311	312	313	314	315	316	317	318	319	320	321	322	323	324	325	326	327	328	329	330	331	332	333	334	335	336	337	338	339	340	341	342	343	344	345	346	347	348	349	350	351	352	353	354	355	356	357	358	359	360	361	362	363	364	365	366	367	368	369	370	371	372	373	374	375	376	377	378	379	380	381	382	383	384	385	386	387	388	389	390	391	392	393	394	395	396	397	398	399	400	401	402	403	404	405	406	407	408	409	410	411	412	413	414	415	416	417	418	419	420	421	422	423	424	425	426	427	428	429	430	431	432	433	434	435	436	437	438	439	440	441	442	443	444	445	446	447	448	449	450	451	452	453	454	455	456	457	458	459	460	461	462	463	464	465	466	467	468	469	470	471	472	473	474	475	476	477	478	479	480	481	482	483	484	485	486	487	488	489	490	491	492	493	494	495	496	497	498	499	500	501	502	503	504	505	506	507	508	509	510	511	512	513	514	515	516	517	518	519	520	521	522	523	524	525	526	527	528	529	530	531	532	533	534	535	536	537	538	539	540	541	542	543	544	545	546	547	548	549	550	551	552	553	554	555	556	557	558	559	560	561	562	563	564	565	566	567	568	569	570	571	572	573	574	575	576	577	578	579	580	581	582	583	584	585	586	587	588	589	590	591	592	593	594	595	596	597	598	599	600	601	602	603	604	605	606	607	608	609	610	611	612	613	614	615	616	617	618	619	620	621	622	623	624	625	626	627	628	629	630	631	632	633	634	635	636	637	638	639	640	641	642	643	644	645	646	647	648	649	650	651	652	653	654	655	656	657	658	659	660	661	662	663	664	665	666	667	668	669	670	671	672	673	674	675	676	677	678	679	680	681	682	683	684	685	686	687	688	689	690	691	692	693	694	695	696	697	698	699	700	701	702	703	704	705	706	707	708	709	7010	7011	7012	7013	7014	7015	7016	7017	7018	7019	7020	7021	7022	7023	7024	7025	7026	7027	7028	7029	7030	7031	7032	7033	7034	7035	7036	7037	7038	7039	7040	7041	7042	7043	7044	7045	7046	7047	7048	7049	7050	7051	7052	7053	7054	7055	7056	7057	7058	7059	7060	7061	7062	7063	7064	7065	7066	7067	7068	7069	7070	7071	7072	7073	7074	7075	7076	7077	7078	7079	7080	7081	7082	7083	7084	7085	7086	7087	7088	7089	7090	7091	7092	7093	7094	7095	7096	7097	7098	7099	70100	70101	70102	70103	70104	70105	70106	70107	70108	70109	70110	70111	70112	70113	70114	70115	70116	70117	70118	70119	70120	70121	70122	70123	70124	70125	70126	70127	70128	70129	70130	70131	70132	70133	70134	70135	70136	70137	70138	70139	70140	70141	70142	70143	70144	70145	70146	70147	70148	70149	70150	70151	70152	70153	70154	70155	70156	70157	70158	70159	70160	70161	70162	70163	70164	70165	70166	70167	70168	70169	70170	70171	70172	70173	70174	70175	70176	70177	70178	70179	70180	70181	70182	70183	70184	70185	70186	70187	70188	70189	70190	70191	70192	70193	70194	70195	70196	70197	70198	70199	70200	70201	70202	70203	70204	70205	70206	70207	70208	70209	70210	70211	70212	70213	70214	70215	70216	70217	70218	70219	70220	70221	70222	70223	70224	70225	70226	70227	70228	70229	70230	70231	70232	70233	70234	70235	70236	70237	70238	70239	70240	70241	70242	70243	70244	70245	70246	70247	70248	70249	70250	70251	70252	70253	70254	70255	70256	70257	70258	70259	70260	70261	70262	70263	70264	70265	70266	70267	70268	70269	70270	70271	70272	70273	70274	70275	70276	70277	70278	70279	70280	70281	70282	70283	70284	70285	70286	70287	70288	70289	70290	70291	70292	70293	70294	70295	70296	70297	70298	70299	70300	70301	70302	70303	70304	70305	70306	70307	70308	70309	70310	70311	70312	70313	70314	70315	70316	70317	70318	70319	70320	70321	70322	70323	70324	70325	70326	70327	70328	70329	70330	70331	70332	70333	70334	70335	70336	70337	70338	70339	70340	70341	70342	70343	70344	70345	70346	70347	70348	70349	70350	70351	70352	70353	70354	70355	70356	70357	70358	70359	70360	70361	70362	70363	70364	70365	70366	70367	70368	70369	70370	70371	70372	70373	70374	70375	70376	70377	70378	70379	70380	70381	70382	70383	70384	70385	70386	70387	70388	70389	70390	70391	70392	70393	70394	70395	70396	70397	70398	70399	70400	70401	70402	70403	70404	70405	70406	70407	70408	70409	70410	70411	70412	70413	70414	70415	70416	70417	70418	70419	70420	70421	70422	70423	70424	70425	70426	70427	70428	70429	70430	70431	70432	70433	70434	70435	70436	70437	70438	70439	70440	70441	70442	70443	70444	70445	70446	70447	70448	70449	70450	70451	70452	70453	70454	70455	70456	70457	70458	70459	70460	70461	70462	70463	70464	70465	70466	70467	70468	70469	70470	70471	70472	70473	70474	70475	70476	70477	70478	70479	70480	70481	70482	70483	70484	70485	70486	70487	70488	70489	70490	70491	70492	70493	70494	70495	70496	70497	70498	70499	70500	70501	70502	70503	70504	70505	70506	70507	70508	70509	70510	70511	70512	70513	70514	70515	70516	70517	70518	70519	70520	70521	70522	70523	70524	70525	70526	70527	70528	70529	70530	70531	70532	70533	70534	70535	70536	70537	70538	70539	70540	70541	70542	70543	70544	70545	70546	70547	70548	70549	70550	70551	70552	70553	70554	70555	70556	70557	70558	70559	70560	70561	70562	70563	70564	70565	70566	70567	70568	70569	70570	70571	70572	70573	70574	70575	70576	70577	70578	70579	70580	70581	70582	70583</td

15 16 17 18 19 20 21 22 23 24 25 26 27 28 29 30 31 32 33 34 35 36 37 38 39 40 41

.....

.....

.....

		PROPERTY CASES FOR TWO ELEMENTS WHICH HAVE FAILED			
		0.01	0.05		
CLASS	4400	7.032+3	100	-	-
CLASS	4401	1.104	100	-	-
CLASS	4402	7.032+3	110	-	-
				TRIANGLE NUMBER	
				2	
				222221	22
				222221	26
				222221	32
				222221	38
				222221	44
				222221	50
				222221	56
				222221	62
				222221	68
				222221	74
				222221	80
				222221	86
				222221	92
				222221	98
				222221	104
				222221	110
				222221	116
				222221	122
				222221	128
				222221	134
				222221	140
				222221	146
				222221	152
				222221	158
				222221	164
				222221	170
				222221	176
				222221	182
				222221	188
				222221	194
				222221	200
				222221	206
				222221	212
				222221	218
				222221	224
				222221	230
				222221	236
				222221	242
				222221	248
				222221	254
				222221	260
				222221	266
				222221	272
				222221	278
				222221	284
				222221	290
				222221	296
				222221	302
				222221	308
				222221	314
				222221	320
				222221	326
				222221	332
				222221	338
				222221	344
				222221	350
				222221	356
				222221	362
				222221	368
				222221	374
				222221	380
				222221	386
				222221	392
				222221	398
				222221	404
				222221	410
				222221	416
				222221	422
				222221	428
				222221	434
				222221	440
				222221	446
				222221	452
				222221	458
				222221	464
				222221	470
				222221	476
				222221	482
				222221	488
				222221	494
				222221	500
				222221	506
				222221	512
				222221	518
				222221	524
				222221	530
				222221	536
				222221	542
				222221	548
				222221	554
				222221	560
				222221	566
				222221	572
				222221	578
				222221	584
				222221	590
				222221	596
				222221	602
				222221	608
				222221	614
				222221	620
				222221	626
				222221	632
				222221	638
				222221	644
				222221	650
				222221	656
				222221	662
				222221	668
				222221	674
				222221	680
				222221	686
				222221	692
				222221	698
				222221	704
				222221	710
				222221	716
				222221	722
				222221	728
				222221	734
				222221	740
				222221	746
				222221	752
				222221	758
				222221	764
				222221	770
				222221	776
				222221	782
				222221	788
				222221	794
				222221	800
				222221	806
				222221	812
				222221	818
				222221	824
				222221	830
				222221	836
				222221	842
				222221	848
				222221	854
				222221	860
				222221	866
				222221	872
				222221	878
				222221	884
				222221	890
				222221	896
				222221	902
				222221	908
				222221	914
				222221	920
				222221	926
				222221	932
				222221	938
				222221	944
				222221	950
				222221	956
				222221	962
				222221	968
				222221	974
				222221	980
				222221	986
				222221	992
				222221	998
				222221	1004
				222221	1010
				222221	1016
				222221	1022
				222221	1028
				222221	1034
				222221	1040
				222221	1046
				222221	1052
				222221	1058
				222221	1064
				222221	1070
				222221	1076
				222221	1082
				222221	1088
				222221	1094
				222221	1100
				222221	1106
				222221	1112
				222221	1118
				222221	1124
				222221	1130
				222221	1136
				222221	1142
				222221	1148
				222221	1154
				222221	1160
				222221	1166
				222221	1172
				222221	1178
				222221	1184
				222221	1190
				222221	1196
				222221	1202
				222221	1208
				222221	1214
				222221	1220
				222221	1226
				222221	1232
				222221	1238
				222221	1244
				222221	1250
				222221	1256
				222221	1262
				222221	1268
				222221	1274
				222221	1280
				222221	1286
				222221	1292
				222221	1298
				222221	1304
				222221	1310
				222221	1316
				222221	1322
				222221	1328
				222221	1334
				222221	1340
				222221	1346
				222221	1352
				222221	1358
				222221	1364
				222221	1370
				222221	1376
				222221	1382
				222221	1388
				222221	1394
				222221	1400
				222221	1406
				222221	1412
				222221	1418
				222221	1424
				222221	1430
				222221	1436
				222221	1442
				222221	1448
				222221	1454
				222221	1460
				222221	1466
				222221	1472
				222221	1478
				222221	1484
				222221	1490
				222221	1496
				222221	1502
				222221	1508
				222221	1514
				222221	1520
				222221	1526
				222221	1532
				222221	1538
				222221	1544
				222221	1550
				222221	1556
				222221	1562
				222221	1568
				222221	1574
				222221	1580
				222221	1586
				222221	1592
				222221	1598
				222221	1604
				222221	1610
				222221	1616
				222221	1622
				222221	1628
				222221	1634

A scatter plot showing the relationship between Net Loading Conditions (Y-axis) and Range (X-axis). The Y-axis ranges from -2 to 4, and the X-axis ranges from 100 to 300. Data points are represented by small circles. A horizontal dashed line is drawn at Net Loading Condition = 0.

APPENDIX E

FINITE ELEMENT MODEL C LISTING

DATA DECK FOR
P-52 VINE PROJECT - UNARMED VINE
MODEL C STATIC CASE
SPARS AND RIBS: CROO AND CSHR
STRUTS: CROO
SEAL PANELS: CROO
NO TORSIONAL STIFFNESS IN SPANS

THE VINE ALUMINUM IS 100% TO 100% OF THE VINE AIRCRAFT STEEL
THE VINE SPAN RIBS ARE 9 CH-100 AIRCRAFT STEEL

DATA POINTS: TOP OF VINE

DATA POINTS: BOTTOM OF VINE

PROPERTY CARDS FOR BUCKLED SKIN PANELS ADJACENT TO DAMAGE		PROPERTY CARDS FOR BUCKLED SKIN PANELS AWAY FROM DAMAGE		PROPERTY CARDS FOR SKIN PANELS WHICH HAVE FAILED	
PoM1	2	222227	3	222227	3
PoM1	3	222228	3	222228	3
PoM1	4	222229	3	222229	3
PoM1	5	222230	3	222230	3
PoM1	6	222231	3	222231	3
PoM1	7	222232	3	222232	3
PoM1	8	222233	3	222233	3
PoM1	9	222234	3	222234	3
PoM1	10	222235	3	222235	3
PoM1	11	222236	3	222236	3
PoM1	12	222237	3	222237	3
PoM1	13	222238	3	222238	3
PoM1	14	222239	3	222239	3
PoM1	15	222240	3	222240	3
PoM1	16	222241	3	222241	3
PoM1	17	222242	3	222242	3
PoM1	18	222243	3	222243	3
PoM1	19	222244	3	222244	3
PoM1	20	222245	3	222245	3
PoM1	21	222246	3	222246	3
PoM1	22	222247	3	222247	3
PoM1	23	222248	3	222248	3
PoM1	24	222249	3	222249	3
PoM1	25	222250	3	222250	3
PoM1	26	222251	3	222251	3
PoM1	27	222252	3	222252	3
PoM1	28	222253	3	222253	3
PoM1	29	222254	3	222254	3
PoM1	30	222255	3	222255	3
PoM1	31	222256	3	222256	3
PoM1	32	222257	3	222257	3
PoM1	33	222258	3	222258	3
PoM1	34	222259	3	222259	3
PoM1	35	222260	3	222260	3
PoM1	36	222261	3	222261	3
PoM1	37	222262	3	222262	3
PoM1	38	222263	3	222263	3
PoM1	39	222264	3	222264	3
PoM1	40	222265	3	222265	3
PoM1	41	222266	3	222266	3
PoM1	42	222267	3	222267	3
PoM1	43	222268	3	222268	3
PoM1	44	222269	3	222269	3
PoM1	45	222270	3	222270	3
PoM1	46	222271	3	222271	3
PoM1	47	222272	3	222272	3
PoM1	48	222273	3	222273	3
PoM1	49	222274	3	222274	3
PoM1	50	222275	3	222275	3
PoM1	51	222276	3	222276	3
PoM1	52	222277	3	222277	3
PoM1	53	222278	3	222278	3
PoM1	54	222279	3	222279	3
PoM1	55	222280	3	222280	3
PoM1	56	222281	3	222281	3
PoM1	57	222282	3	222282	3
PoM1	58	222283	3	222283	3
PoM1	59	222284	3	222284	3
PoM1	60	222285	3	222285	3
PoM1	61	222286	3	222286	3
PoM1	62	222287	3	222287	3
PoM1	63	222288	3	222288	3
PoM1	64	222289	3	222289	3
PoM1	65	222290	3	222290	3
PoM1	66	222291	3	222291	3
PoM1	67	222292	3	222292	3
PoM1	68	222293	3	222293	3
PoM1	69	222294	3	222294	3
PoM1	70	222295	3	222295	3
PoM1	71	222296	3	222296	3
PoM1	72	222297	3	222297	3
PoM1	73	222298	3	222298	3
PoM1	74	222299	3	222299	3
PoM1	75	222300	3	222300	3
PoM1	76	222301	3	222301	3
PoM1	77	222302	3	222302	3
PoM1	78	222303	3	222303	3
PoM1	79	222304	3	222304	3
PoM1	80	222305	3	222305	3
PoM1	81	222306	3	222306	3
PoM1	82	222307	3	222307	3
PoM1	83	222308	3	222308	3
PoM1	84	222309	3	222309	3
PoM1	85	222310	3	222310	3
PoM1	86	222311	3	222311	3
PoM1	87	222312	3	222312	3
PoM1	88	222313	3	222313	3
PoM1	89	222314	3	222314	3
PoM1	90	222315	3	222315	3
PoM1	91	222316	3	222316	3
PoM1	92	222317	3	222317	3
PoM1	93	222318	3	222318	3
PoM1	94	222319	3	222319	3
PoM1	95	222320	3	222320	3
PoM1	96	222321	3	222321	3
PoM1	97	222322	3	222322	3
PoM1	98	222323	3	222323	3
PoM1	99	222324	3	222324	3
PoM1	100	222325	3	222325	3
PoM1	101	222326	3	222326	3
PoM1	102	222327	3	222327	3
PoM1	103	222328	3	222328	3
PoM1	104	222329	3	222329	3
PoM1	105	222330	3	222330	3
PoM1	106	222331	3	222331	3
PoM1	107	222332	3	222332	3
PoM1	108	222333	3	222333	3
PoM1	109	222334	3	222334	3
PoM1	110	222335	3	222335	3
PoM1	111	222336	3	222336	3
PoM1	112	222337	3	222337	3
PoM1	113	222338	3	222338	3
PoM1	114	222339	3	222339	3
PoM1	115	222340	3	222340	3
PoM1	116	222341	3	222341	3
PoM1	117	222342	3	222342	3
PoM1	118	222343	3	222343	3
PoM1	119	222344	3	222344	3
PoM1	120	222345	3	222345	3
PoM1	121	222346	3	222346	3
PoM1	122	222347	3	222347	3
PoM1	123	222348	3	222348	3
PoM1	124	222349	3	222349	3
PoM1	125	222350	3	222350	3
PoM1	126	222351	3	222351	3
PoM1	127	222352	3	222352	3
PoM1	128	222353	3	222353	3
PoM1	129	222354	3	222354	3
PoM1	130	222355	3	222355	3
PoM1	131	222356	3	222356	3
PoM1	132	222357	3	222357	3
PoM1	133	222358	3	222358	3
PoM1	134	222359	3	222359	3
PoM1	135	222360	3	222360	3
PoM1	136	222361	3	222361	3
PoM1	137	222362	3	222362	3
PoM1	138	222363	3	222363	3
PoM1	139	222364	3	222364	3
PoM1	140	222365	3	222365	3
PoM1	141	222366	3	222366	3
PoM1	142	222367	3	222367	3
PoM1	143	222368	3	222368	3
PoM1	144	222369	3	222369	3
PoM1	145	222370	3	222370	3
PoM1	146	222371	3	222371	3
PoM1	147	222372	3	222372	3
PoM1	148	222373	3	222373	3
PoM1	149	222374	3	222374	3
PoM1	150	222375	3	222375	3
PoM1	151	222376	3	222376	3
PoM1	152	222377	3	222377	3
PoM1	153	222378	3	222378	3
PoM1	154	222379	3	222379	3
PoM1	155	222380	3	222380	3
PoM1	156	222381	3	222381	3
PoM1	157	222382	3	222382	3
PoM1	158	222383	3	222383	3
PoM1	159	222384	3	222384	3
PoM1	160	222385	3	222385	3
PoM1	161	222386	3	222386	3
PoM1	162	222387	3	222387	3
PoM1	163	222388	3	222388	3
PoM1	164	222389	3	222389	3
PoM1	165	222390	3	222390	3
PoM1	166	222391	3	222391	3
PoM1	167	222392	3	222392	3
PoM1	168	222393	3	222393	3
PoM1	169	222394	3	222394	3
PoM1	170	222395	3	222395	3
PoM1	171	222396	3	222396	3
PoM1	172	222397	3	222397	3
PoM1	173	222398	3	222398	3
PoM1	174	222399	3	222399	3
PoM1	175	222400	3	222400	3
PoM1	176	222401	3	222401	3
PoM1	177	222402	3	222402	3
PoM1	178	222403	3	222403	3
PoM1	179	222404	3	222404	3
PoM1	180	222405	3	222405	3
PoM1	181	222406	3	222406	3
PoM1	182	222407	3	222407	3
PoM1	183	222408	3	222408	3
PoM1	184	222409	3	222409	3
PoM1	185	222410	3	222410	3
PoM1	186	222411	3	222411	3
PoM1	187	222412	3	222412	3
PoM1	188	222413	3	222413	3
PoM1	189	222414	3	222414	3
PoM1	190	222415	3	222415	3
PoM1	191	222416	3	222416	3
PoM1	192	222417	3	222417	3
PoM1	193	222418	3	222418	3
PoM1	194	222419	3	222419	3
PoM1	195	222420	3	222420	3
PoM1	196	222421	3	222421	3
PoM1	197	222422	3	222422	3
PoM1	198	222423	3	222423	3
PoM1	199	222424	3	222424	3
PoM1	200	222425	3	222425	3
PoM1	201	222426	3	222426	3
PoM1	202	222427	3	222427	3
PoM1	203	222428	3		

1-15
 1-16
 1-17
 1-18
 1-19
 1-20
 1-21
 1-22
 1-23
 1-24
 1-25
 1-26
 1-27
 1-28
 1-29
 1-30
 1-31
 1-32
 1-33
 1-34
 1-35
 1-36
 1-37
 1-38
 1-39
 1-40
 1-41
 1-42
 1-43
 1-44
 1-45
 1-46
 1-47
 1-48
 1-49
 1-50
 1-51
 1-52
 1-53
 1-54
 1-55
 1-56
 1-57
 1-58
 1-59
 1-60
 1-61
 1-62
 1-63
 1-64
 1-65
 1-66
 1-67
 1-68
 1-69
 1-70
 1-71
 1-72
 1-73
 1-74
 1-75
 1-76
 1-77
 1-78
 1-79
 1-80
 1-81
 1-82
 1-83
 1-84
 1-85
 1-86
 1-87
 1-88
 1-89
 1-90
 1-91
 1-92
 1-93
 1-94
 1-95
 1-96
 1-97
 1-98
 1-99
 1-100
 1-101
 1-102
 1-103
 1-104
 1-105
 1-106
 1-107
 1-108
 1-109
 1-110
 1-111
 1-112
 1-113
 1-114
 1-115
 1-116
 1-117
 1-118
 1-119
 1-120
 1-121
 1-122
 1-123
 1-124
 1-125
 1-126
 1-127
 1-128
 1-129
 1-130
 1-131
 1-132
 1-133
 1-134
 1-135
 1-136
 1-137
 1-138
 1-139
 1-140
 1-141
 1-142
 1-143
 1-144
 1-145
 1-146
 1-147
 1-148
 1-149
 1-150
 1-151
 1-152
 1-153
 1-154
 1-155
 1-156
 1-157
 1-158
 1-159
 1-160
 1-161
 1-162
 1-163
 1-164
 1-165
 1-166
 1-167
 1-168
 1-169
 1-170
 1-171
 1-172
 1-173
 1-174
 1-175
 1-176
 1-177
 1-178
 1-179
 1-180
 1-181
 1-182
 1-183
 1-184
 1-185
 1-186
 1-187
 1-188
 1-189
 1-190
 1-191
 1-192
 1-193
 1-194
 1-195
 1-196
 1-197
 1-198
 1-199
 1-200
 1-201
 1-202
 1-203
 1-204
 1-205
 1-206
 1-207
 1-208
 1-209
 1-210
 1-211
 1-212
 1-213
 1-214
 1-215
 1-216
 1-217
 1-218
 1-219
 1-220
 1-221
 1-222
 1-223
 1-224
 1-225
 1-226
 1-227
 1-228
 1-229
 1-230
 1-231
 1-232
 1-233
 1-234
 1-235
 1-236
 1-237
 1-238
 1-239
 1-240
 1-241
 1-242
 1-243
 1-244
 1-245
 1-246
 1-247
 1-248
 1-249
 1-250
 1-251
 1-252
 1-253
 1-254
 1-255
 1-256
 1-257
 1-258
 1-259
 1-260
 1-261
 1-262
 1-263
 1-264
 1-265
 1-266
 1-267
 1-268
 1-269
 1-270
 1-271
 1-272
 1-273
 1-274
 1-275
 1-276
 1-277
 1-278
 1-279
 1-280
 1-281
 1-282
 1-283
 1-284
 1-285
 1-286
 1-287
 1-288
 1-289
 1-290
 1-291
 1-292
 1-293
 1-294
 1-295
 1-296
 1-297
 1-298
 1-299
 1-300
 1-301
 1-302
 1-303
 1-304
 1-305
 1-306
 1-307
 1-308
 1-309
 1-310
 1-311
 1-312
 1-313
 1-314
 1-315
 1-316
 1-317
 1-318
 1-319
 1-320
 1-321
 1-322
 1-323
 1-324
 1-325
 1-326
 1-327
 1-328
 1-329
 1-330
 1-331
 1-332
 1-333
 1-334
 1-335
 1-336
 1-337
 1-338
 1-339
 1-340
 1-341
 1-342
 1-343
 1-344
 1-345
 1-346
 1-347
 1-348
 1-349
 1-350
 1-351
 1-352
 1-353
 1-354
 1-355
 1-356
 1-357
 1-358
 1-359
 1-360
 1-361
 1-362
 1-363
 1-364
 1-365
 1-366
 1-367
 1-368
 1-369
 1-370
 1-371
 1-372
 1-373
 1-374
 1-375
 1-376
 1-377
 1-378
 1-379
 1-380
 1-381
 1-382
 1-383
 1-384
 1-385
 1-386
 1-387
 1-388
 1-389
 1-390
 1-391
 1-392
 1-393
 1-394
 1-395
 1-396
 1-397
 1-398
 1-399
 1-400
 1-401
 1-402
 1-403
 1-404
 1-405
 1-406
 1-407
 1-408
 1-409
 1-410
 1-411
 1-412
 1-413
 1-414
 1-415
 1-416
 1-417
 1-418
 1-419
 1-420
 1-421
 1-422
 1-423
 1-424
 1-425
 1-426
 1-427
 1-428
 1-429
 1-430
 1-431
 1-432
 1-433
 1-434
 1-435
 1-436
 1-437
 1-438
 1-439
 1-440
 1-441
 1-442
 1-443
 1-444
 1-445
 1-446
 1-447
 1-448
 1-449
 1-450
 1-451
 1-452
 1-453
 1-454
 1-455
 1-456
 1-457
 1-458
 1-459
 1-460
 1-461
 1-462
 1-463
 1-464
 1-465
 1-466
 1-467
 1-468
 1-469
 1-470
 1-471
 1-472
 1-473
 1-474
 1-475
 1-476
 1-477
 1-478
 1-479
 1-480
 1-481
 1-482
 1-483
 1-484
 1-485
 1-486
 1-487
 1-488
 1-489
 1-490
 1-491
 1-492
 1-493
 1-494
 1-495
 1-496
 1-497
 1-498
 1-499
 1-500
 1-501
 1-502
 1-503
 1-504
 1-505
 1-506
 1-507
 1-508
 1-509
 1-510
 1-511
 1-512
 1-513
 1-514
 1-515
 1-516
 1-517
 1-518
 1-519
 1-520
 1-521
 1-522
 1-523
 1-524
 1-525
 1-526
 1-527
 1-528
 1-529
 1-530
 1-531
 1-532
 1-533
 1-534
 1-535
 1-536
 1-537
 1-538
 1-539
 1-540
 1-541
 1-542
 1-543
 1-544
 1-545
 1-546
 1-547
 1-548
 1-549
 1-550
 1-551
 1-552
 1-553
 1-554
 1-555
 1-556
 1-557
 1-558
 1-559
 1-560
 1-561
 1-562
 1-563
 1-564
 1-565
 1-566
 1-567
 1-568
 1-569
 1-570
 1-571
 1-572
 1-573
 1-574
 1-575
 1-576
 1-577
 1-578
 1-579
 1-580
 1-581
 1-582
 1-583
 1-584
 1-585
 1-586
 1-587
 1-588
 1-589
 1-590
 1-591
 1-592
 1-593
 1-594
 1-595
 1-596
 1-597
 1-598
 1-599
 1-600
 1-601
 1-602
 1-603
 1-604
 1-605
 1-606
 1-607
 1-608
 1-609
 1-610
 1-611
 1-612
 1-613
 1-614
 1-615
 1-616
 1-617
 1-618
 1-619
 1-620
 1-621
 1-622
 1-623
 1-624
 1-625
 1-626
 1-627
 1-628
 1-629
 1-630
 1-631
 1-632
 1-633
 1-634
 1-635
 1-636
 1-637
 1-638
 1-639
 1-640
 1-641
 1-642
 1-643
 1-644
 1-645
 1-646
 1-647
 1-648
 1-649
 1-650
 1-651
 1-652
 1-653
 1-654
 1-655
 1-656
 1-657
 1-658
 1-659
 1-660
 1-661
 1-662
 1-663
 1-664
 1-665
 1-666
 1-667
 1-668
 1-669
 1-670
 1-671
 1-672
 1-673
 1-674
 1-675
 1-676
 1-677
 1-678
 1-679
 1-680
 1-681
 1-682
 1-683
 1-684
 1-685
 1-686
 1-687
 1-688
 1-689
 1-690
 1-691
 1-692
 1-693
 1-694
 1-695
 1-696
 1-697
 1-698
 1-699
 1-700
 1-701
 1-702
 1-703
 1-704
 1-705
 1-706
 1-707
 1-708
 1-709
 1-710
 1-711
 1-712
 1-713
 1-714
 1-715
 1-716
 1-717
 1-718
 1-719
 1-720
 1-721
 1-722
 1-723
 1-724
 1-725
 1-726
 1-727
 1-728
 1-729
 1-730
 1-731
 1-732
 1-733
 1-734
 1-735
 1-736
 1-737
 1-738
 1-739
 1-740
 1-741
 1-742
 1-743
 1-744
 1-745
 1-746
 1-747
 1-748
 1-749
 1-750
 1-751
 1-752
 1-753
 1-754
 1-755
 1-756
 1-757
 1-758
 1-759
 1-760
 1-761
 1-762
 1-763
 1-764
 1-765
 1-766
 1-767
 1-768
 1-769
 1-770
 1-771
 1-772
 1-773
 1-774
 1-775
 1-776
 1-777
 1-778
 1-779
 1-780
 1-781
 1-782
 1-783
 1-784
 1-785
 1-786
 1-787
 1-788
 1-789
 1-790
 1-791
 1-792
 1-793
 1-794
 1-795
 1-796
 1-797
 1-798
 1-799
 1-800
 1-801
 1-802
 1-803
 1-804
 1-805
 1-806
 1-807
 1-808
 1-809
 1-810
 1-811
 1-812
 1-813
 1-814
 1-815
 1-816
 1-817
 1-818
 1-819
 1-820
 1-821
 1-822
 1-823
 1-824
 1-825
 1-826
 1-827
 1-828
 1-829
 1-830
 1-831
 1-832
 1-833
 1-834
 1-835
 1-836
 1-837
 1-838
 1-839
 1-840
 1-841
 1-842
 1-843
 1-844
 1-845
 1-846
 1-847
 1-848
 1-849
 1-850
 1-851
 1-852
 1-853
 1-854
 1-855
 1-856
 1-857
 1-858
 1-859
 1-860
 1-861
 1-862
 1-863
 1-864
 1-865
 1-866
 1-867
 1-868
 1-869
 1-870
 1-871
 1-872
 1-873
 1-874
 1-875
 1-876
 1-877
 1-878
 1-879
 1-880
 1-881
 1-882
 1-883
 1-884
 1-885
 1-886
 1-887
 1-888
 1-889
 1-890
 1-891
 1-892
 1-893
 1-894
 1-895
 1-896
 1-897
 1-898
 1-899
 1-900
 1-901
 1-902
 1-903
 1-904
 1-905
 1-906
 1-907
 1-908
 1-909
 1-910
 1-911
 1-912
 1-913
 1-914
 1-915
 1-916
 1-917
 1-918
 1-919
 1-920
 1-921
 1-922
 1-923
 1-924
 1-925
 1-926
 1-927
 1-928
 1-929
 1-930
 1-931
 1-932
 1-933
 1-934
 1-935
 1-936
 1-937
 1-938
 1-939
 1-940
 1-941
 1-942
 1-943
 1-944
 1-945
 1-946
 1-947
 1-948
 1-949
 1-950
 1-951
 1-952
 1-953
 1-954
 1-955
 1-956
 1-957
 1-958
 1-959
 1-960
 1-961
 1-962
 1-963
 1-964
 1-965
 1-966
 1-967
 1-968
 1-969
 1-970
 1-971
 1-972
 1-973
 1-974
 1-975
 1-976
 1-977
 1-978
 1-979
 1-980
 1-981
 1-982
 1-983
 1-984
 1-985
 1-986
 1-987
 1-988
 1-989
 1-990
 1-991
 1-992
 1-993
 1-994
 1-995
 1-996
 1-997
 1-998
 1-999
 1-1000

PROPERTY CARDS FOR TWO ELEMENTS AWAY FROM EDGE

FOR HOLES BETWEEN SPARS, PANELS 0 AND 7

FOR HOLES BETWEEN SPARS, PANELS 1 THRU 9

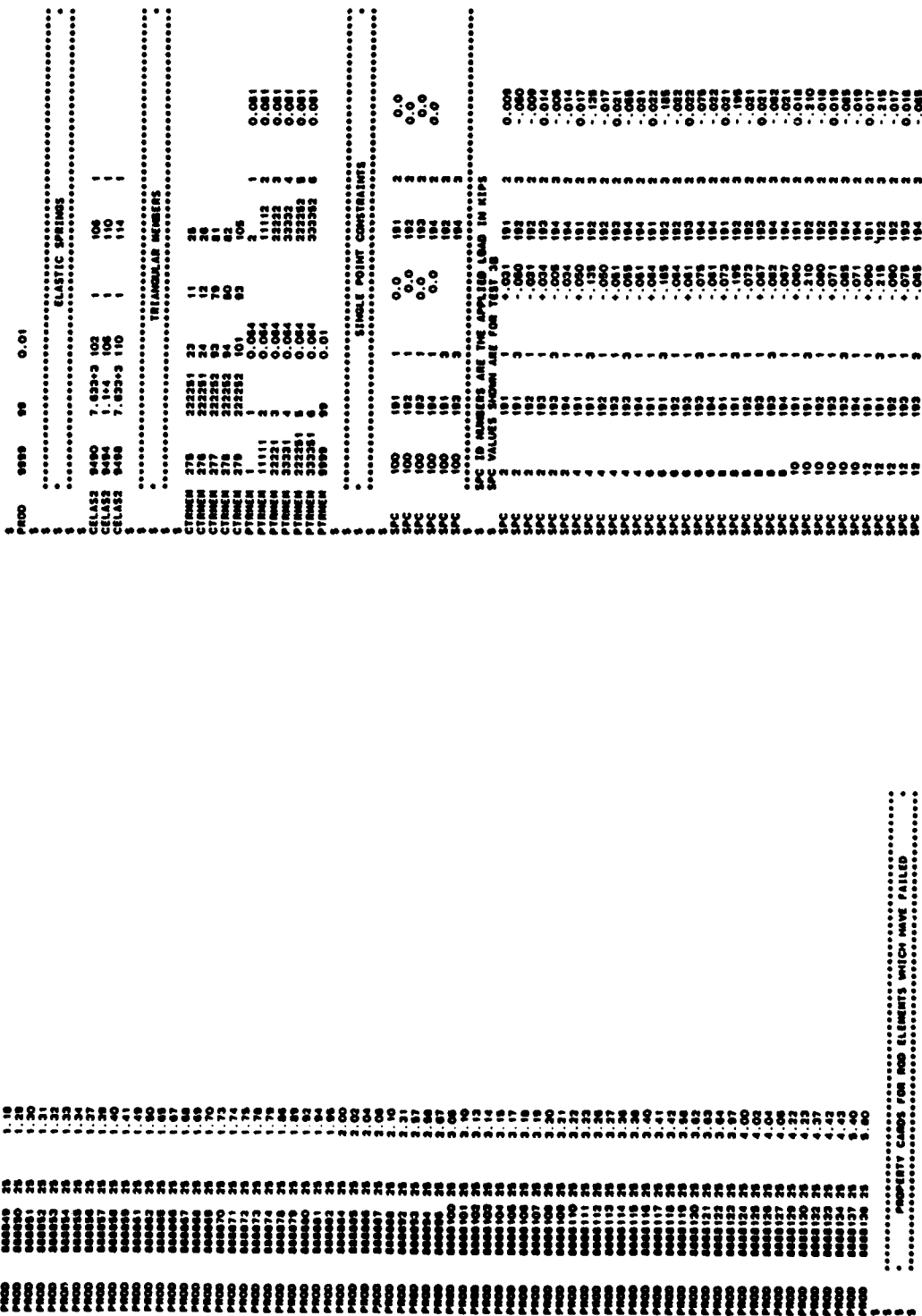
FOR HOLES BETWEEN FORWARD SPAR AND LEADING EDGE AND

FOR HOLES BETWEEN SPARS, PANELS 1 THRU 9

FOR HOLES IN SPARS AND FOR ALL VERTICAL HOLES

FOR 2000S BETWEEN SPANS AND LEADING EDGE AND
FOR 2000S BETWEEN SPANS. PANELS 1 THRU 9

1-1670
1-1671
1-1672
1-1673
1-1674
1-1675
1-1676
1-1677
1-1678
1-1679
1-1680
1-1681
1-1682
1-1683
1-1684
1-1685
1-1686
1-1687
1-1688
1-1689
1-1690
1-1691
1-1692
1-1693
1-1694
1-1695
1-1696
1-1697
1-1698
1-1699
1-1700
1-1701
1-1702
1-1703
1-1704
1-1705
1-1706
1-1707
1-1708
1-1709
1-1710
1-1711
1-1712
1-1713
1-1714
1-1715
1-1716
1-1717
1-1718
1-1719
1-1720
1-1721
1-1722
1-1723
1-1724
1-1725
1-1726
1-1727
1-1728
1-1729
1-1730
1-1731
1-1732
1-1733
1-1734
1-1735
1-1736
1-1737
1-1738



SC	12	194	1	- .075	194	2	- .016
MULTIPOINT CONSTRAINTS							
	100	104	1	- 1.0			
	100	104	2	- 1.0			
	100	104	3	- 1.0			
	100	104	4	- 1.0			
	100	104	5	- 1.0			
	100	104	6	- 1.0			
	100	104	7	- 1.0			
	100	104	8	- 1.0			
	100	104	9	- 1.0			
	100	104	10	- 1.0			
	100	104	11	- 1.0			
	100	104	12	- 1.0			
	100	104	13	- 1.0			
	100	104	14	- 1.0			
	100	104	15	- 1.0			
	100	104	16	- 1.0			
	100	104	17	- 1.0			
	100	104	18	- 1.0			
	100	104	19	- 1.0			
	100	104	20	- 1.0			
	100	104	21	- 1.0			
	100	104	22	- 1.0			
	100	104	23	- 1.0			
	100	104	24	- 1.0			
	100	104	25	- 1.0			
	100	104	26	- 1.0			
	100	104	27	- 1.0			
	100	104	28	- 1.0			
	100	104	29	- 1.0			
	100	104	30	- 1.0			
	100	104	31	- 1.0			
	100	104	32	- 1.0			
	100	104	33	- 1.0			
	100	104	34	- 1.0			
	100	104	35	- 1.0			
	100	104	36	- 1.0			
	100	104	37	- 1.0			
	100	104	38	- 1.0			
	100	104	39	- 1.0			
	100	104	40	- 1.0			
	100	104	41	- 1.0			
	100	104	42	- 1.0			
	100	104	43	- 1.0			
	100	104	44	- 1.0			
	100	104	45	- 1.0			
	100	104	46	- 1.0			
	100	104	47	- 1.0			
	100	104	48	- 1.0			
	100	104	49	- 1.0			
	100	104	50	- 1.0			
	100	104	51	- 1.0			
	100	104	52	- 1.0			
	100	104	53	- 1.0			
	100	104	54	- 1.0			
	100	104	55	- 1.0			
	100	104	56	- 1.0			
	100	104	57	- 1.0			
	100	104	58	- 1.0			
	100	104	59	- 1.0			
	100	104	60	- 1.0			
	100	104	61	- 1.0			
	100	104	62	- 1.0			
	100	104	63	- 1.0			
	100	104	64	- 1.0			
	100	104	65	- 1.0			
	100	104	66	- 1.0			
	100	104	67	- 1.0			
	100	104	68	- 1.0			
	100	104	69	- 1.0			
	100	104	70	- 1.0			
	100	104	71	- 1.0			
	100	104	72	- 1.0			
	100	104	73	- 1.0			
	100	104	74	- 1.0			
	100	104	75	- 1.0			
	100	104	76	- 1.0			
	100	104	77	- 1.0			
	100	104	78	- 1.0			
	100	104	79	- 1.0			
	100	104	80	- 1.0			
	100	104	81	- 1.0			
	100	104	82	- 1.0			
	100	104	83	- 1.0			
	100	104	84	- 1.0			
	100	104	85	- 1.0			
	100	104	86	- 1.0			
	100	104	87	- 1.0			
	100	104	88	- 1.0			
	100	104	89	- 1.0			
	100	104	90	- 1.0			
	100	104	91	- 1.0			
	100	104	92	- 1.0			
	100	104	93	- 1.0			
	100	104	94	- 1.0			
	100	104	95	- 1.0			
	100	104	96	- 1.0			
	100	104	97	- 1.0			
	100	104	98	- 1.0			
	100	104	99	- 1.0			
	100	104	100	- 1.0			

SC	12	194	1	- .075	194	2	- .016
MATERIAL CARDS FOR SPANS AND RIBS AWAY FROM DAMAGE							
	11	10.306	2.976	3.14-3			
	12	7.764	2.624				
	13	10.306	3.966	3.14-3			
	14	9.310	2.974				
	15	10.306	3.966	3.14-3			
	16	9.310	2.974				
	17	10.306	3.966	3.14-3			
	18	9.310	2.974				
	19	10.306	3.966	3.14-3			
	20	9.310	2.974				
	21	10.306	3.966	3.14-3			
	22	10.306	3.966	3.14-3			
	23	10.306	3.966	3.14-3			
	24	10.306	3.966	3.14-3			
	25	10.306	3.966	3.14-3			
	26	10.306	3.966	3.14-3			
	27	10.306	3.966	3.14-3			
	28	10.306	3.966	3.14-3			
	29	10.306	3.966	3.14-3			
	30	10.306	3.966	3.14-3			
	31	10.306	3.966	3.14-3			
	32	10.306	3.966	3.14-3			
	33	10.306	3.966	3.14-3			
	34	10.306	3.966	3.14-3			
	35	10.306	3.966	3.14-3			
	36	10.306	3.966	3.14-3			
	37	10.306	3.966	3.14-3			
	38	10.306	3.966	3.14-3			
	39	10.306	3.966	3.14-3			
	40	10.306	3.966	3.14-3			
	41	10.306	3.966	3.14-3			
	42	10.306	3.966	3.14-3			
	43	10.306	3.966	3.14-3			
	44	10.306	3.966	3.14-3			
	45	10.306	3.966	3.14-3			
	46	10.306	3.966	3.14-3			
	47	10.306	3.966	3.14-3			
	48	10.306	3.966	3.14-3			
	49	10.306	3.966	3.14-3			
	50	10.306	3.966	3.14-3			
	51	10.306	3.966	3.14-3			
	52	10.306	3.966	3.14-3			
	53	10.306	3.966	3.14-3			
	54	10.306	3.966	3.14-3			
	55	10.306	3.966	3.14-3			
	56	10.306	3.966	3.14-3			
	57	10.306	3.966	3.14-3			
	58	10.306	3.966	3.14-3			
	59	10.306	3.966	3.14-3			
	60	10.306	3.966	3.14-3			
	61	10.306	3.966	3.14-3			
	62	10.306	3.966	3.14-3			
	63	10.306	3.966	3.14-3			
	64	10.306	3.966	3.14-3			
	65	10.306	3.966	3.14-3			
	66	10.306	3.966	3.14-3			
	67	10.306	3.966	3.14-3			
	68	10.306	3.966	3.14-3			
	69	10.306	3.966	3.14-3			
	70	10.306	3.966	3.14-3			
	71	10.306	3.966	3.14-3			
	72	10.306	3.966	3.14-3			
	73	10.306	3.966	3.14-3			
	74	10.306	3.966	3.14-3			
	75	10.306	3.966	3.14-3			
	76	10.306	3.966	3.14-3			
	77	10.306	3.966	3.14-3			
	78	10.306	3.966	3.14-3			
	79	10.306	3.966	3.14-3			
	80	10.306	3.966	3.14-3			
	81	10.306	3.966	3.14-3			
	82	10.306	3.966	3.14-3			
	83	10.306	3.966	3.14-3			
	84	10.306	3.966	3.14-3			
	85	10.306	3.966	3.14-3			
	86	10.306	3.966	3.14-3			
	87	10.306	3.966	3.14-3			
	88	10.306	3.966	3.14-3			
	89	10.306	3.966	3.14-3			
	90	10.306	3.966	3.14-3			
	91	10.306	3.966	3.14-3			
	92	10.306	3.966	3.14-3			
	93	10.306	3.966	3.14-3			
	94	10.306	3.966	3.14-3			
	95	10.306	3.966	3.14-3			
	96	10.306	3.966	3.14-3			
	97	10.306	3.966	3.14-3			
	98	10.306	3.966	3.14-3			
	99	10.306	3.966	3.14-3			
	100						

APPENDIX F

FINITE ELEMENT TORSIONAL ROD LISTING

These cards convert wind input A to model B by adding torsional stiffness to the front spar and to the rear spar.

Coordinate System Definitions for Tension

Card #	Line #	Front Spar Centerline	Rear Spar Centerline
1000	1	114	114
1000	2	3000	3000
1000	3	0.0	0.0
1000	4	0.0	0.0
1000	5	0.0	0.0
1000	6	0.0	0.0
1000	7	0.0	0.0
1000	8	0.0	0.0
1000	9	0.0	0.0
1000	10	0.0	0.0
1000	11	0.0	0.0
1000	12	0.0	0.0
1000	13	0.0	0.0
1000	14	0.0	0.0
1000	15	0.0	0.0
1000	16	0.0	0.0
1000	17	0.0	0.0
1000	18	0.0	0.0
1000	19	0.0	0.0
1000	20	0.0	0.0
1000	21	0.0	0.0
1000	22	0.0	0.0
1000	23	0.0	0.0
1000	24	0.0	0.0
1000	25	0.0	0.0
1000	26	0.0	0.0
1000	27	0.0	0.0
1000	28	0.0	0.0
1000	29	0.0	0.0
1000	30	0.0	0.0
1000	31	0.0	0.0
1000	32	0.0	0.0
1000	33	0.0	0.0
1000	34	0.0	0.0
1000	35	0.0	0.0
1000	36	0.0	0.0
1000	37	0.0	0.0
1000	38	0.0	0.0
1000	39	0.0	0.0
1000	40	0.0	0.0
1000	41	0.0	0.0
1000	42	0.0	0.0
1000	43	0.0	0.0
1000	44	0.0	0.0
1000	45	0.0	0.0
1000	46	0.0	0.0
1000	47	0.0	0.0
1000	48	0.0	0.0
1000	49	0.0	0.0
1000	50	0.0	0.0
1000	51	0.0	0.0
1000	52	0.0	0.0
1000	53	0.0	0.0
1000	54	0.0	0.0
1000	55	0.0	0.0
1000	56	0.0	0.0
1000	57	0.0	0.0
1000	58	0.0	0.0
1000	59	0.0	0.0
1000	60	0.0	0.0
1000	61	0.0	0.0
1000	62	0.0	0.0
1000	63	0.0	0.0
1000	64	0.0	0.0
1000	65	0.0	0.0
1000	66	0.0	0.0
1000	67	0.0	0.0
1000	68	0.0	0.0
1000	69	0.0	0.0
1000	70	0.0	0.0
1000	71	0.0	0.0
1000	72	0.0	0.0
1000	73	0.0	0.0
1000	74	0.0	0.0
1000	75	0.0	0.0
1000	76	0.0	0.0
1000	77	0.0	0.0
1000	78	0.0	0.0
1000	79	0.0	0.0
1000	80	0.0	0.0
1000	81	0.0	0.0
1000	82	0.0	0.0
1000	83	0.0	0.0
1000	84	0.0	0.0
1000	85	0.0	0.0
1000	86	0.0	0.0
1000	87	0.0	0.0
1000	88	0.0	0.0
1000	89	0.0	0.0
1000	90	0.0	0.0
1000	91	0.0	0.0
1000	92	0.0	0.0
1000	93	0.0	0.0
1000	94	0.0	0.0
1000	95	0.0	0.0
1000	96	0.0	0.0
1000	97	0.0	0.0
1000	98	0.0	0.0
1000	99	0.0	0.0
1000	100	0.0	0.0
1000	101	0.0	0.0
1000	102	0.0	0.0
1000	103	0.0	0.0
1000	104	0.0	0.0
1000	105	0.0	0.0
1000	106	0.0	0.0
1000	107	0.0	0.0
1000	108	0.0	0.0
1000	109	0.0	0.0
1000	110	0.0	0.0
1000	111	0.0	0.0
1000	112	0.0	0.0
1000	113	0.0	0.0
1000	114	0.0	0.0
1000	115	0.0	0.0
1000	116	0.0	0.0
1000	117	0.0	0.0
1000	118	0.0	0.0
1000	119	0.0	0.0
1000	120	0.0	0.0
1000	121	0.0	0.0
1000	122	0.0	0.0
1000	123	0.0	0.0
1000	124	0.0	0.0
1000	125	0.0	0.0
1000	126	0.0	0.0
1000	127	0.0	0.0
1000	128	0.0	0.0
1000	129	0.0	0.0
1000	130	0.0	0.0
1000	131	0.0	0.0
1000	132	0.0	0.0
1000	133	0.0	0.0
1000	134	0.0	0.0
1000	135	0.0	0.0
1000	136	0.0	0.0
1000	137	0.0	0.0
1000	138	0.0	0.0
1000	139	0.0	0.0
1000	140	0.0	0.0
1000	141	0.0	0.0
1000	142	0.0	0.0
1000	143	0.0	0.0
1000	144	0.0	0.0
1000	145	0.0	0.0
1000	146	0.0	0.0
1000	147	0.0	0.0
1000	148	0.0	0.0
1000	149	0.0	0.0
1000	150	0.0	0.0
1000	151	0.0	0.0
1000	152	0.0	0.0
1000	153	0.0	0.0
1000	154	0.0	0.0
1000	155	0.0	0.0
1000	156	0.0	0.0
1000	157	0.0	0.0
1000	158	0.0	0.0
1000	159	0.0	0.0
1000	160	0.0	0.0
1000	161	0.0	0.0
1000	162	0.0	0.0
1000	163	0.0	0.0
1000	164	0.0	0.0
1000	165	0.0	0.0
1000	166	0.0	0.0
1000	167	0.0	0.0
1000	168	0.0	0.0
1000	169	0.0	0.0
1000	170	0.0	0.0
1000	171	0.0	0.0
1000	172	0.0	0.0
1000	173	0.0	0.0
1000	174	0.0	0.0
1000	175	0.0	0.0
1000	176	0.0	0.0
1000	177	0.0	0.0
1000	178	0.0	0.0
1000	179	0.0	0.0
1000	180	0.0	0.0
1000	181	0.0	0.0
1000	182	0.0	0.0
1000	183	0.0	0.0
1000	184	0.0	0.0
1000	185	0.0	0.0
1000	186	0.0	0.0
1000	187	0.0	0.0
1000	188	0.0	0.0
1000	189	0.0	0.0
1000	190	0.0	0.0
1000	191	0.0	0.0
1000	192	0.0	0.0
1000	193	0.0	0.0
1000	194	0.0	0.0
1000	195	0.0	0.0
1000	196	0.0	0.0
1000	197	0.0	0.0
1000	198	0.0	0.0
1000	199	0.0	0.0
1000	200	0.0	0.0
1000	201	0.0	0.0
1000	202	0.0	0.0
1000	203	0.0	0.0
1000	204	0.0	0.0
1000	205	0.0	0.0
1000	206	0.0	0.0
1000	207	0.0	0.0
1000	208	0.0	0.0
1000	209	0.0	0.0
1000	210	0.0	0.0
1000	211	0.0	0.0
1000	212	0.0	0.0
1000	213	0.0	0.0
1000	214	0.0	0.0
1000	215	0.0	0.0
1000	216	0.0	0.0
1000	217	0.0	0.0
1000	218	0.0	0.0
1000	219	0.0	0.0
1000	220	0.0	0.0
1000	221	0.0	0.0
1000	222	0.0	0.0
1000	223	0.0	0.0
1000	224	0.0	0.0
1000	225	0.0	0.0
1000	226	0.0	0.0
1000	227	0.0	0.0
1000	228	0.0	0.0
1000	229	0.0	0.0
1000	230	0.0	0.0
1000	231	0.0	0.0
1000	232	0.0	0.0
1000	233	0.0	0.0
1000	234	0.0	0.0
1000	235	0.0	0.0
1000	236	0.0	0.0
1000	237	0.0	0.0
1000	238	0.0	0.0
1000	239	0.0	0.0
1000	240	0.0	0.0
1000	241	0.0	0.0
1000	242	0.0	0.0
1000	243	0.0	0.0
1000	244	0.0	0.0
1000	245	0.0	0.0
1000	246	0.0	0.0
1000	247	0.0	0.0
1000	248	0.0	0.0
1000	249	0.0	0.0
1000	250	0.0	0.0
1000	251	0.0	0.0
1000	252	0.0	0.0
1000	253	0.0	0.0
1000	254	0.0	0.0
1000	255	0.0	0.0
1000	256	0.0	0.0
1000	257	0.0	0.0
1000	258	0.0	0.0
1000	259	0.0	0.0
1000	260	0.0	0.0
1000	261	0.0	0.0
1000	262	0.0	0.0
1000	263	0.0	0.0
1000	264	0.0	0.0
1000	265	0.0	0.0
1000	266	0.0	0.0
1000	267	0.0	0.0
1000	268	0.0	0.0
1000	269	0.0	0.0
1000	270	0.0	0.0
1000	271	0.0	0.0
1000	272	0.0	0.0
1000	273	0.0	0.0
1000	274	0.0	0.0
1000	275	0.0	0.0
1000	276	0.0	0.0
1000	277	0.0	0.0
1000	278	0.0	0.0
1000	279	0.0	0.0
1000	280	0.0	0.0
1000	281	0.0	0.0
1000	282	0.0	0.0
1000	283	0.0	0.0
1000	284	0.0	0.0
1000	285	0.0	0.0
1000	286	0.0	0.0
1000	287	0.0	0.0
1000	288	0.0	0.0
1000	289	0.0	0.0
1000	290	0.0	0.0
1000	291	0.0	0.0
1000	292	0.0	0.0
1000	293	0.0	0.0
1000	294	0.0	0.0
1000	295	0.0	0.0
1000	296	0.0	0.0
1000	297	0.0	0.0
1000	298	0.0	0.0
1000	299	0.0	0.0
1000	300	0.0	0.0
1000	301	0.0	0.0
1000	302	0.0	0.0
1000	303	0.0	0.0
1000	304	0.0	0.0
1000	305	0.0	

APPENDIX G

FINITE ELEMENT INITIAL DAMAGE MODELING

BULK DATA DECK FOR TEST 1 (SIMPLE DAMAGE)
F-BAR VING PROJECT - DAMAGED VING
MODEL A - STATIC CASE
SPARS AND RIBS CROWN AND COWSHR
STIFFENERS CROWN
SKIN PANELS COWSHR
NO TENSIONAL STIFFNESS IN SPARS

卷之三

VEGETAL TISSUE

NEU 247	NEW P10-3333902	OLD P10-2122202
NEU 248	NEW P10-3333901	OLD P10-21222402
NEU 249	NEW P10-3333901	OLD P10-21222501

Digitized by srujanika@gmail.com

BULK DATA BACK UP TEST - (SAMPLE CHANNEL)	
7-01	VINYL PRODUCT - BLENDED VINE
7-02	WAX
7-03	STATIC CASH
SPARES	LINE ITEM
7-04	CD-ROM AND CD-RW
7-05	CD-R
7-06	CD-RW
7-07	SCSI DRIVE
7-08	SCSI BACKUP

• • • • •

BULK DATA DECK FOR TEST 2C
F-SAF WING PROJECT - DAMAGED WING
MODEL A - STATIC CASE
SPARS AND RIBS - CROD AND CSHEAR
STIFFENERS - CROD
SKIN PANELS - CSHEAR
NO TORSIONAL STIFFNESS IN SPARS

SHEAR PANELS - TOP OF WING

CHANGE CROD 83 NEW PID-9999 OLD PID-322292
CHANGE CROD 84 NEW PID-11112 OLD PID-2

VERTICAL SHEAR PANELS

CHANGE CSHEAR 237 NEW PID-9999 OLD PID-3222401

HORIZONTAL RODS

CHANGE CROD 500 NEW PID-9999 OLD PID-322252
CHANGE CROD 510 NEW PID-9999 OLD PID-322253
CHANGE CROD 511 NEW PID-9999 OLD PID-322254

SPECIAL PROPERTY AND MATERIAL CARDS FOR INITIAL DAMAGE

MA11	99	10.0	5.0	3.14-3	•499
MA99	99.99	99.99	99.99	99.99	PROD
				99.99	0.49

•499

BULK DATA DECK FOR TEST 28
F-SAF WIND PROJECT - DAMAGED WIND
MODEL A - STATIC CASE
SPANS AND RIBS: CROD AND CSHEAR
STIFFNESS: CROD
SHELL PANELS: CSHEAR
NO TORSIONAL STIFFNESS IN SPARS

SHEAR PANELS - BOTTOM OF WIND

CHANGE CROD 102 AND 104 NEW PID-0000 OLD PID-222252
CHANGE CROD 106 AND 108 NEW PID-0000 OLD PID-2

VERTICAL SHEAR PANELS

CHANGE CSHEAR 237 NEW PID-111101 OLD PID-222201
CHANGE CSHEAR 243 NEW PID-111118 OLD PID-222202
CHANGE CSHEAR 248 NEW PID-11112 OLD PID-2

HORIZONTAL RODS

CHANGE CROD 509 NEW PID-0000 OLD PID-0000
CHANGE CROD 510 NEW PID-0000 OLD PID-0000
CHANGE CROD 511 NEW PID-0000 OLD PID-0000
CHANGE CROD 512 NEW PID-0000 OLD PID-0000
CHANGE CROD 513 NEW PID-0000 OLD PID-0000
CHANGE CROD 514 NEW PID-0000 OLD PID-0000
CHANGE CROD 515 NEW PID-0000 OLD PID-0000
CHANGE CROD 516 NEW PID-0000 OLD PID-0000
CHANGE CROD 517 NEW PID-0000 OLD PID-0000
CHANGE CROD 518 NEW PID-0000 OLD PID-0000
CHANGE CROD 519 NEW PID-0000 OLD PID-0000
CHANGE CROD 520 NEW PID-0000 OLD PID-0000
CHANGE CROD 521 NEW PID-0000 OLD PID-0000
CHANGE CROD 522 NEW PID-0000 OLD PID-0000
CHANGE CROD 523 NEW PID-0000 OLD PID-0000
CHANGE CROD 524 NEW PID-0000 OLD PID-0000
CHANGE CROD 525 NEW PID-0000 OLD PID-0000
CHANGE CROD 526 NEW PID-0000 OLD PID-0000
CHANGE CROD 527 NEW PID-0000 OLD PID-0000
CHANGE CROD 528 NEW PID-0000 OLD PID-0000
CHANGE CROD 529 NEW PID-0000 OLD PID-0000
CHANGE CROD 530 NEW PID-0000 OLD PID-0000

SPECIAL PROPERTY AND MATERIAL CARDS FOR INITIAL DAMAGE

Prop	10.0	1.0	3.14-3	+M99
Prop 1	0.999	0.999		
Prop 2	1.0	0.999		
Prop 3	0.999	0.999		
Prop 4	0.999	0.999		
Prop 5	0.999	0.999		
Prop 6	0.999	0.999		
Prop 7	0.999	0.999		
Prop 8	0.999	0.999		
Prop 9	0.999	0.999		
Prop 10	0.999	0.999		
Prop 11	0.999	0.999		
Prop 12	0.999	0.999		
Prop 13	0.999	0.999		
Prop 14	0.999	0.999		
Prop 15	0.999	0.999		
Prop 16	0.999	0.999		
Prop 17	0.999	0.999		
Prop 18	0.999	0.999		
Prop 19	0.999	0.999		
Prop 20	0.999	0.999		
Prop 21	0.999	0.999		
Prop 22	0.999	0.999		
Prop 23	0.999	0.999		
Prop 24	0.999	0.999		
Prop 25	0.999	0.999		
Prop 26	0.999	0.999		
Prop 27	0.999	0.999		
Prop 28	0.999	0.999		
Prop 29	0.999	0.999		
Prop 30	0.999	0.999		
Prop 31	0.999	0.999		
Prop 32	0.999	0.999		
Prop 33	0.999	0.999		
Prop 34	0.999	0.999		
Prop 35	0.999	0.999		
Prop 36	0.999	0.999		
Prop 37	0.999	0.999		
Prop 38	0.999	0.999		
Prop 39	0.999	0.999		
Prop 40	0.999	0.999		
Prop 41	0.999	0.999		
Prop 42	0.999	0.999		
Prop 43	0.999	0.999		
Prop 44	0.999	0.999		
Prop 45	0.999	0.999		
Prop 46	0.999	0.999		
Prop 47	0.999	0.999		
Prop 48	0.999	0.999		
Prop 49	0.999	0.999		
Prop 50	0.999	0.999		
Prop 51	0.999	0.999		
Prop 52	0.999	0.999		
Prop 53	0.999	0.999		
Prop 54	0.999	0.999		
Prop 55	0.999	0.999		
Prop 56	0.999	0.999		
Prop 57	0.999	0.999		
Prop 58	0.999	0.999		
Prop 59	0.999	0.999		
Prop 60	0.999	0.999		
Prop 61	0.999	0.999		
Prop 62	0.999	0.999		
Prop 63	0.999	0.999		
Prop 64	0.999	0.999		
Prop 65	0.999	0.999		
Prop 66	0.999	0.999		
Prop 67	0.999	0.999		
Prop 68	0.999	0.999		
Prop 69	0.999	0.999		
Prop 70	0.999	0.999		
Prop 71	0.999	0.999		
Prop 72	0.999	0.999		
Prop 73	0.999	0.999		
Prop 74	0.999	0.999		
Prop 75	0.999	0.999		
Prop 76	0.999	0.999		
Prop 77	0.999	0.999		
Prop 78	0.999	0.999		
Prop 79	0.999	0.999		
Prop 80	0.999	0.999		
Prop 81	0.999	0.999		
Prop 82	0.999	0.999		
Prop 83	0.999	0.999		
Prop 84	0.999	0.999		
Prop 85	0.999	0.999		
Prop 86	0.999	0.999		
Prop 87	0.999	0.999		
Prop 88	0.999	0.999		
Prop 89	0.999	0.999		
Prop 90	0.999	0.999		
Prop 91	0.999	0.999		
Prop 92	0.999	0.999		
Prop 93	0.999	0.999		
Prop 94	0.999	0.999		
Prop 95	0.999	0.999		
Prop 96	0.999	0.999		
Prop 97	0.999	0.999		
Prop 98	0.999	0.999		
Prop 99	0.999	0.999		
Prop 100	0.999	0.999		
Prop 101	0.999	0.999		
Prop 102	0.999	0.999		
Prop 103	0.999	0.999		
Prop 104	0.999	0.999		
Prop 105	0.999	0.999		
Prop 106	0.999	0.999		
Prop 107	0.999	0.999		
Prop 108	0.999	0.999		
Prop 109	0.999	0.999		
Prop 110	0.999	0.999		
Prop 111	0.999	0.999		
Prop 112	0.999	0.999		
Prop 113	0.999	0.999		
Prop 114	0.999	0.999		
Prop 115	0.999	0.999		
Prop 116	0.999	0.999		
Prop 117	0.999	0.999		
Prop 118	0.999	0.999		
Prop 119	0.999	0.999		
Prop 120	0.999	0.999		
Prop 121	0.999	0.999		
Prop 122	0.999	0.999		
Prop 123	0.999	0.999		
Prop 124	0.999	0.999		
Prop 125	0.999	0.999		
Prop 126	0.999	0.999		
Prop 127	0.999	0.999		
Prop 128	0.999	0.999		
Prop 129	0.999	0.999		
Prop 130	0.999	0.999		
Prop 131	0.999	0.999		
Prop 132	0.999	0.999		
Prop 133	0.999	0.999		
Prop 134	0.999	0.999		
Prop 135	0.999	0.999		
Prop 136	0.999	0.999		
Prop 137	0.999	0.999		
Prop 138	0.999	0.999		
Prop 139	0.999	0.999		
Prop 140	0.999	0.999		
Prop 141	0.999	0.999		
Prop 142	0.999	0.999		
Prop 143	0.999	0.999		
Prop 144	0.999	0.999		
Prop 145	0.999	0.999		
Prop 146	0.999	0.999		
Prop 147	0.999	0.999		
Prop 148	0.999	0.999		
Prop 149	0.999	0.999		
Prop 150	0.999	0.999		
Prop 151	0.999	0.999		
Prop 152	0.999	0.999		
Prop 153	0.999	0.999		
Prop 154	0.999	0.999		
Prop 155	0.999	0.999		
Prop 156	0.999	0.999		
Prop 157	0.999	0.999		
Prop 158	0.999	0.999		
Prop 159	0.999	0.999		
Prop 160	0.999	0.999		
Prop 161	0.999	0.999		
Prop 162	0.999	0.999		
Prop 163	0.999	0.999		
Prop 164	0.999	0.999		
Prop 165	0.999	0.999		
Prop 166	0.999	0.999		
Prop 167	0.999	0.999		
Prop 168	0.999	0.999		
Prop 169	0.999	0.999		
Prop 170	0.999	0.999		
Prop 171	0.999	0.999		
Prop 172	0.999	0.999		
Prop 173	0.999	0.999		
Prop 174	0.999	0.999		
Prop 175	0.999	0.999		
Prop 176	0.999	0.999		
Prop 177	0.999	0.999		
Prop 178	0.999	0.999		
Prop 179	0.999	0.999		
Prop 180	0.999	0.999		
Prop 181	0.999	0.999		
Prop 182	0.999	0.999		
Prop 183	0.999	0.999		
Prop 184	0.999	0.999		
Prop 185	0.999	0.999		
Prop 186	0.999	0.999		
Prop 187	0.999	0.999		
Prop 188	0.999	0.999		
Prop 189	0.999	0.999		
Prop 190	0.999	0.999		
Prop 191	0.999	0.999		
Prop 192	0.999	0.999		
Prop 193	0.999	0.999		
Prop 194	0.999	0.999		
Prop 195	0.999	0.999		
Prop 196	0.999	0.999		
Prop 197	0.999	0.999		
Prop 198	0.999	0.999		
Prop 199	0.999	0.999		
Prop 200	0.999	0.999		
Prop 201	0.999	0.999		
Prop 202	0.999	0.999		
Prop 203	0.999	0.999		
Prop 204	0.999	0.999		
Prop 205	0.999	0.999		
Prop 206	0.999	0.999		
Prop 207	0.999	0.999		
Prop 208	0.999	0.999		
Prop 209	0.999	0.999		
Prop 210	0.999	0.999		
Prop 211	0.999	0.999		
Prop 212	0.999	0.999		
Prop 213	0.999	0.999		
Prop 214	0.999	0.999		
Prop 215	0.999	0.999		
Prop 216	0.999	0.999		
Prop 217	0.999	0.999		
Prop 218	0.999	0.999		
Prop 219	0.999	0.999		
Prop 220	0.999	0.999		
Prop 221	0.999	0.999		
Prop 222	0.999	0.999		
Prop 223	0.999	0.999		
Prop 224	0.999	0.999		
Prop 225	0.999	0.999		
Prop 226	0.999	0.999		
Prop 227	0.999	0.999		
Prop 228	0.999	0.999		
Prop 229	0.999	0.999		
Prop 230	0.999	0.999		
Prop 231	0.999	0.999		
Prop 232	0.999	0.999		
Prop 233	0.999	0.999		
Prop 234	0.999	0.999		
Prop 235	0.999	0.999		
Prop 236	0.999	0.999		
Prop 237	0.999	0.999		
Prop 238	0.999	0.999		
Prop 239	0.999	0.999		
Prop 240	0.999	0.999		
Prop 241	0.999	0.999		
Prop 242	0.999	0.999		
Prop 243	0.999	0.999		
Prop 244	0.999	0.999		

APPENDIX H

PROGRESSIVE STRUCTURAL COLLAPSE ANALYSIS LISTING

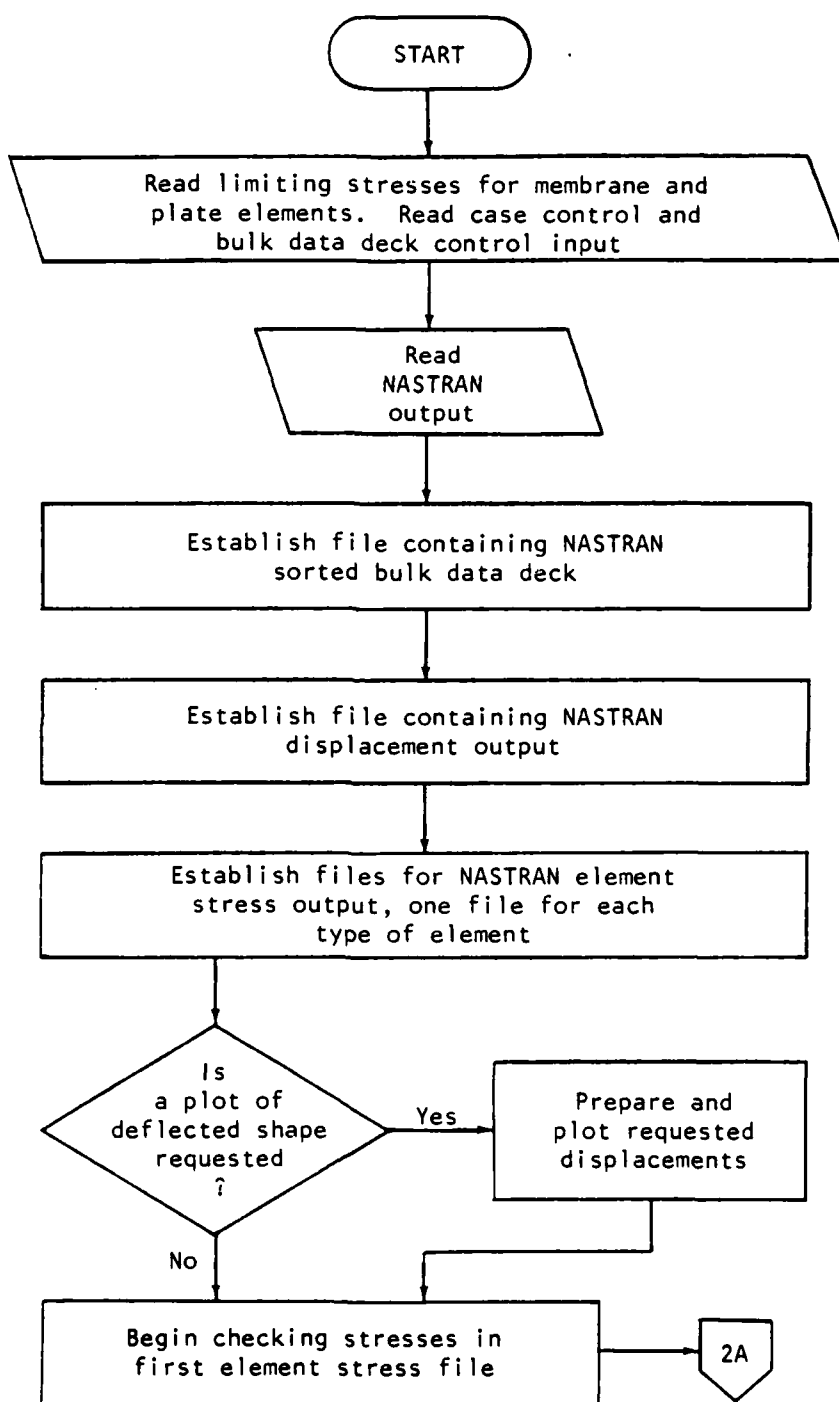


Figure 25. PROSCAN Functional Flow Diagram

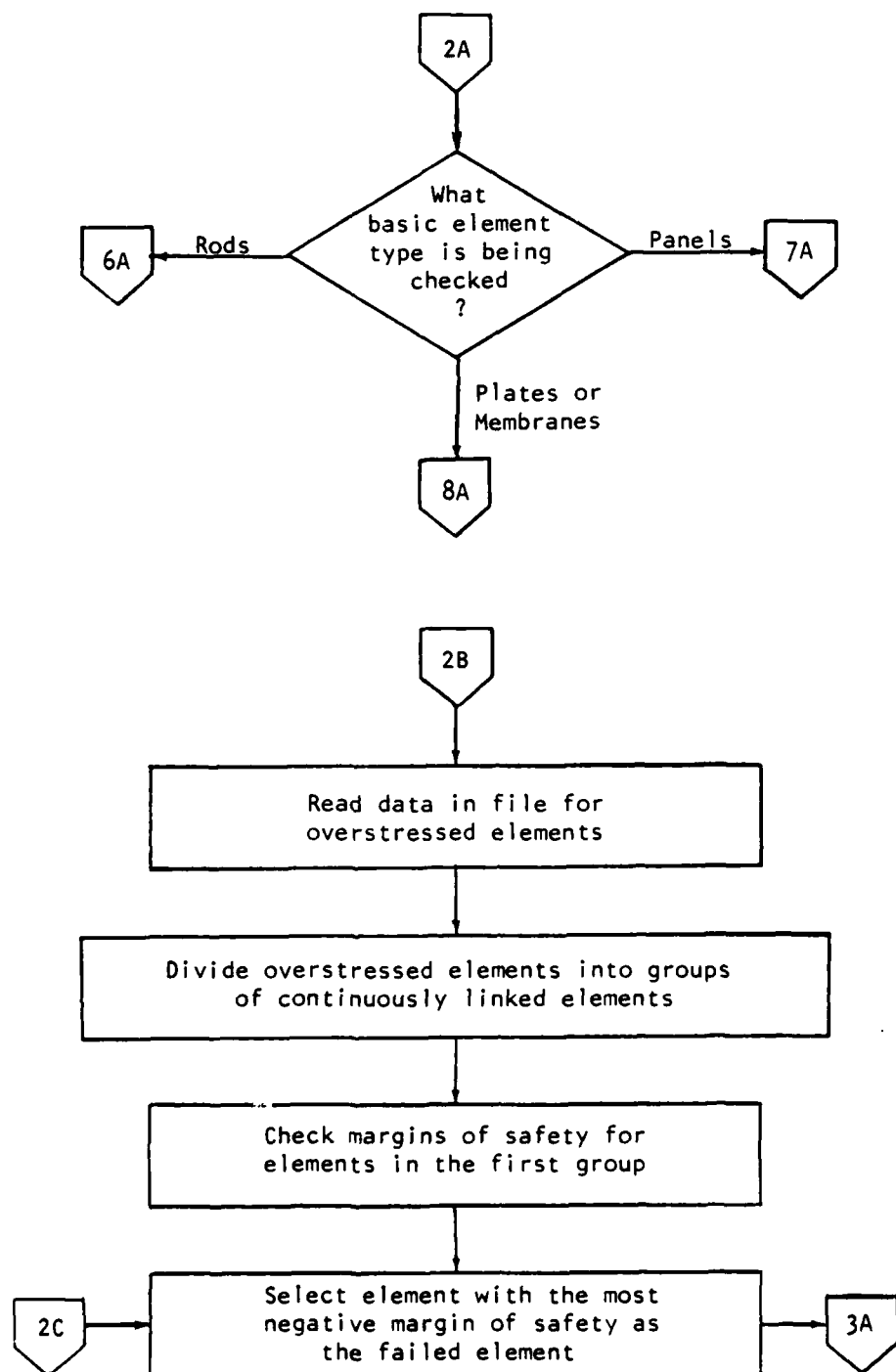


Figure 25. (Continued)

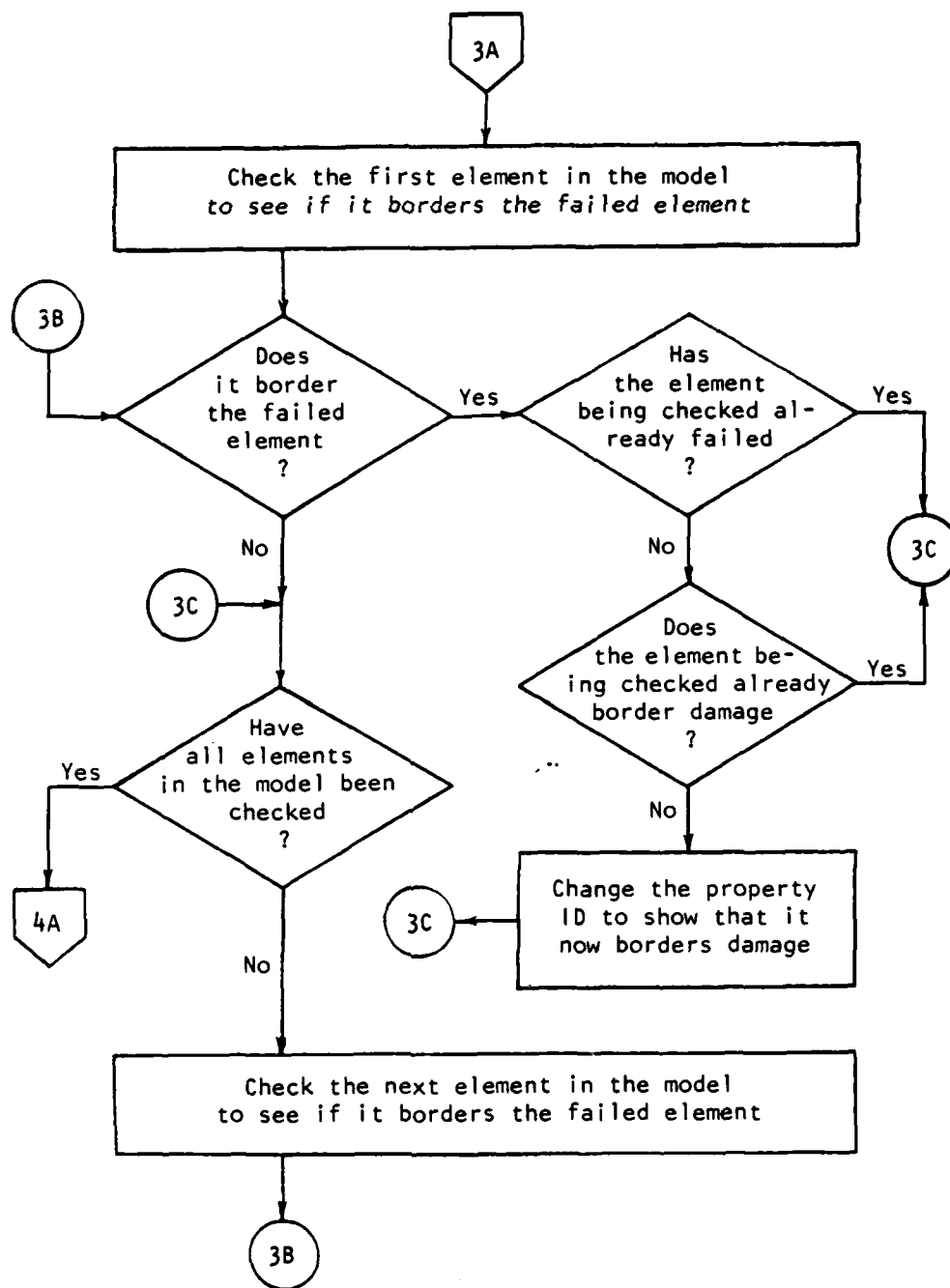


Figure 25. (Continued)

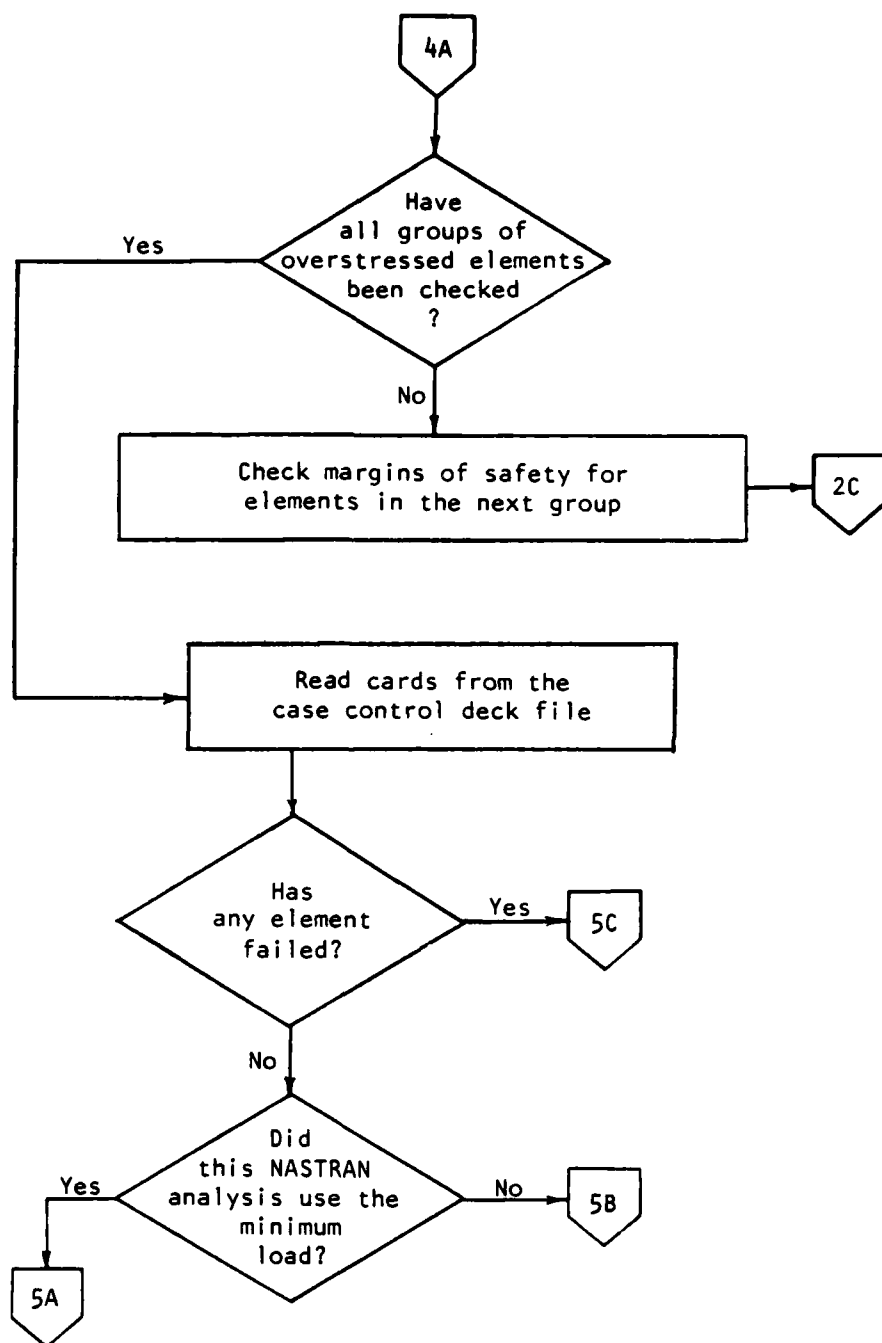


Figure 25. (Continued)

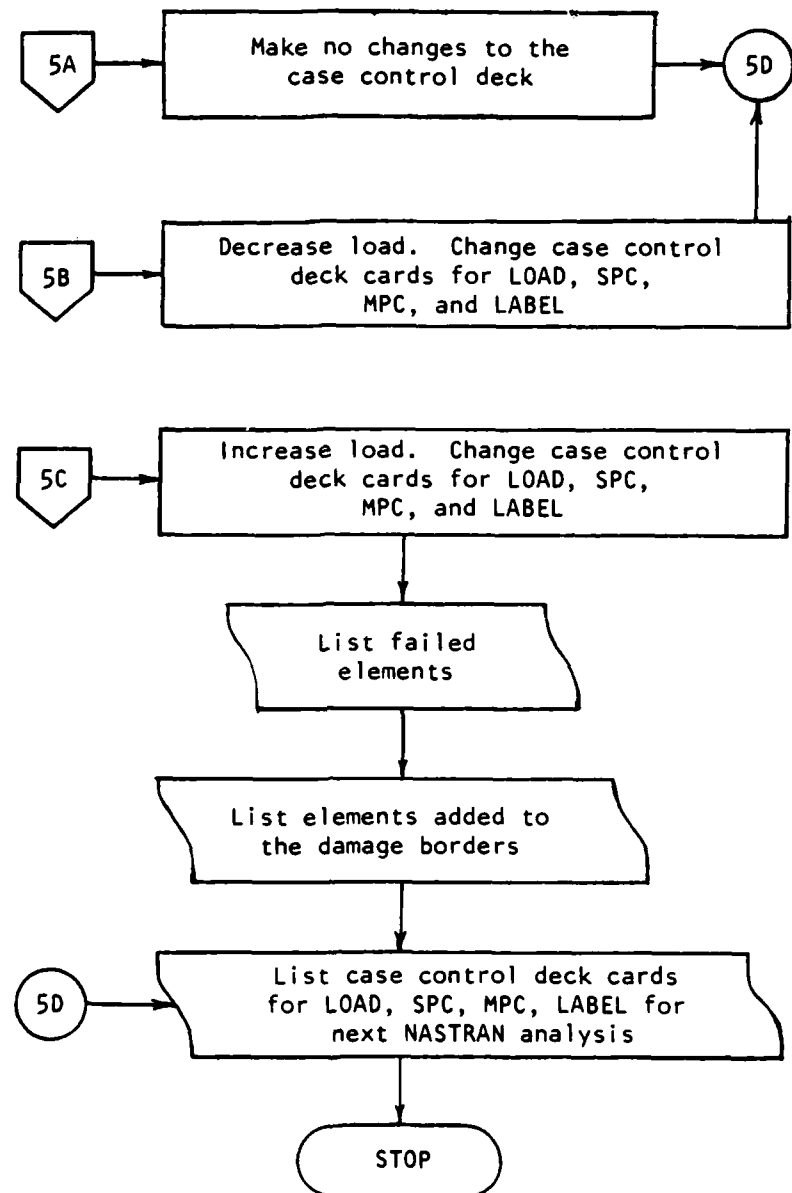


Figure 25. (Continued)

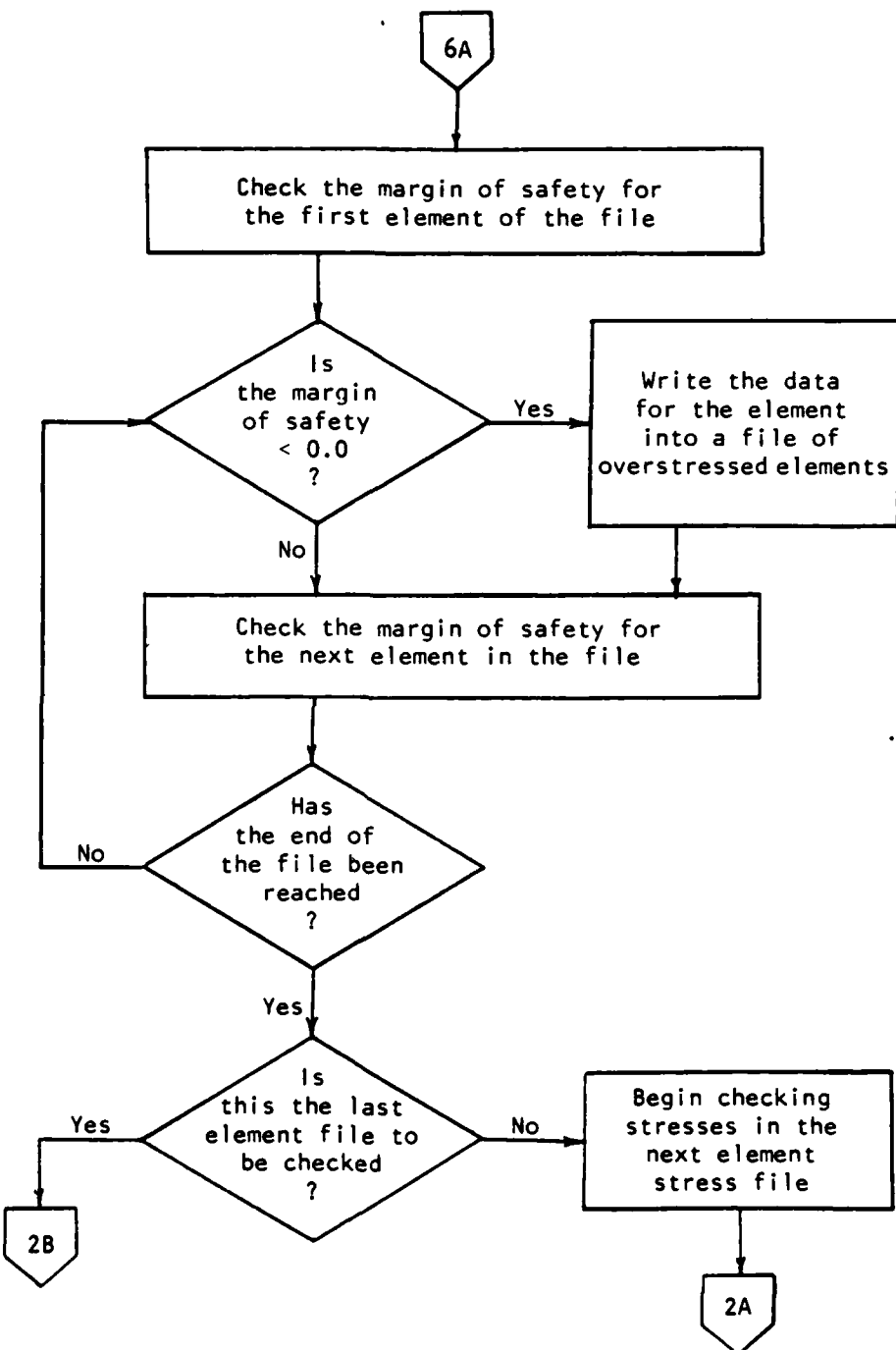


Figure 25. (Continued)

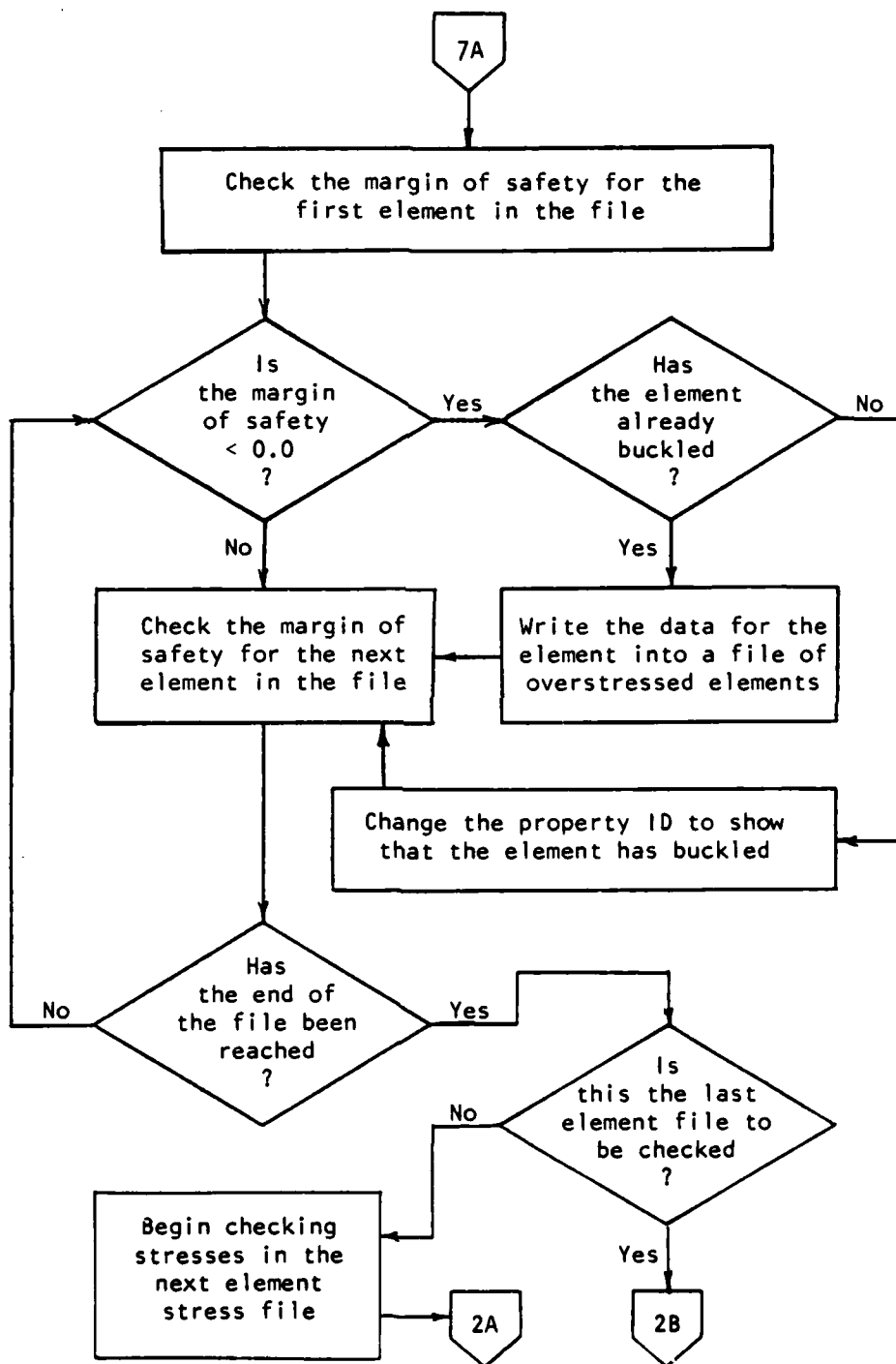


Figure 25. (Continued)

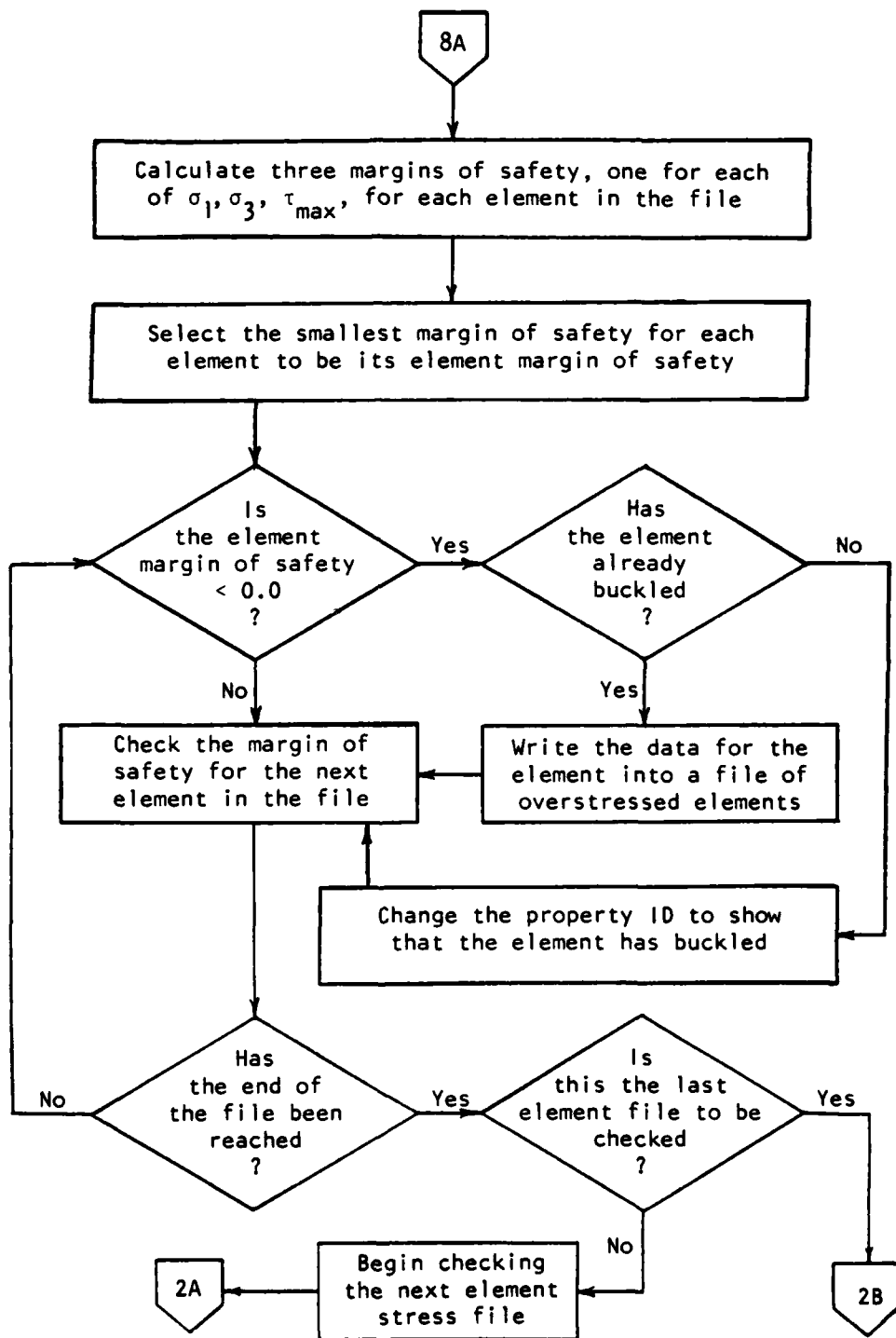


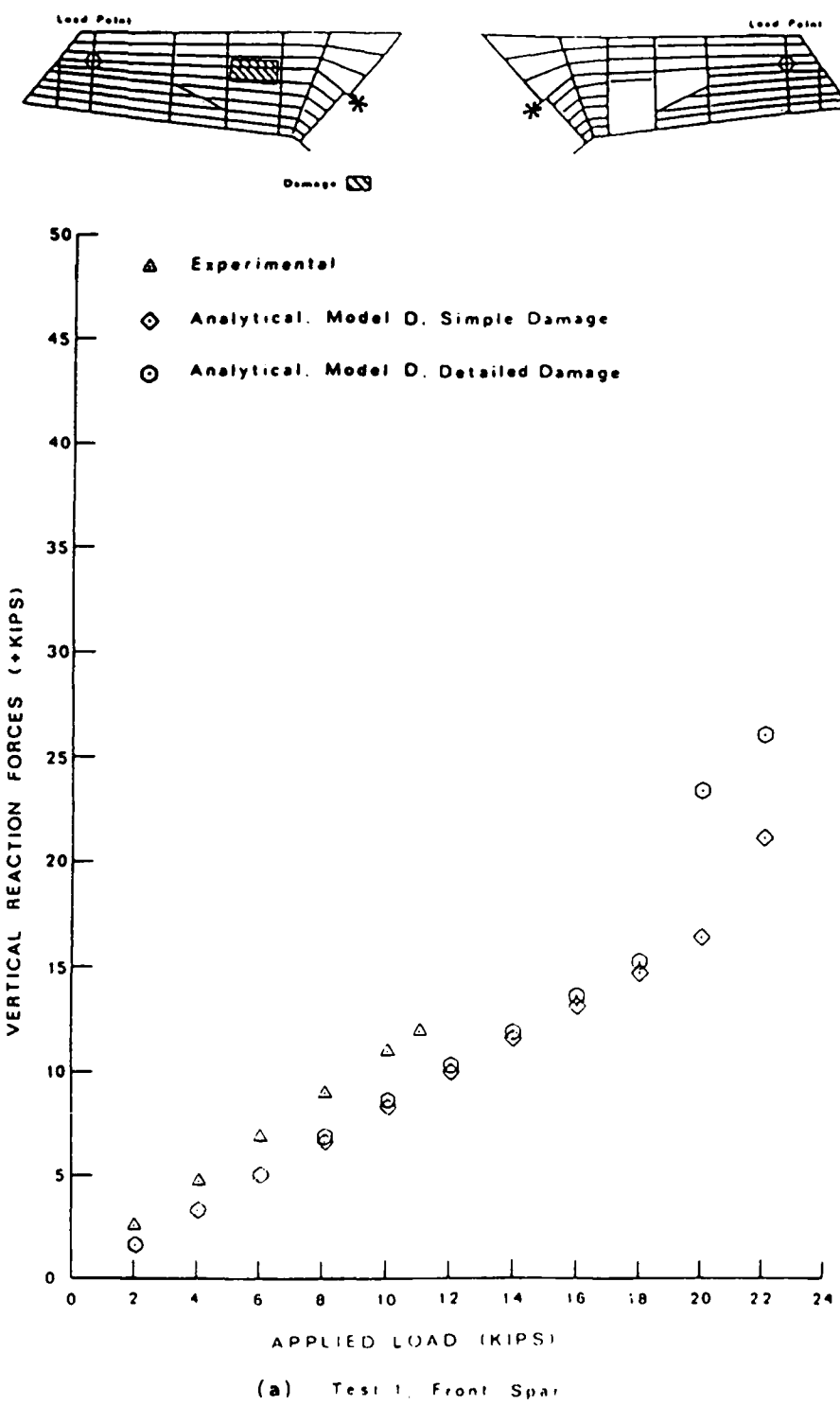
Figure 25. (Continued)

卷之三

LUN	UNIT	NO.	DISPLACEMENT	DATA INPUT
	LOGICAL UNIT	NO.	DISPLACEMENT	DATA OUTPUT
	LOGICAL UNIT	NO.	GRID POINT DATA	INPUT
LUN1	LOGICAL UNIT	NO.1	0	DATA INPUT
LUN2	LOGICAL UNIT	NO.2	0	DATA OUTPUT
LUN3	LOGICAL UNIT	NO.3	0	DATA INPUT
LUN4	LOGICAL UNIT	NO.4	0	DATA OUTPUT

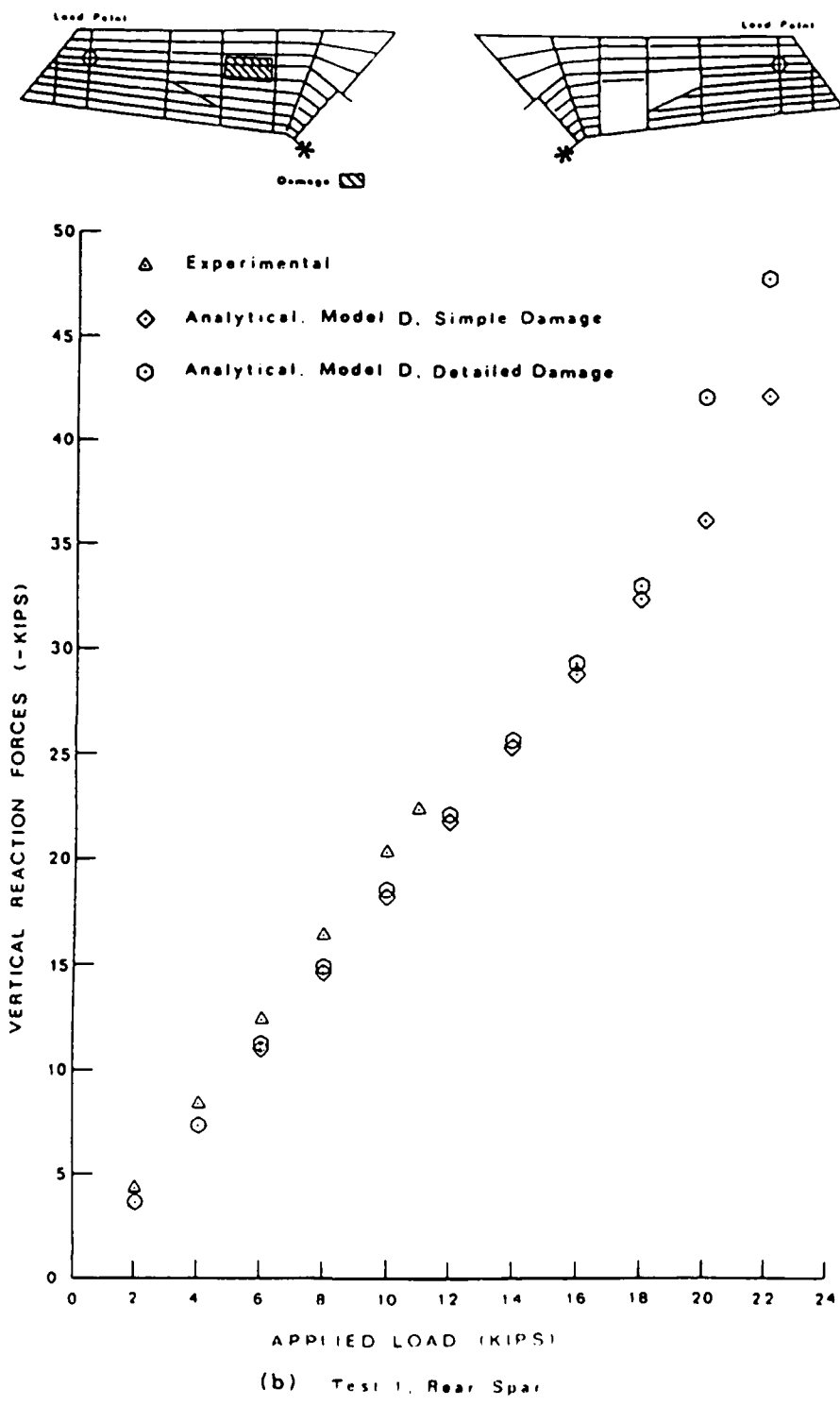
APPENDIX I

PLOTS OF ANALYTICAL AND EXPERIMENTAL DATA



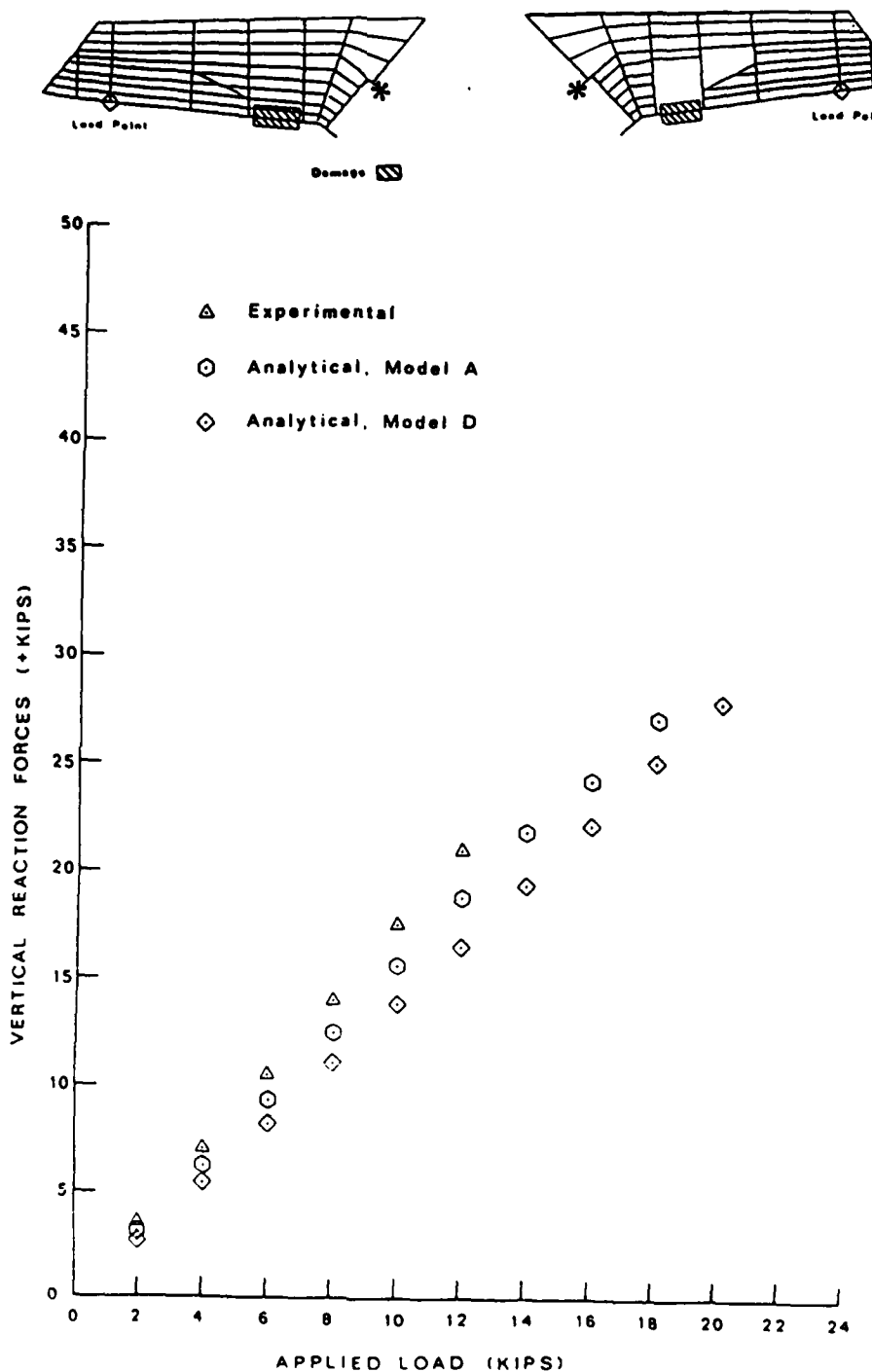
(a) Test 1, Front Spar

Figure 26. Comparison of Vertical Reaction Forces



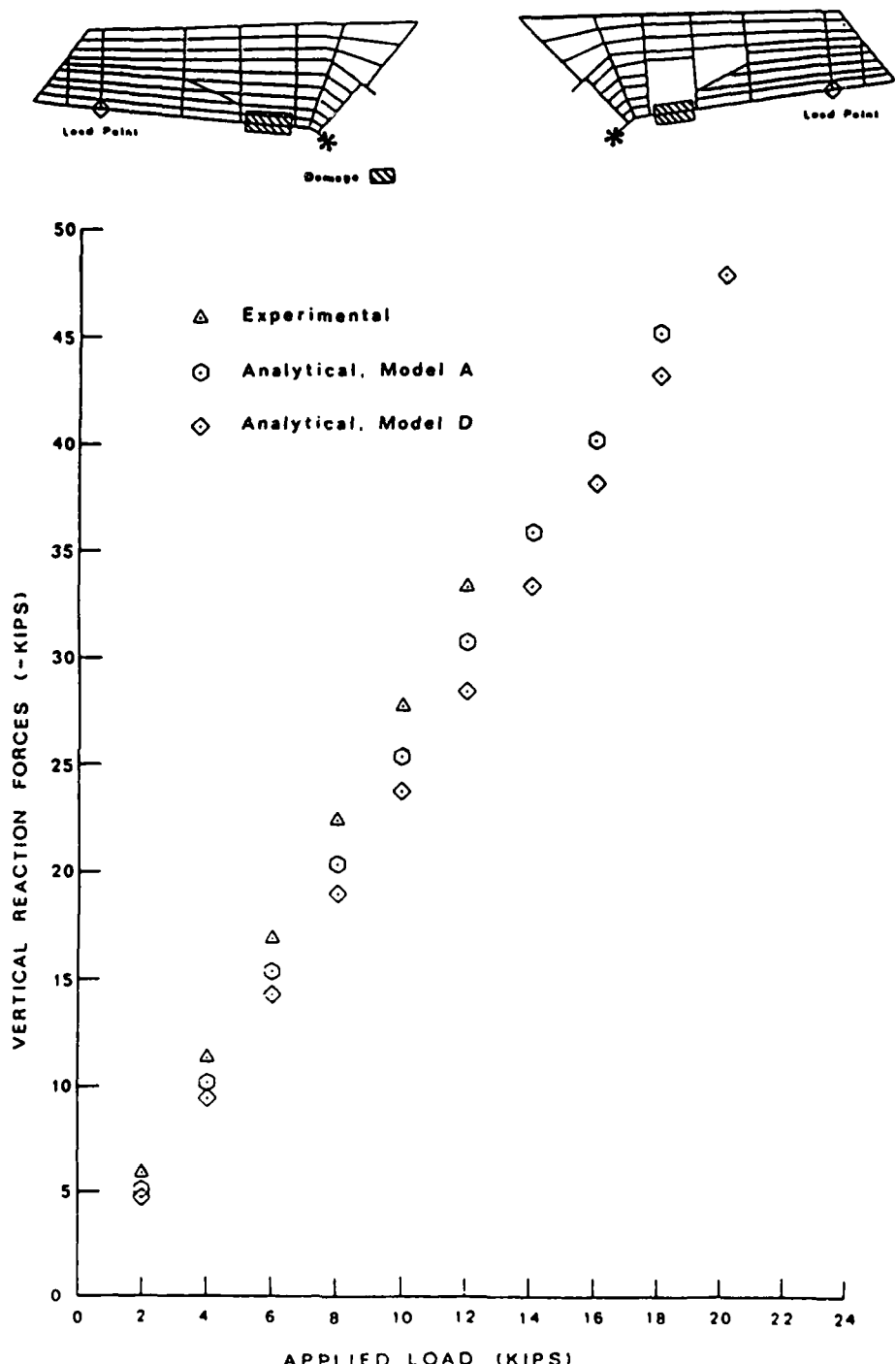
(b) Test 1, Rear Spar

Figure 26. (Continued)



(c) Test 2C, Front Spar

Figure 26. (Continued)



(d) Test 2C, Rear Spar

Figure 26. (Continued)

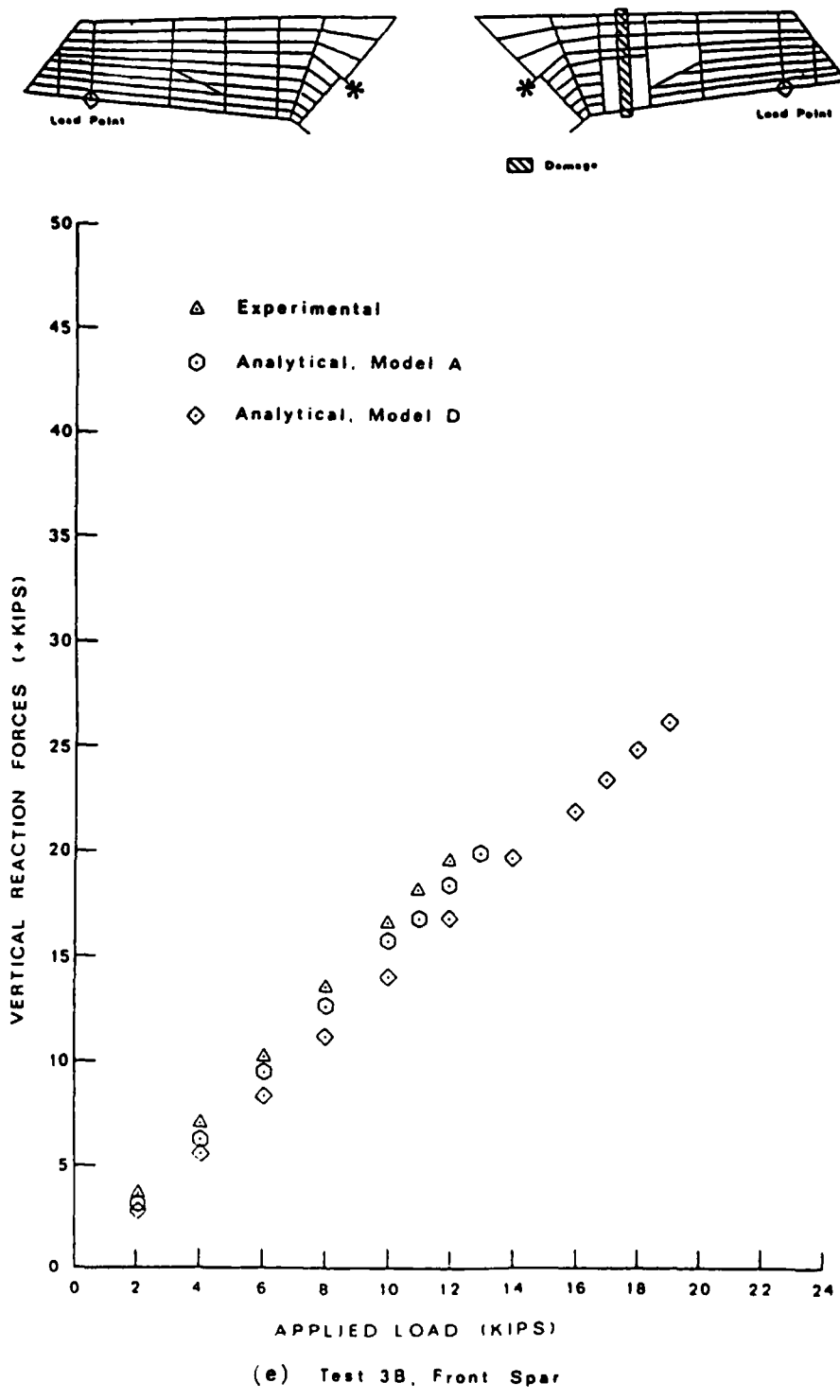
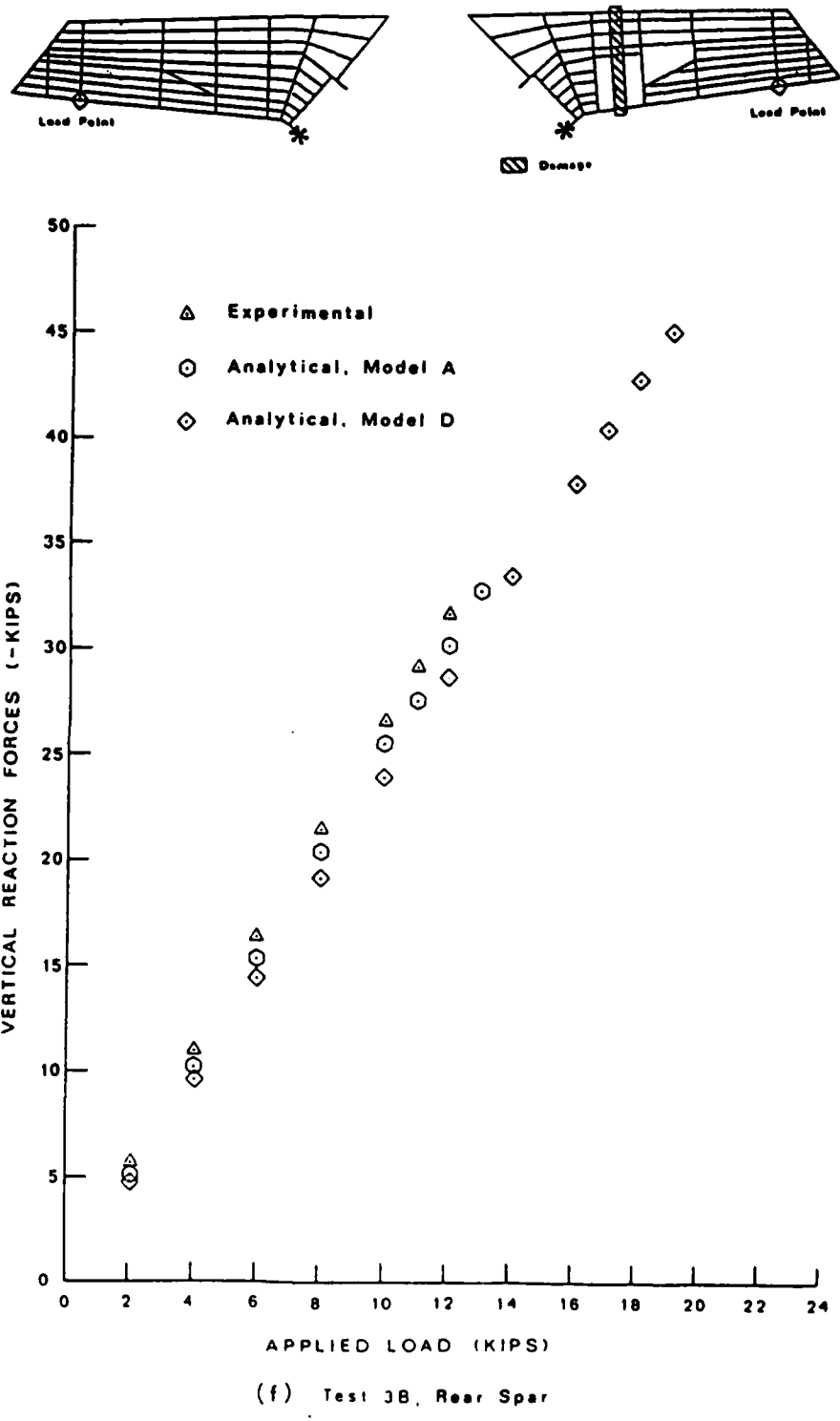
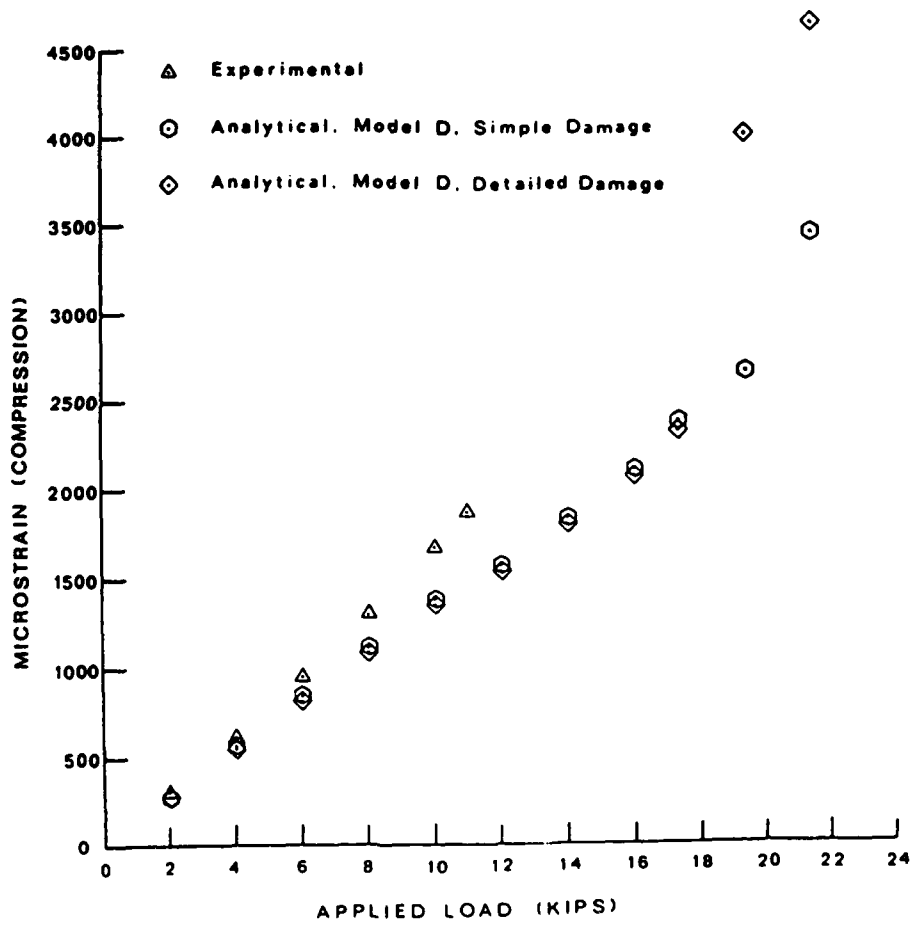
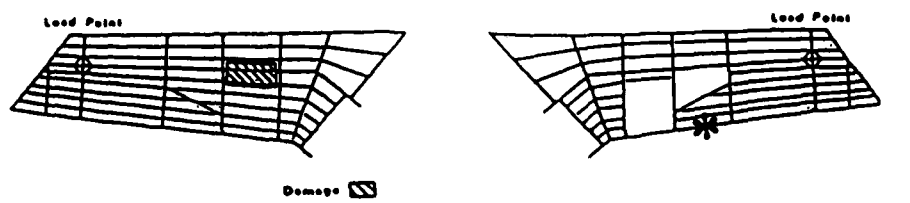


Figure 26. (Continued)



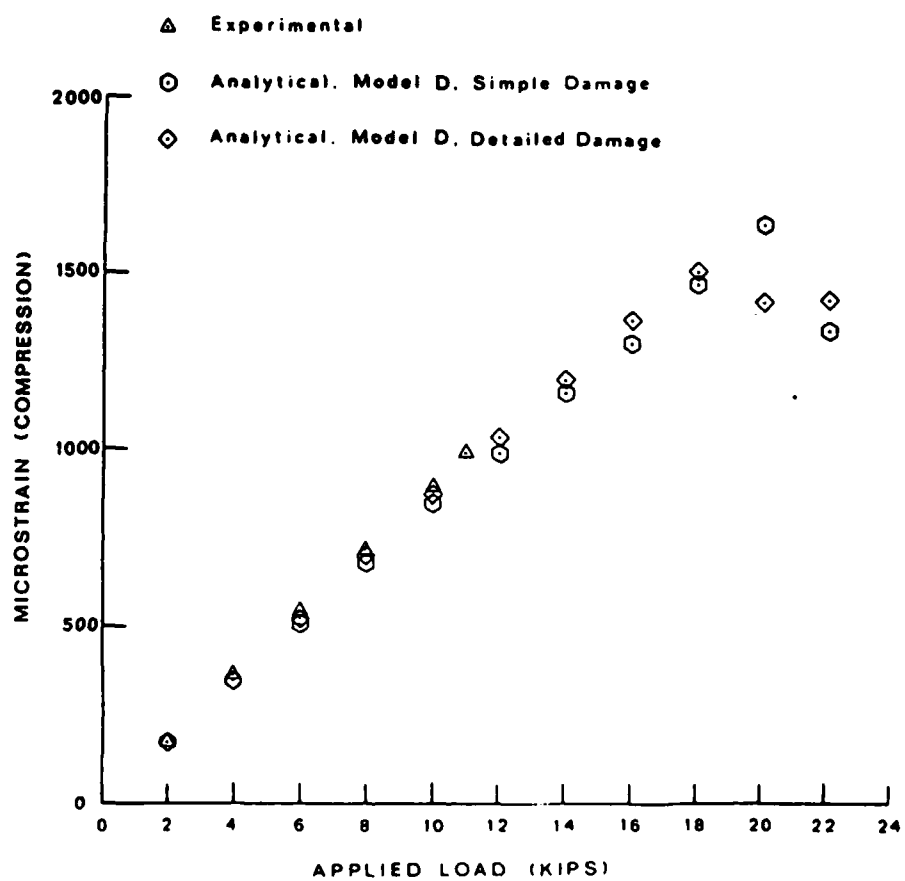
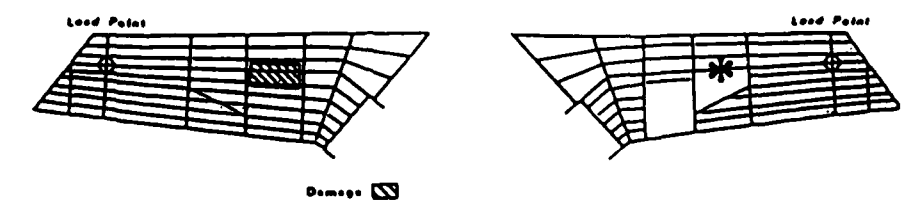
(f) Test 3B, Rear Spar

Figure 26. (Continued)



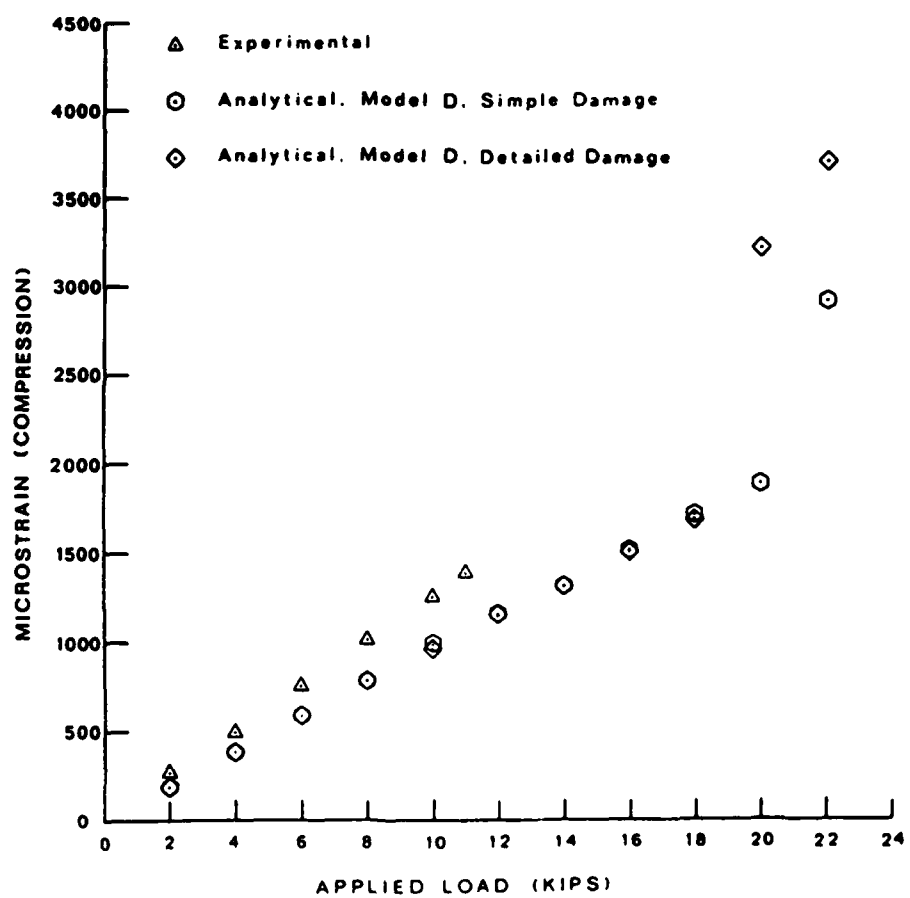
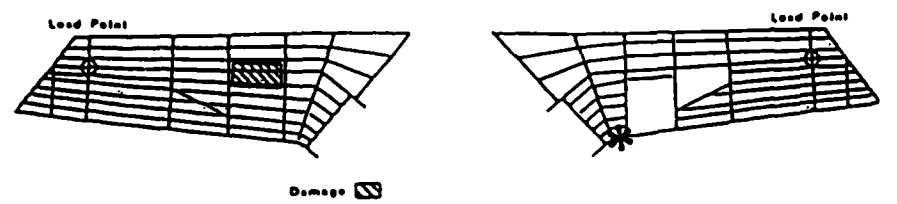
(a) Rod Element 458

Figure 27. Comparison of Strains for Test 1



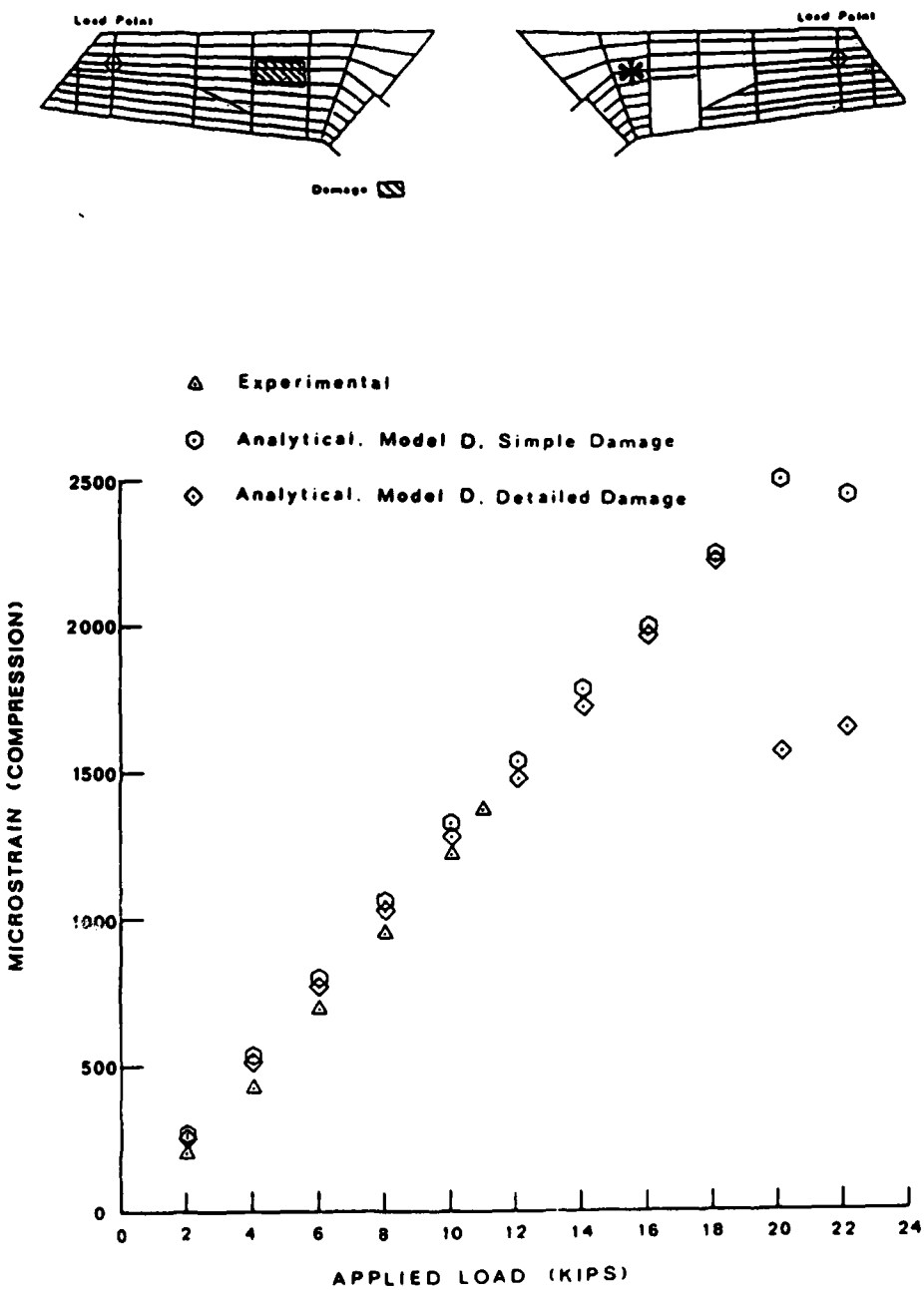
(b) Rod Element 476

Figure 27. (Continued)



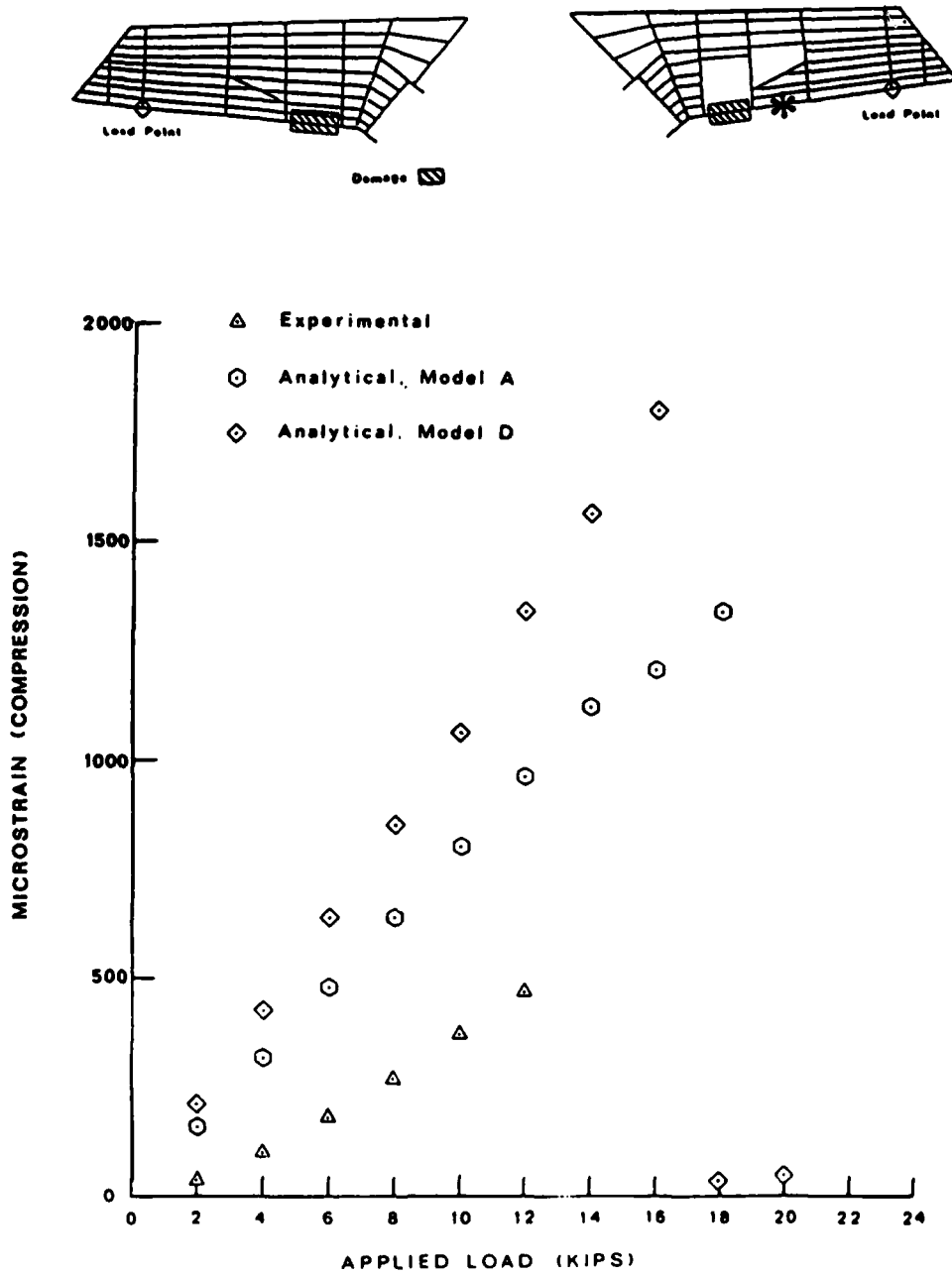
(c) Rod Element 564

Figure 27. (Continued)



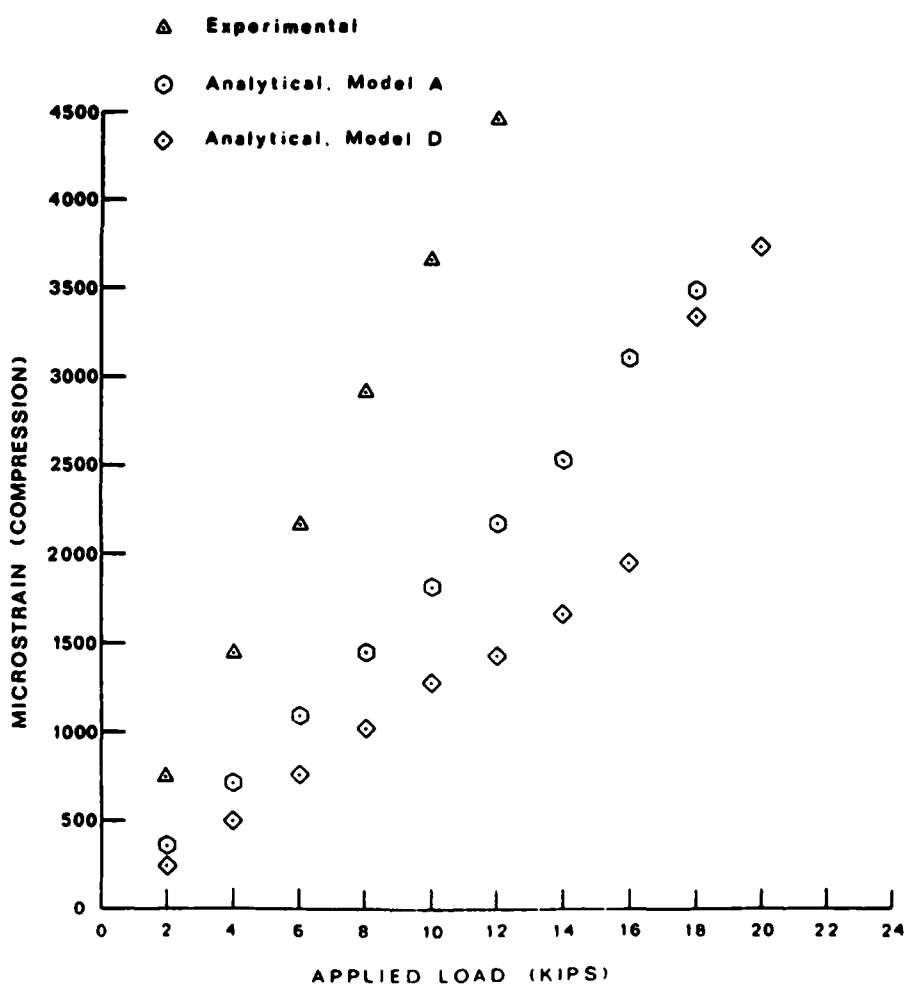
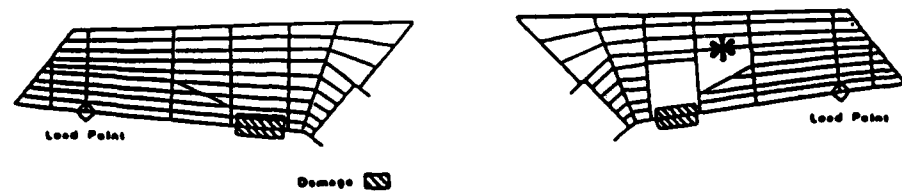
(d) Rod Element 576

Figure 27. (Continued)



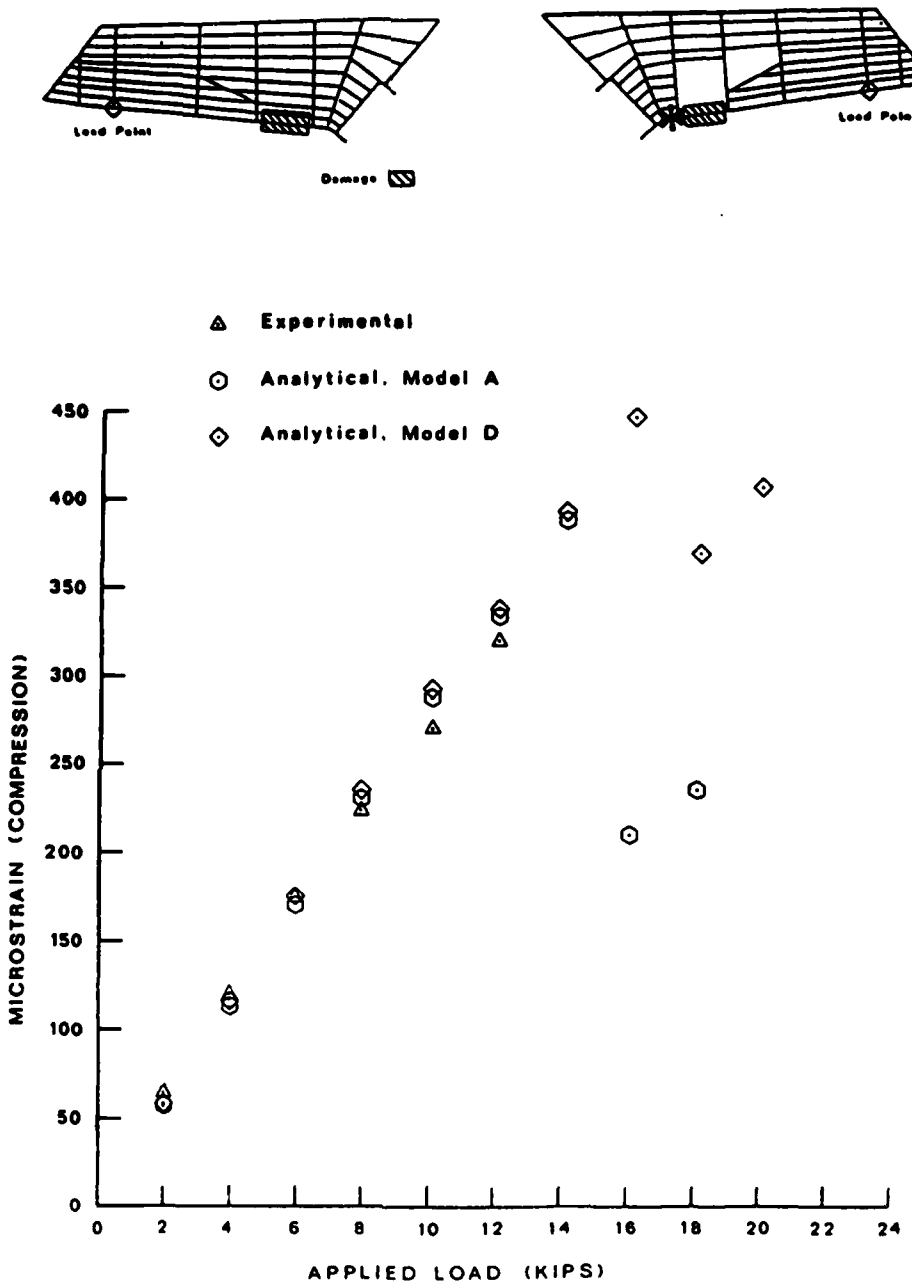
(a) Rod Element 458

Figure 28. Comparison of Strains for Test 2C



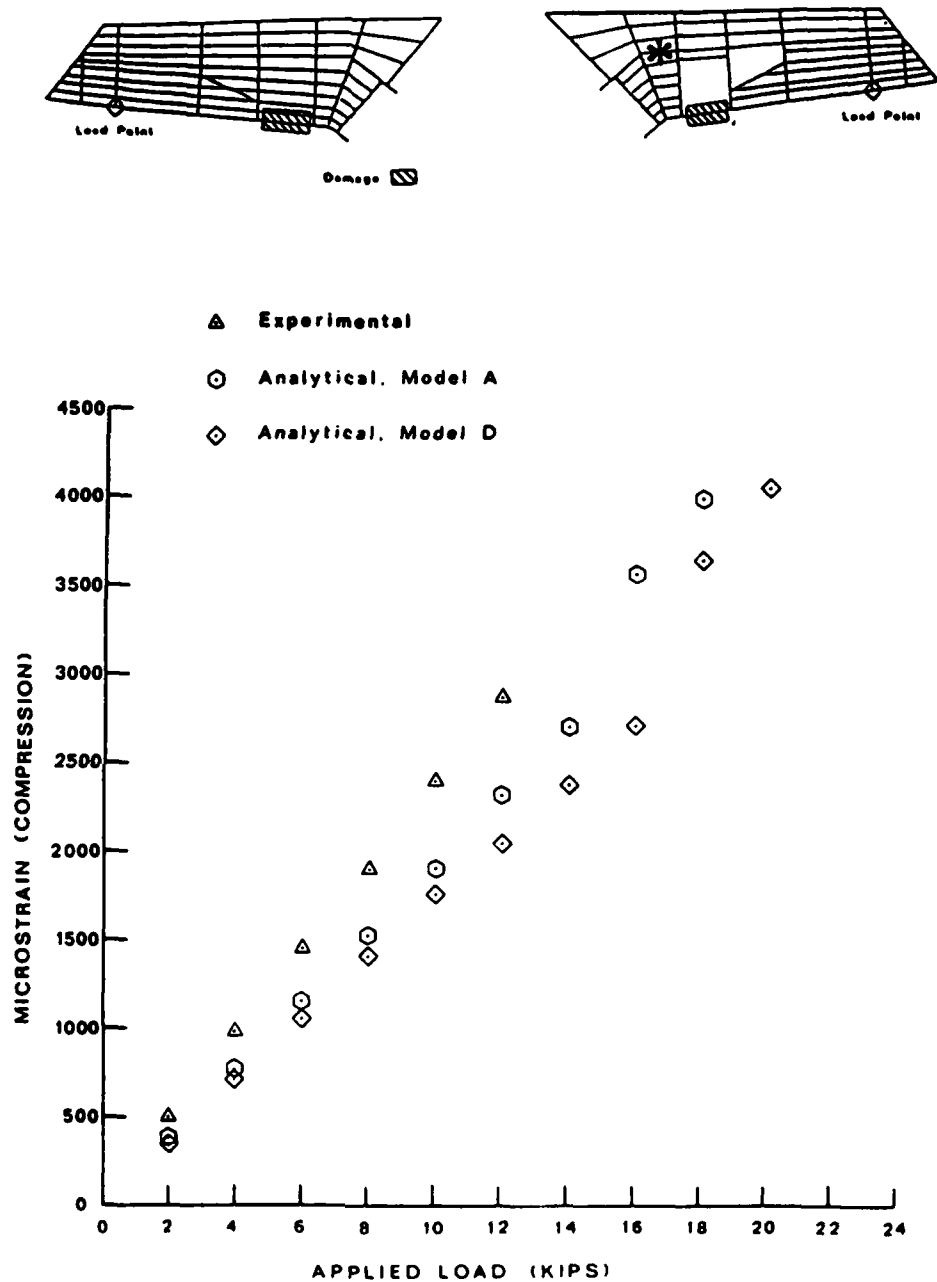
(b) Rod Element 476

Figure 28. (Continued)



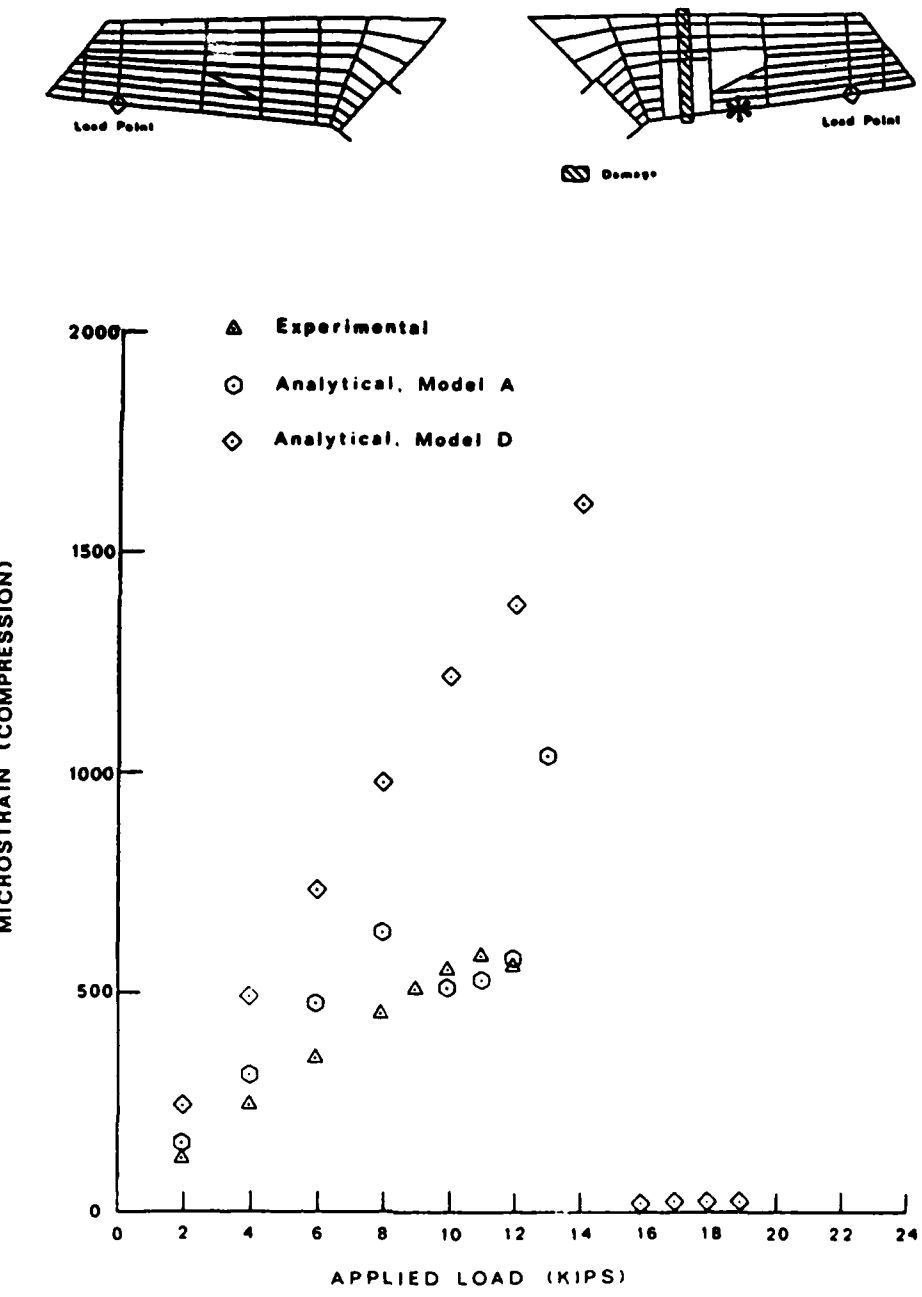
(c) Rod Element 564

Figure 28. (Continued)



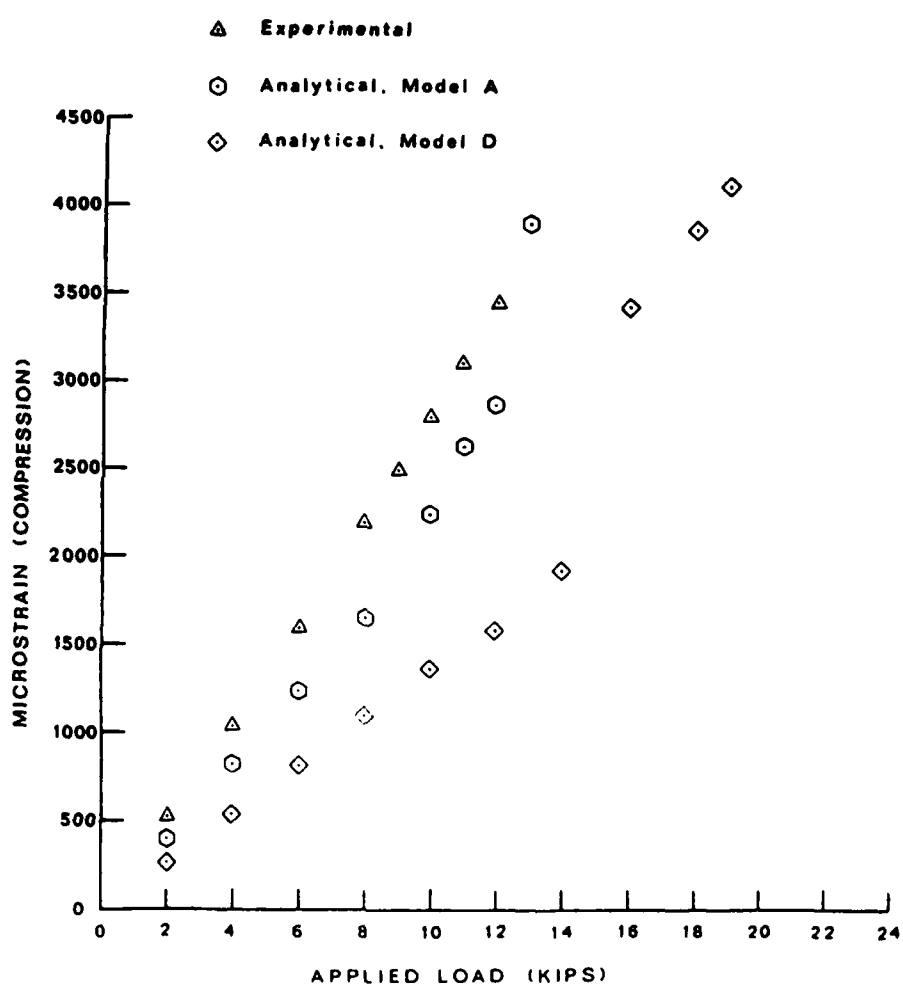
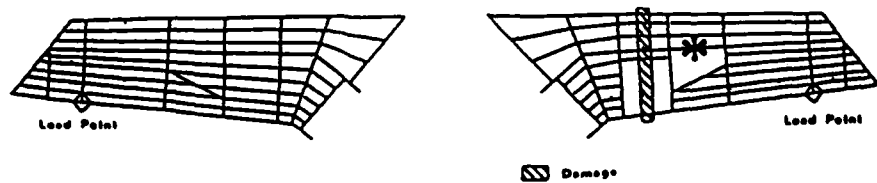
(d) Rod Element 576

Figure 28. (Continued)



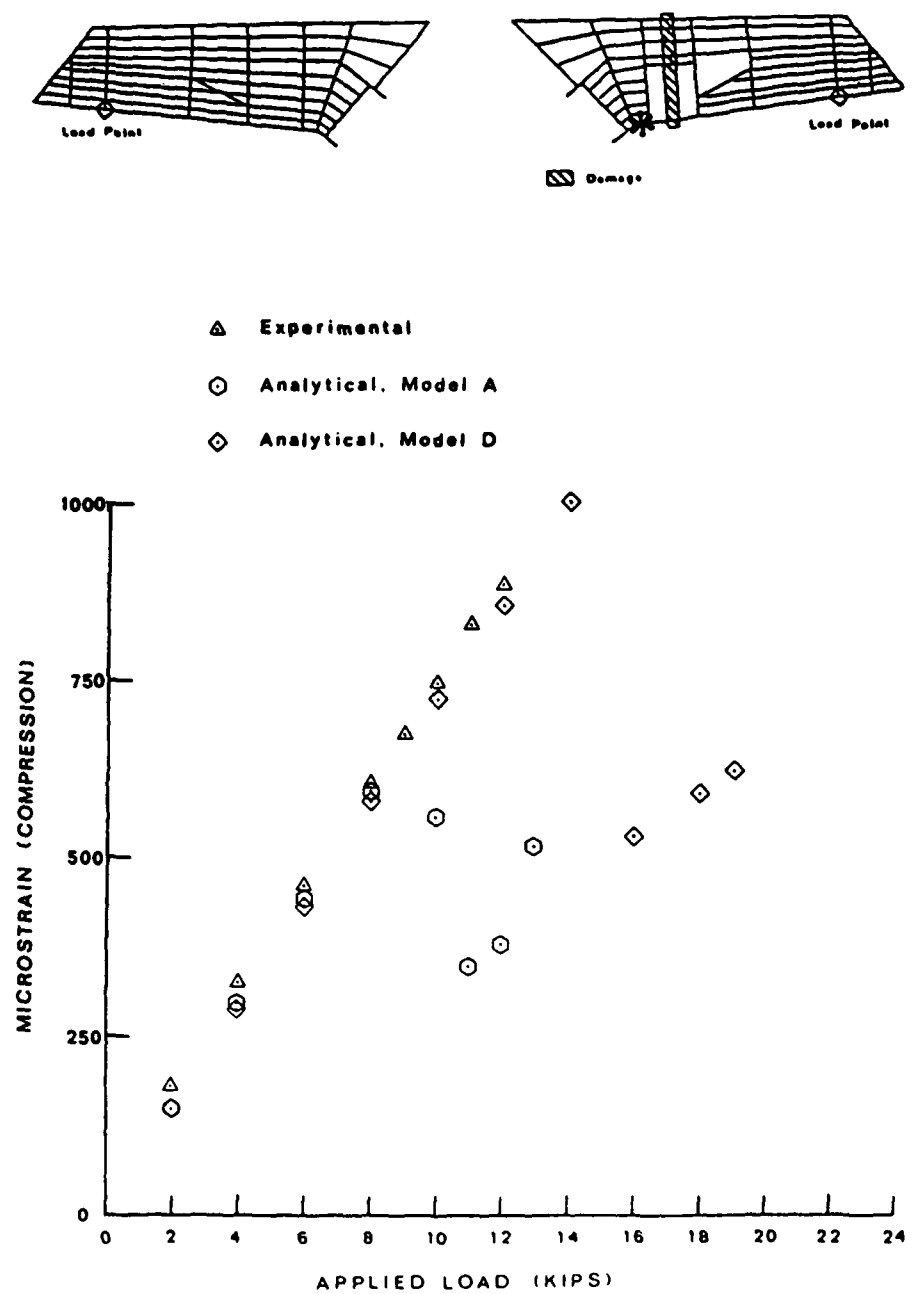
(a) Rod Element 458

Figure 29. Comparison of Strains for Test 3B



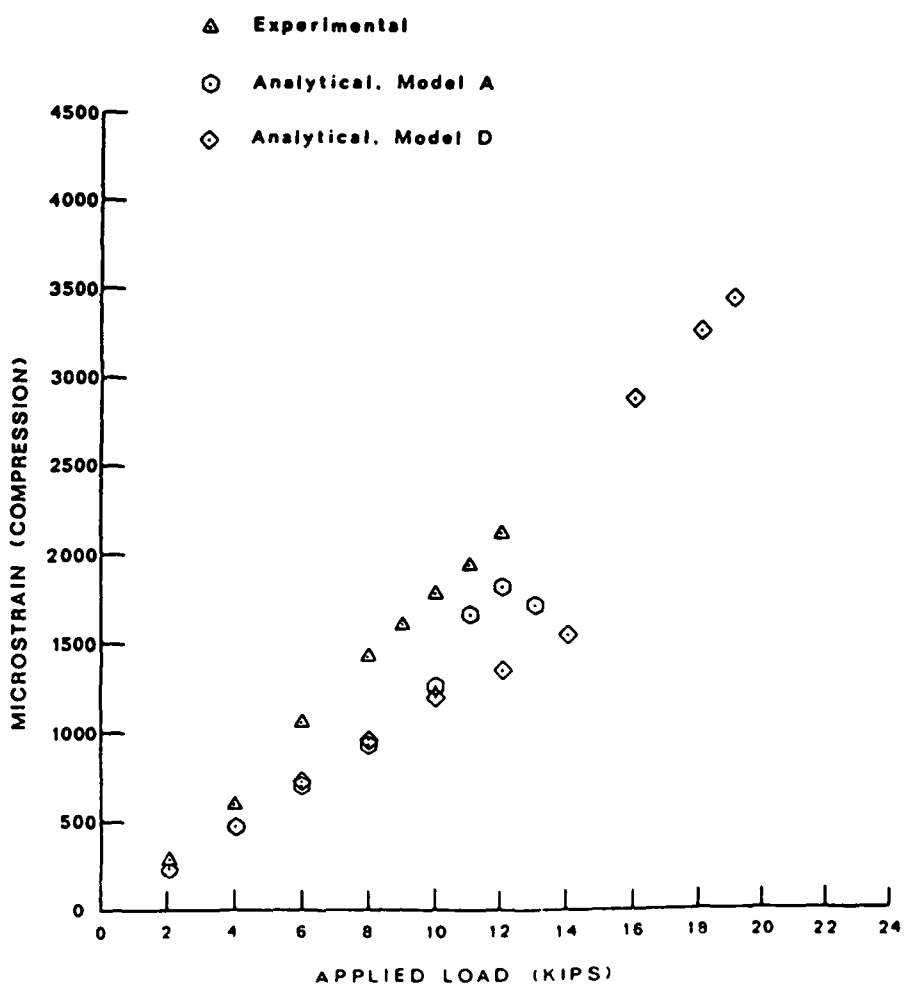
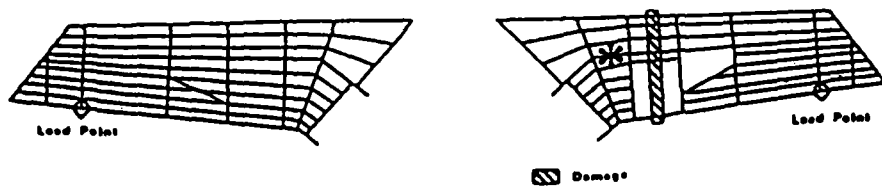
(b) Rod Element 476

Figure 29. (Continued)



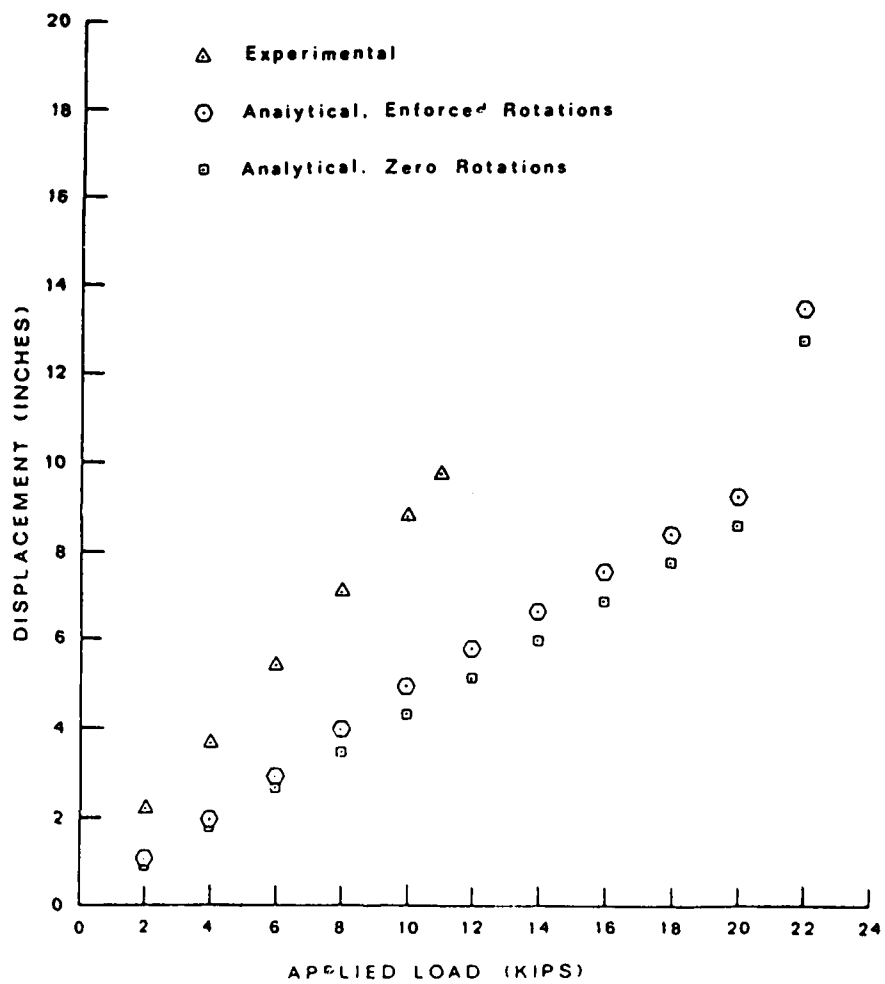
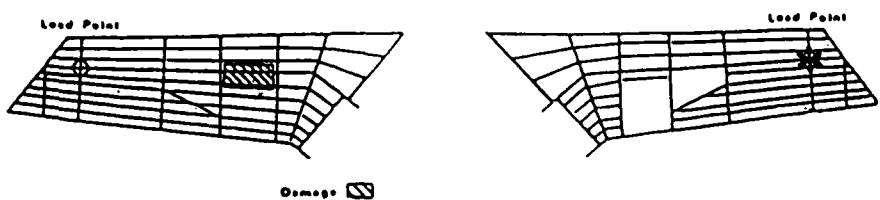
(c) Rod Element 564

Figure 29. (Continued)



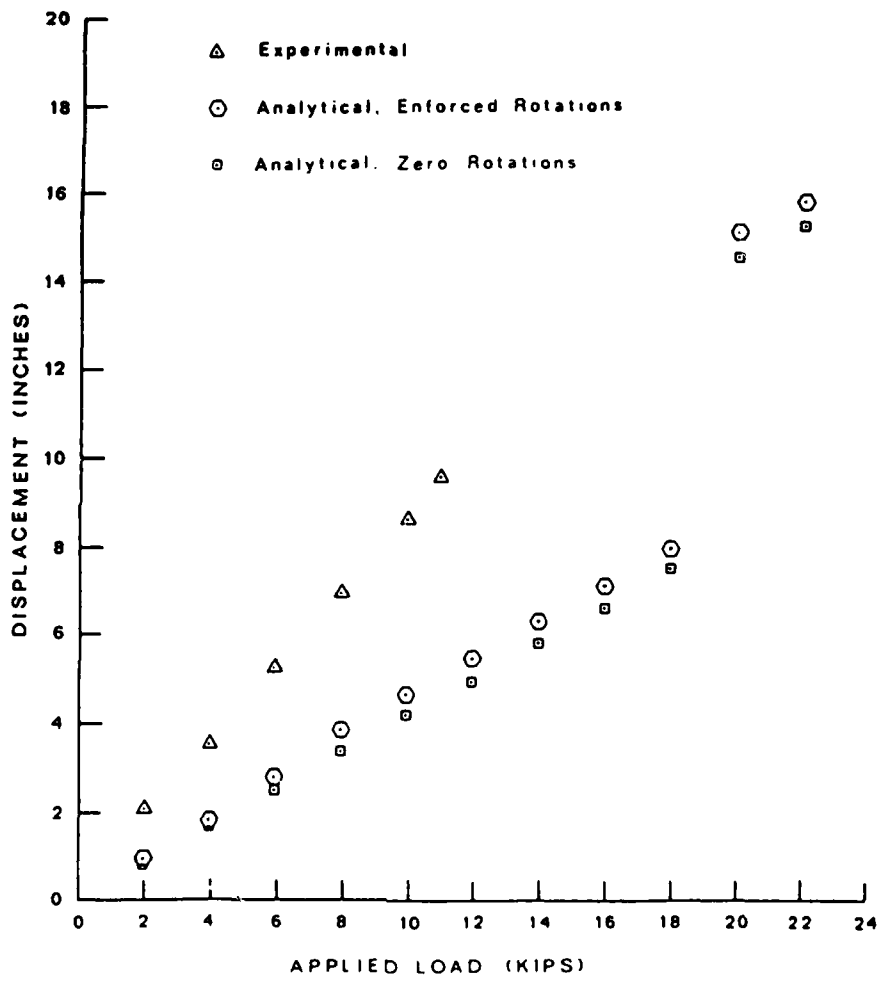
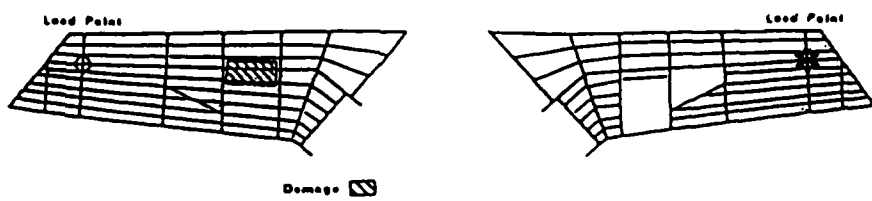
(d) Rod Element 576

Figure 29. (Continued)



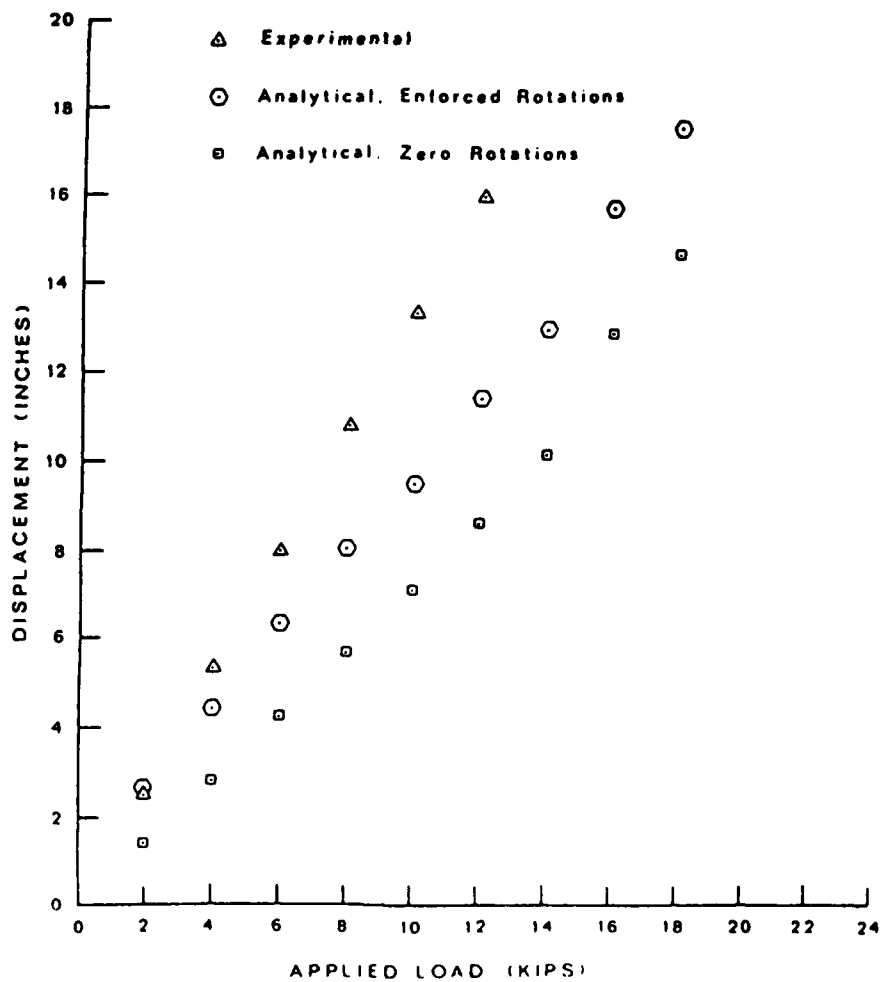
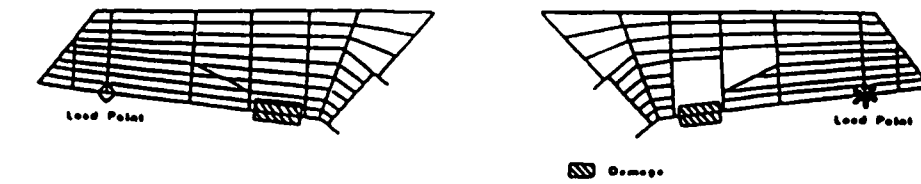
(a) Test 1. Model D (with torsional stiffness rods), Simple

Figure 30. Load Point Displacements for Test 1



(b) Test 1, Model D (with torsional stiffness rods), Detailed

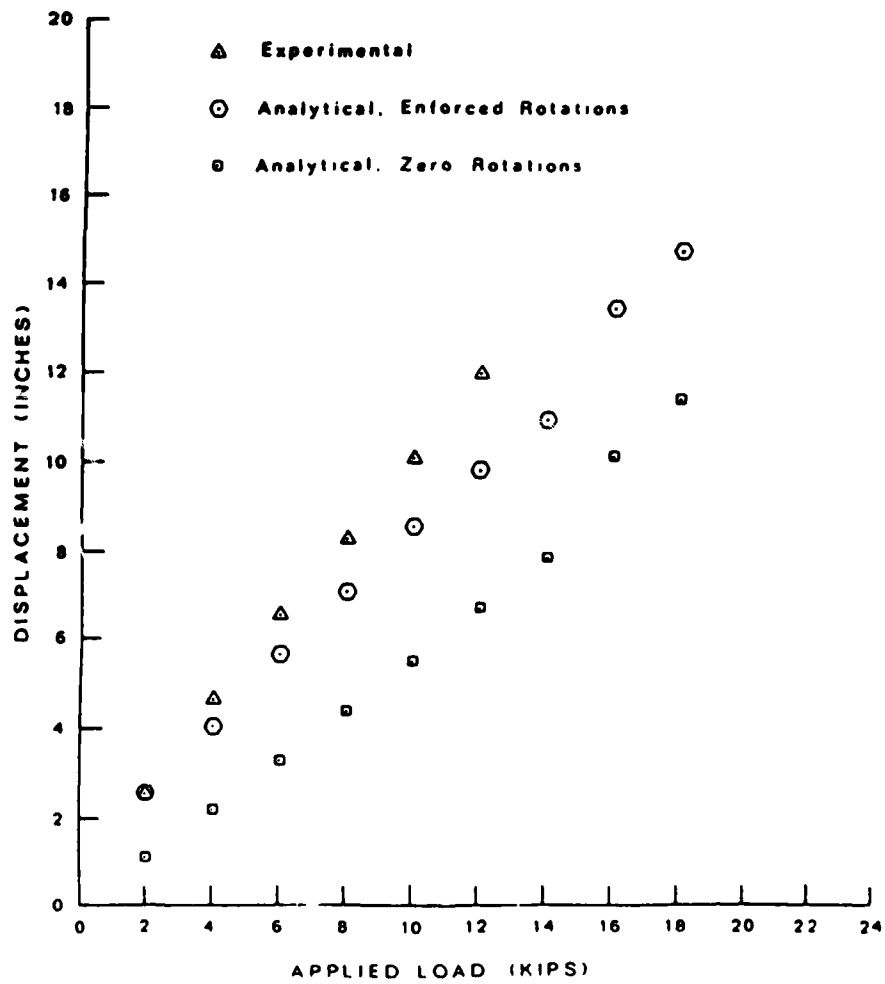
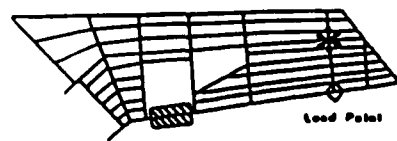
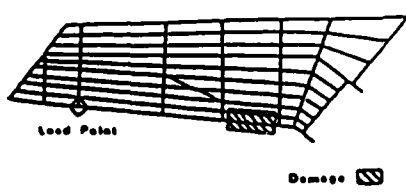
Figure 30. (Continued)



(a) Load Point, Model A (without torsional stiffness rods)

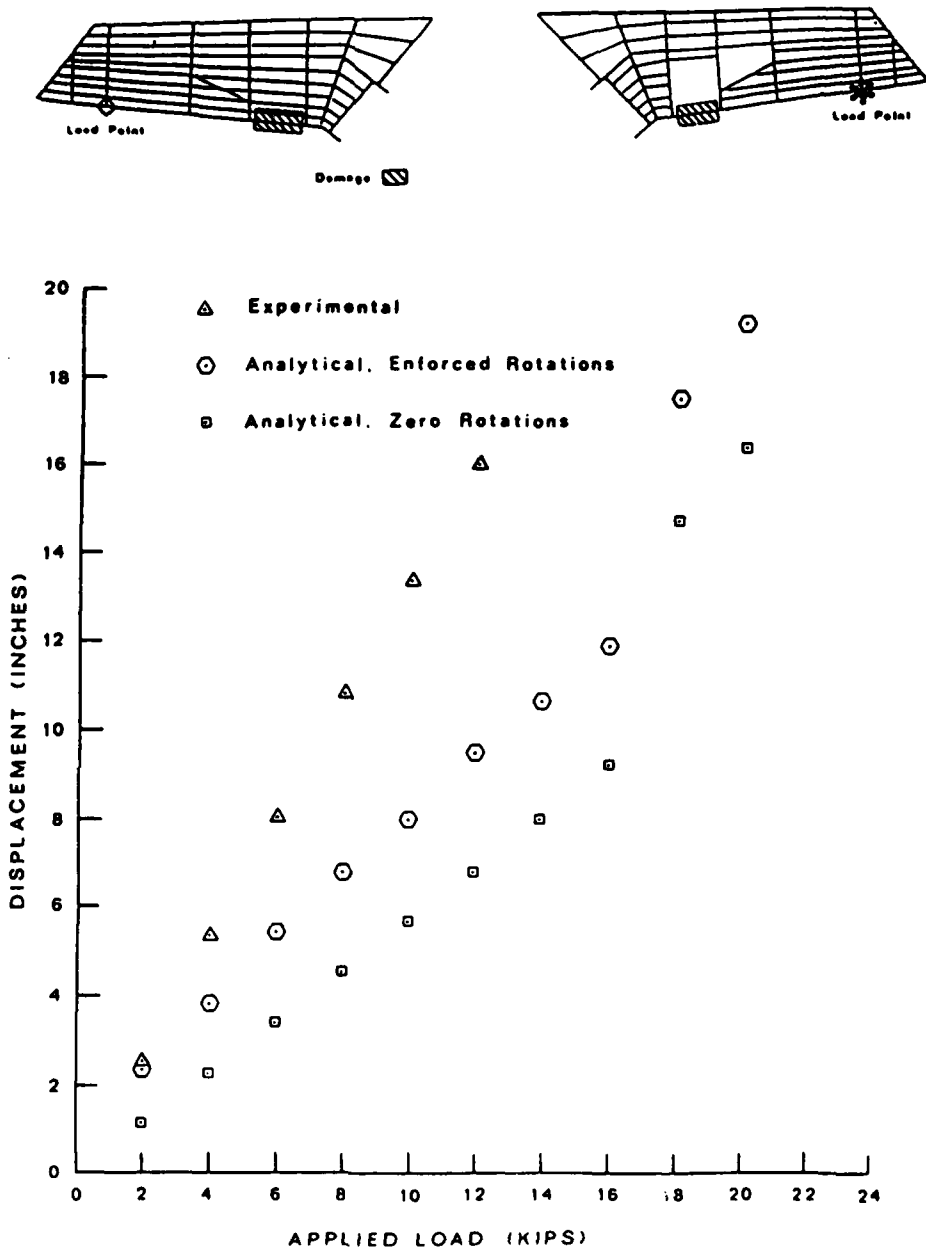
Figure 31. Single-Point Displacements for Test 2C

170



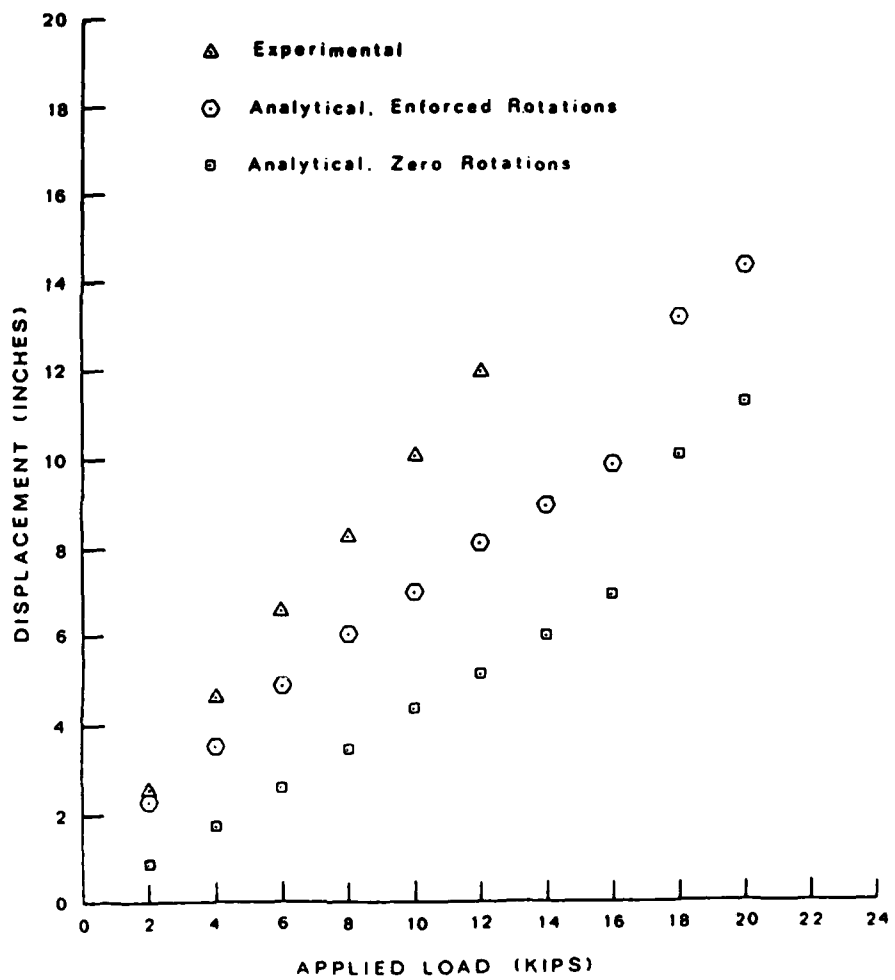
(b) Node 46, Model A (without torsional stiffness rods)

Figure 31. (Continued)



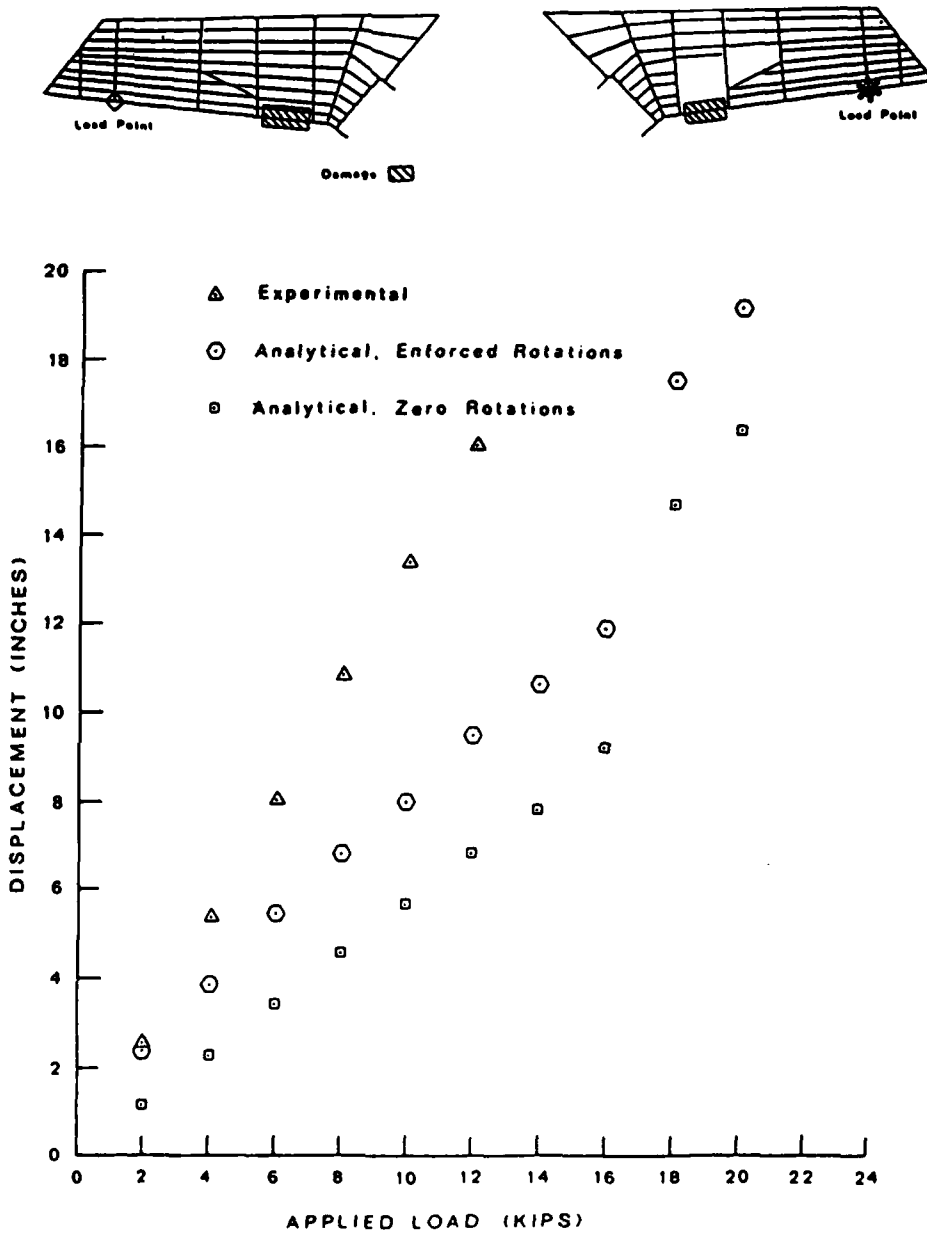
(c) Load Point, Model C (without torsional stiffness rods)

Figure 31. (Continued)



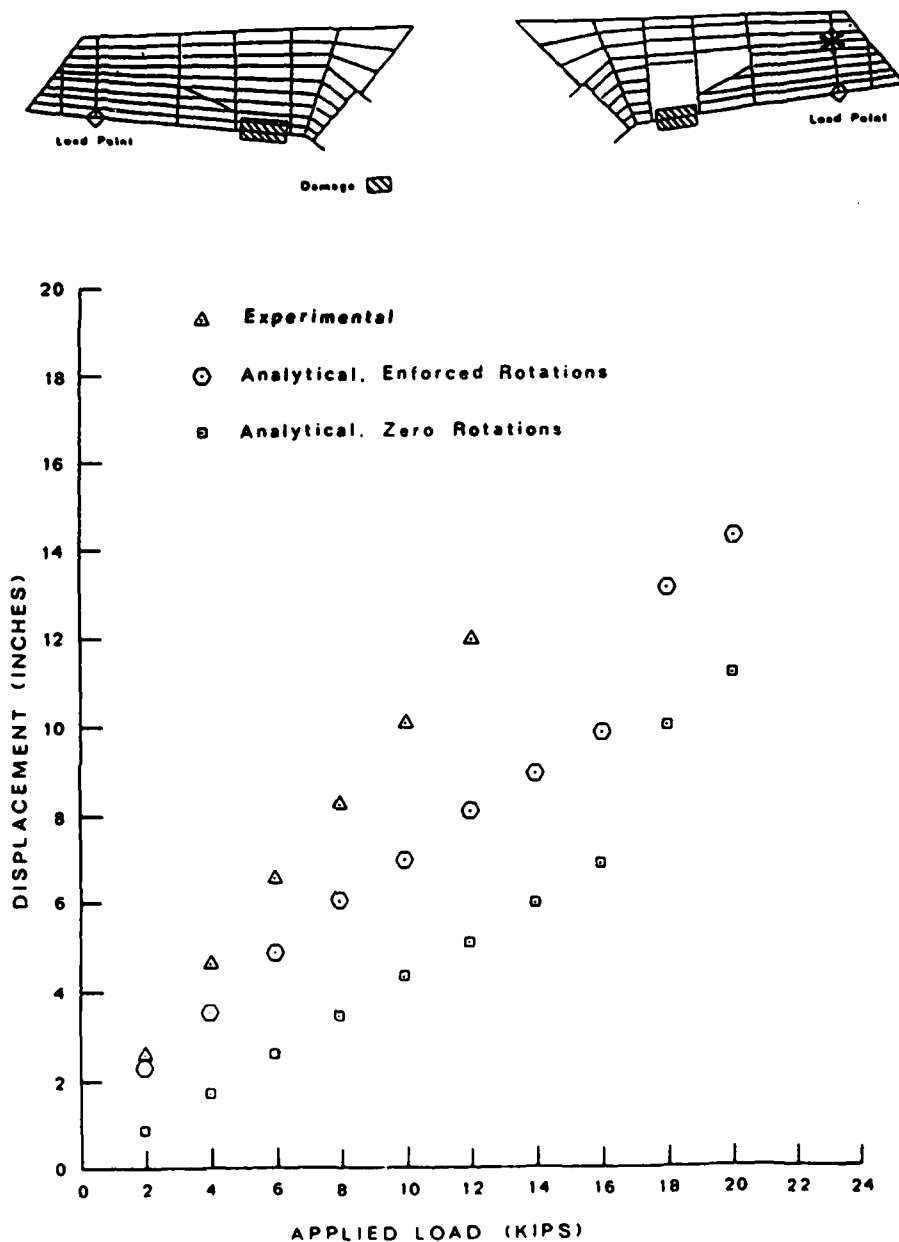
(d) Node 46, Model C (without torsional stiffness rods)

Figure 31. (Continued)



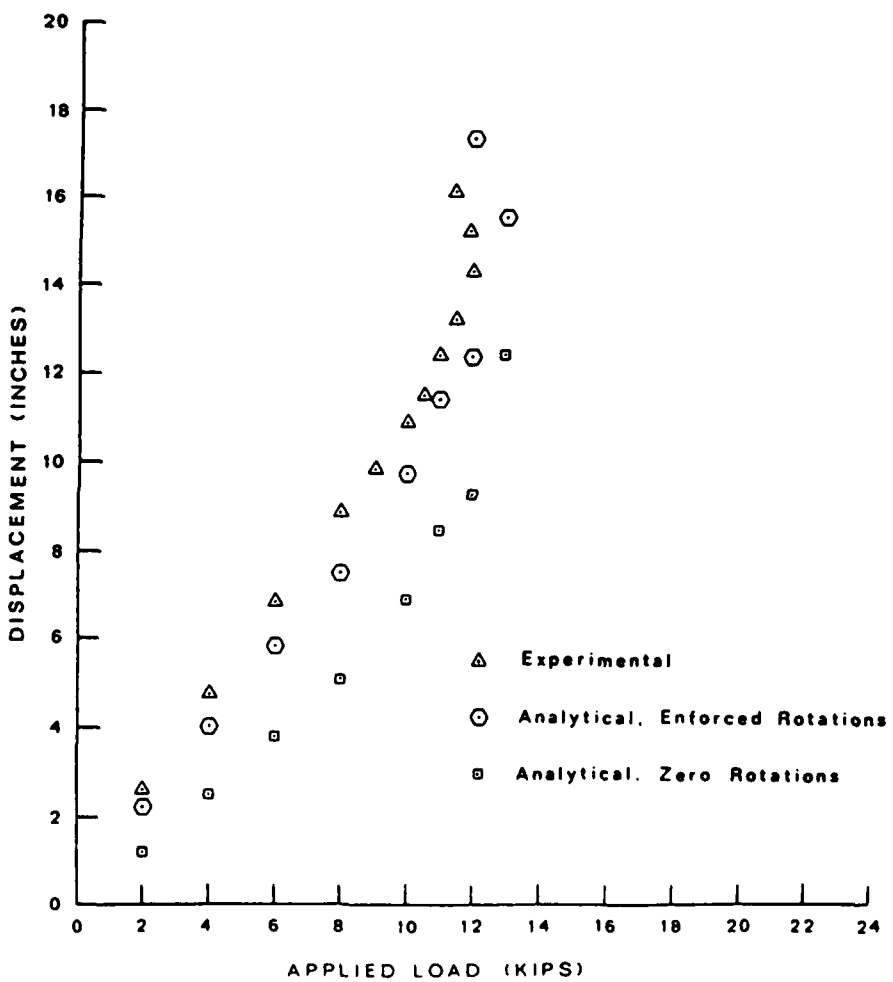
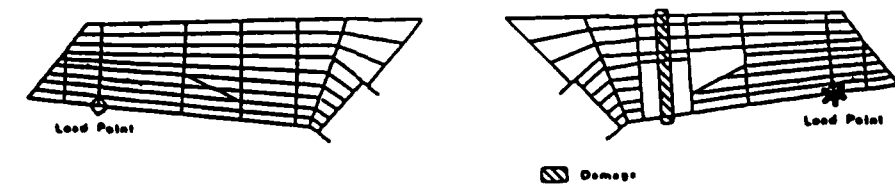
(e) Load Point, Model D (with torsional stiffness rods)

Figure 31. (Continued)



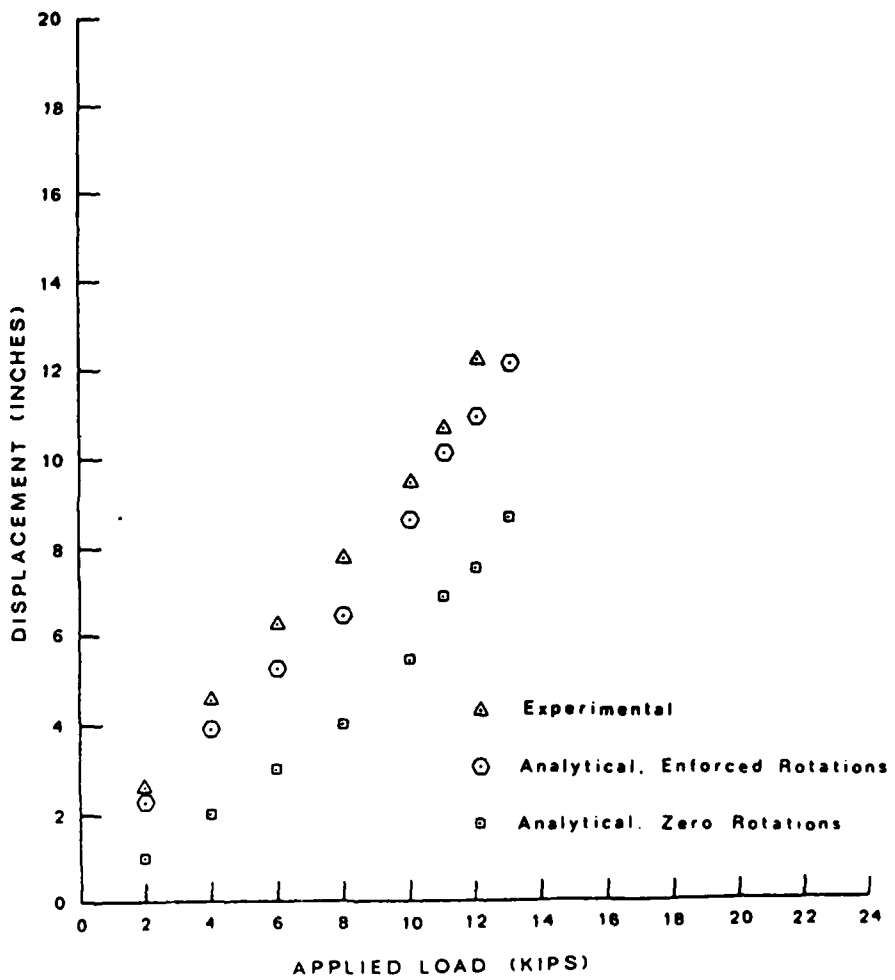
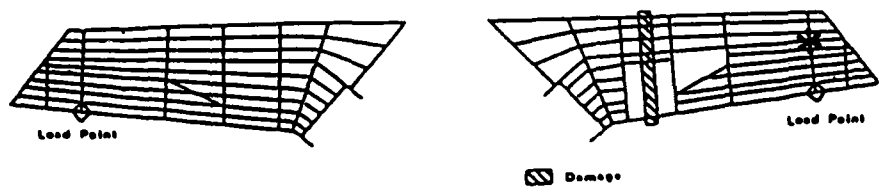
(f) Node 46, Model D (with torsional stiffness rods)

Figure 31. (Continued)



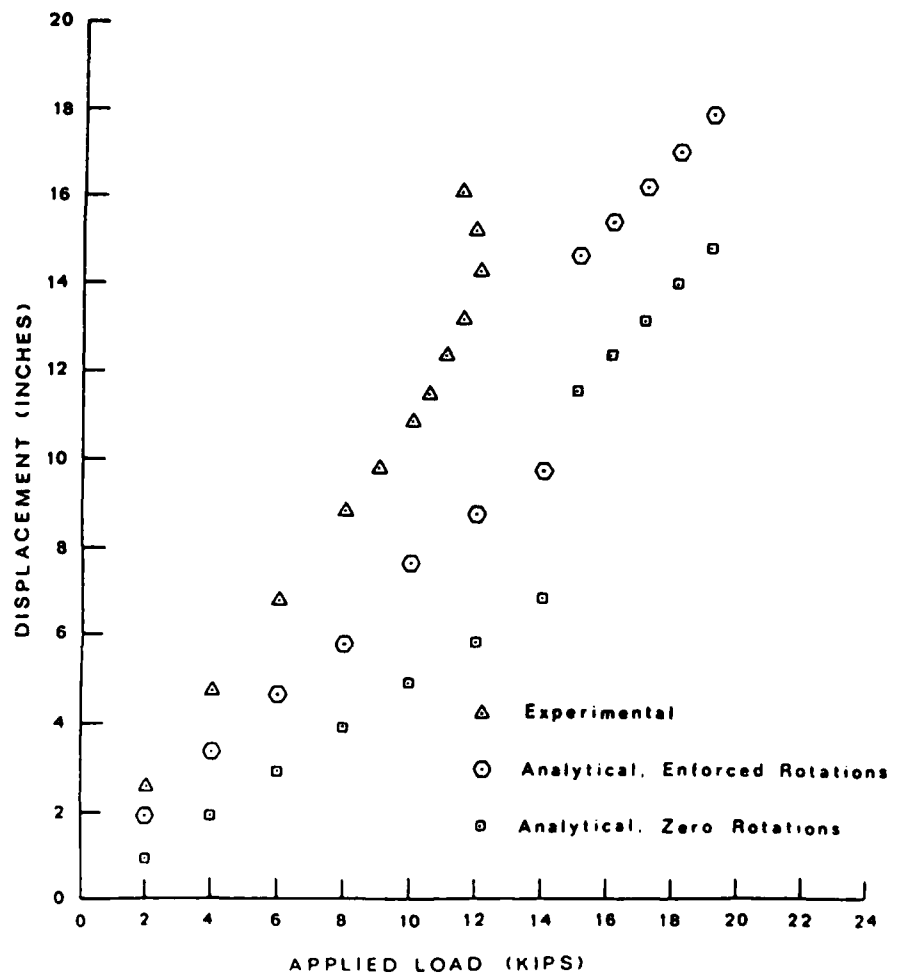
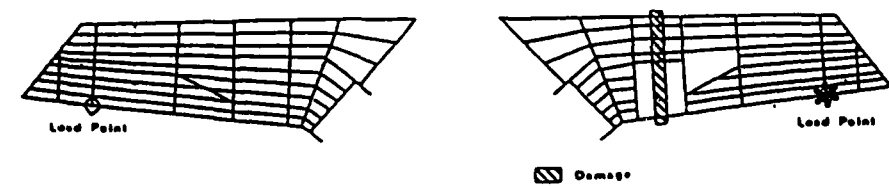
(a) Load Point, Model A (without torsional stiffness rods)

Figure 32. Single-Point Displacements for Test 3B



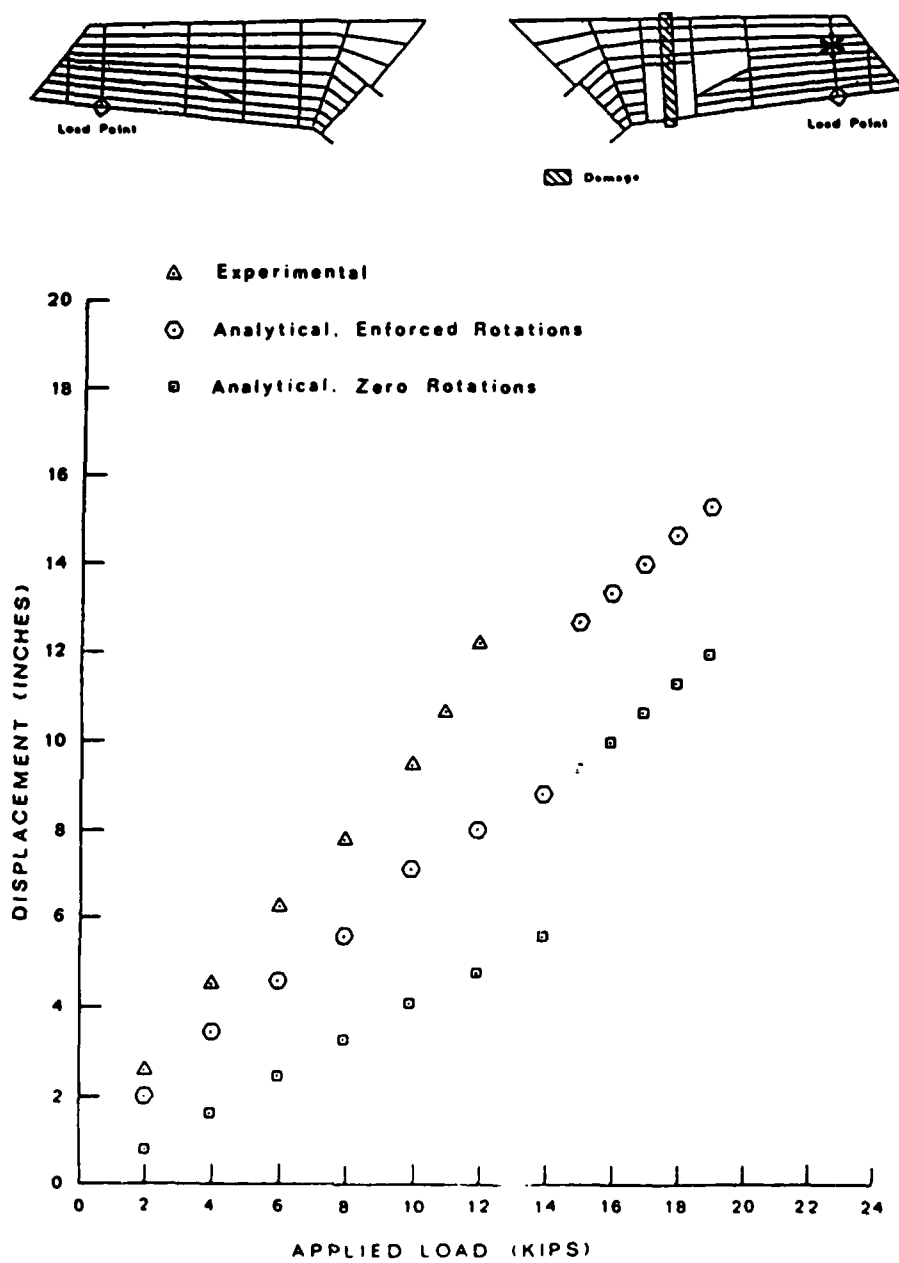
(b) Node 46, Model A (without torsional stiffness rods)

Figure 32. (Continued)



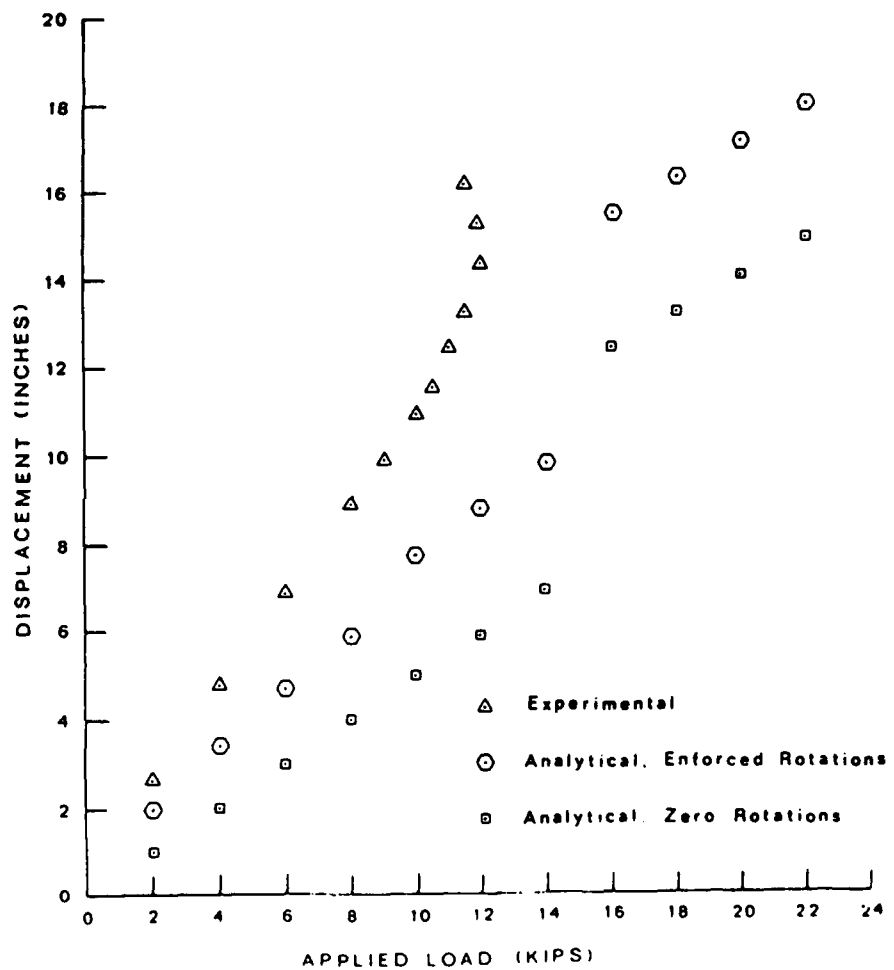
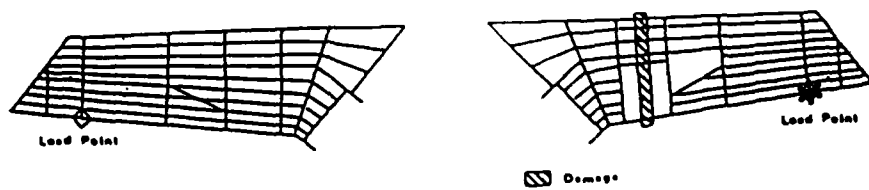
(c) Load Point, Model C (without torsional stiffness rods)

Figure 32. (Continued)



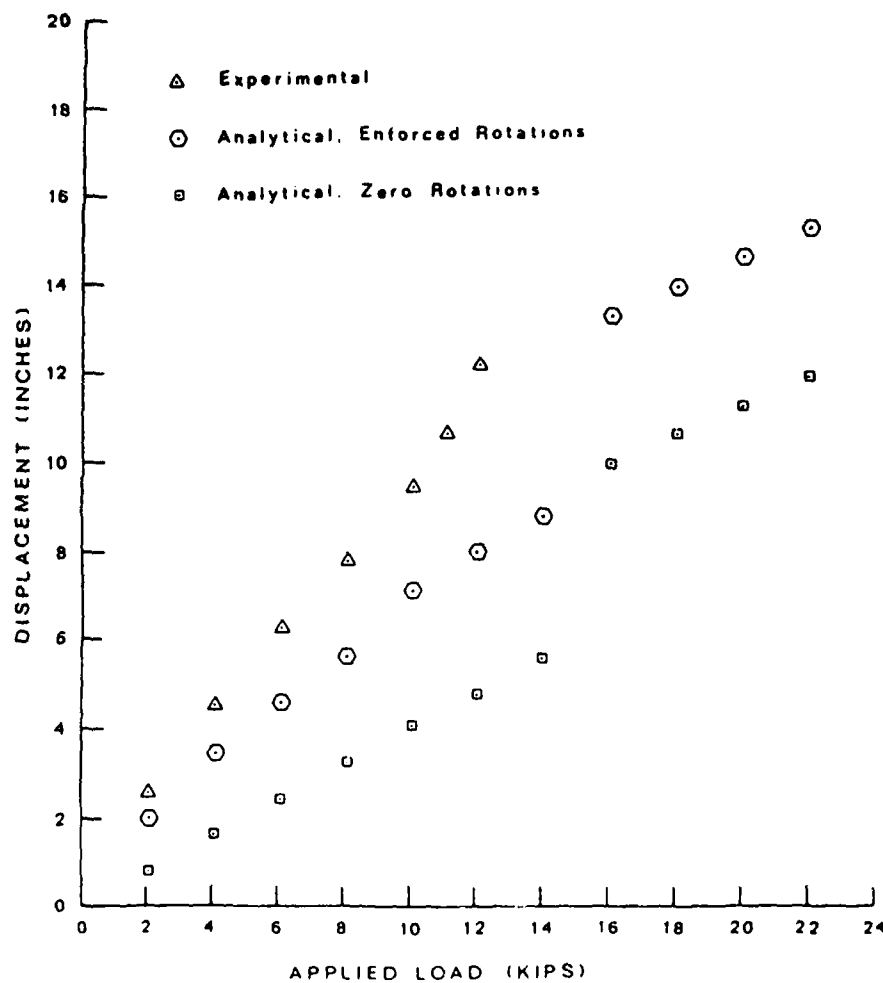
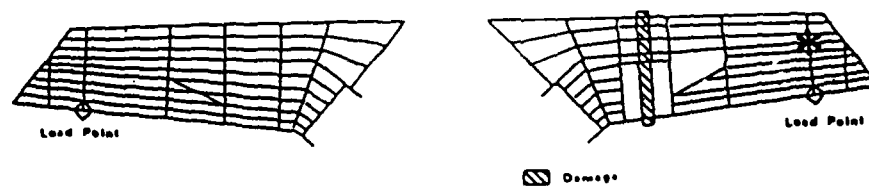
(d) Node 48, Model C (without torsional stiffness rods)

Figure 32. (Continued)



(e) Load Point, Model D (with torsional stiffness rods)

Figure 32. (Continued)



(f) Node 46, Model D (with torsional stiffness rods)

Figure 32. (Continued)

AD-A125 266

ANALYSIS OF PROGRESSIVE COLLAPSE OF COMPLEX STRUCTURES
(U) AIR FORCE INST OF TECH WRIGHT-PATTERSON AFB OH
G E RIGGS DEC 82 AFIT/CI/NR-82-63D

3/3

UNCLASSIFIED

F/G 12/1 NL

END
DATA
FILED
83
DTIC



MICROCOPY RESOLUTION TEST CHART
NATIONAL BUREAU OF STANDARDS-1963-A

APPENDIX J

SUMMARY OF ANALYTICAL RESULTS

TABLE V
SUMMARY OF RESULTS FOR TEST 1,
MODEL D, SIMPLE DAMAGE

Iteration No.	Load	Buckled Elements	Overstressed Elements	Failed Elements
1	10	68 118	---	---
2	12	56 112	---	---
3	14	136	---	---
4	16	54 80 106 124 135 255	529	529
5	14	---	---	---
6	16	---	---	---
7	18	82	---	---
8	20	111 117 132 134 258	---	---
9	22	64 116	117	117
10	20	---	137 573	573
11	18	---	119	119
12	16	---	135 571	135
13	14	---	531	531
14	12	---	---	---
15	14	---	---	---
16	16	105 257	---	---
17	18	85	105 121	105
18	16	123	533	533
19	14	---	---	---
20	16	---	123	123
21	14	---	---	---
22	16	---	---	---
23	18	---	579	579
24	16	---	---	---
25	18	---	---	---
26	20	---	---	---
27	22	52 62 89 107 125 75 248	---	248
28	20	93 114 143 256	107 125 213 257	125

TABLE V (Continued)

Iteration No.	Load	Buckled Elements	Overstressed Elements	Failed Elements
29	18	126	107 256 257 581	257
30	16	---	581	581
31	14	---	126	126
32	12	---	582	582
33	10	---	---	---
34	12	---	---	---
35	14	---	---	---

TABLE VI
SUMMARY OF RESULTS FOR TEST 1,
MODEL D, DETAILED DAMAGE

Iteration No.	Load	Buckled Elements	Overstressed Elements	Failed Elements
1	10	68 118	---	---
2	12	56 112 136	---	---
3	14	---	---	---
4	16	80 135	---	---
5	18	54 106 124 132	---	---
6	20	116 117 134 254 255 258	121	121
7	18	---	117 137	137
8	16	111	119	119
9	14	256 257	577	577
10	12	---	---	---
11	14	123	---	---
12	16	82 105 126	123 531 9529	123 9529
13	14	---	579	579
14	12	---	---	---
15	14	125	---	---
16	16	85 143	105 125	125
17	14	---	257	257
18	12	---	---	---
19	14	---	581	581
20	12	---	---	---
21	14	---	---	---
22	16	114	---	---
23	18	62 64 89	---	---
24	20	52 93	68 256	68 256
25	18	50 130	---	---
26	20	55	---	---
27	22	---	126	126
28	20	---	582	582
29	18	---	---	---

TABLE VI (Continued)

Iteration No.	Load	Buckled Elements	Overstressed Elements	Failed Elements
30	20	---	---	---
31	22	---	75	75
32	20	67 73	55 57 473	473
33	18	97	57 73	73
34	16	---	55 471	55
35	14	53	427	427

TABLE VII
SUMMARY OF RESULTS FOR TEST 2C,
MODEL A, SIMPLE DAMAGE

Iteration No.	Load	Buckled Elements	Overstressed Elements	Failed Elements
1	10	111 135	---	---
2	12	80	---	---
3	14	49 81 82 133 136 255	---	---
4	16	68 129 134	109	109
5	14	114 131	127	127
6	12	132	---	---
7	14	130	---	---
8	16	56	---	---
9	18	50 79 107 108	137	137
10	16	---	119 575	575
11	14	113 123 125 143 144	119 129 133 135 139 573 577 579	119 129 579
12	12	142	103 121 131 133 135 139 531 567 577 581 605 615	131 577 581
13	10	85 93 97 105 112 115 116 117 118 124 126 141 254 256 257	113 121 125 133 135 139 140 213 223 224 225 226 227 228 535 536 567 569 573 580 582 589 591 607 611 620 625	133 582
14	8	106	97 108 115 117 121 123 125 126 135 139 140 141 223 224 225 226 227 228 257 528 534 535 536 569 571 573 578 580 589 591 609 611 625 627 629 631 632	135 528
15	6	73	97 104 108 110 113 115 117 121 123 125 126 128 139 140 141 144 212 213 223 224 225 226 227 228 257 530 534 535 536 569 578 580 591 593 601	580

TABLE VII (Continued)

Iteration No.	Load	Buckled Elements	Overstressed Elements	Failed Elements
15 (Cont.)			618 625 627 628 629 630 631 632	
16	4	---	97 104 111 115 117 118 121 123 124 125 126 128 139 140 141 142 212 213 222 223 224 225 226 227 228 249 257 532 534 535 536 552 555 567 569 578 589 591 593 595 601 616 623 625 627 628 629 630 631 632	111 552 578

TABLE VIII
SUMMARY OF RESULTS FOR TEST 2C,
MODEL D, DETAILED DAMAGE

Iteration No.	Load	Buckled Elements	Overstressed Elements	Failed Elements
1	10	56 68 80 112 114 118 126	---	---
2	12	106 132	---	---
3	14	62 82 111 135 256	---	---
4	16	49 50 108 124 134 255	---	---
5	18	116 117 133 258	68	68
6	16	---	---	---
7	18	---	66	66
8	16	79 81 113 129	460	460
9	14	---	---	---
10	16	---	462	462
11	14	---	---	---
12	16	---	---	---
13	18	61 105 107	70	70
14	16	54	---	---
15	18	52 115	---	---
16	20	---	56	56
17	18	63	430	430
18	16	---	---	---
19	18	---	58 432	58
20	16	64	432	432
21	14	---	---	---
22	16	---	---	---
23	18	---	62 255 434	62 255
24	16	254	64 78 81 82 187 434	81 434
25	14	---	64 78 79 82 105 254 436	78 79 254
26	12	55	64 77 82 105 436 477 479	64 479

TABLE VIII (Continued)

Iteration No.	Load	Buckled Elements	Overstressed Elements	Failed Elements
27	10	85	77 82 105 436 477 481	77 436 481
28	8	---	---	---
29	10	131	54 80 428 475 477	54 80 475 477
30	8	73 126	52 75 82 428 438	52 75 428 438
31	6	---	55 473	55
32	4	---	---	---
33	6	---	427 429	427 429
34	4	---	---	---

TABLE IX
SUMMARY OF RESULTS FOR TEST 3B,
MODEL A, SIMPLE DAMAGE

Iteration No.	Load	Buckled Elements	Overstressed Elements	Failed Elements
1	10	---	510	510
2	8	---	---	---
3	10	---	---	---
4	11	49 114 134 136	110	110
5	10	130 132	128	128
6	8	---	---	---
7	10	135	---	---
8	11	---	---	---
9	12	---	---	---
10	13	116 133	66	66
11	12	56	---	---
12	13	111	460 462	460 462
13	12	52 55 82	424 432	424 432
14	10	80 113	58	58
15	8	---	528	528
16	6	---	---	---
17	8	81 254	434	434
18	6	---	436	436
19	4	---	---	---
20	6	79 256	---	---
21	8	61 129 197 213	52 438 482	52 438
22	6	62	---	---
23	8	63 107 115 257	109 127 437 582	127 437 582
24	6	---	109	109
25	4	---	---	---
26	6	---	---	---
27	8	51	78 111	78 111
28	6	---	60	60
29	4	54	532	532

TABLE X
SUMMARY OF RESULTS FOR TEST 3B,
MODEL D, DETAILED DAMAGE

Iteration No.	Load	Buckled Elements	Overstressed Elements	Failed Elements
1	10	56 68 112 114 118 136	---	---
2	12	132 256	---	---
3	14	62 134	---	---
4	16	49 80 116 135	510	510
5	14	---	110	110
6	12	130	112 128	112
7	10	---	566	566
8	8	---	---	---
9	10	---	---	---
10	12	---	---	---
11	14	---	114	114
12	12	50 82	568	568
13	10	---	---	---
14	12	---	---	---
15	14	124	---	---
16	16	258	---	---
17	17	67 117	---	---
18	18	111 254	---	---
19	19	---	530	530
20	18	---	528 532 534 574	528 532 534
21	17	55 64 73 97 107 113 126 129 143 255 257	118 120 256 552 574	120 256
22	16	115 125	116 117 118 138 257 536 552 574 592	117 118 536
23	14	51 63 85 123 131 133 141	56 58 79 81 85 107 115 119 137 257 279 430 476 499 535 573 574	73 107 115 279 476 573 574

TABLE X (Continued)

Iteration No.	Load	Buckled Elements	Overstressed Elements	Failed Elements
24	12	105	55 56 57 58 69 71 75 78 113 119 197 429 430 467 471 473 535 571	71 113 119 535 571
25	10	---	55 58 75 78 79 80 105 111 121 197 429 430 467 471 473 478 569 575	105 111 467 473 569
26	8	---	58 75 77 78 80 109 197 429 430 471 533 567	58 109 471 533 567

VITA

Gregory Edward Riggs

Candidate for the Degree of
Doctor of Philosophy

Thesis: ANALYSIS OF PROGRESSIVE COLLAPSE OF COMPLEX STRUCTURES

Major Field: Civil Engineering

Biographical:

Personal Data: Born in Wichita, Kansas, April 13, 1950, the son of Mr. and Mrs. C. Edward Riggs.

Education: Graduated from Thomas A. Edison High School, Tulsa, Oklahoma, in May, 1968; received the Bachelor of Science in Civil Engineering degree from the United States Air Force Academy Colorado Springs, Colorado, in June, 1972; received the Master of Science degree in Civil Engineering from the University of Illinois, Urbana, Illinois, in February, 1973; completed the requirements for the Doctor of Philosophy degree at Oklahoma State University in December, 1982.

Professional Experience: Base civil engineering officer, U.S. Air Force, 1973-1975; staff civil engineering officer, U.S. Air Force, 1975-1977; Civil Engineering Instructor, U.S. Air Force Academy, 1977-1979; Civil Engineering Assistant Professor, U.S. Air Force Academy, 1979-1980.

Professional Organizations: Chi Epsilon, National Society of Professional Engineers, Society of American Military Engineers.

Professional Registration: Registered Professional Engineer in Colorado.